Stony Brook University

Function and Evolution of the Cranial Sinuses in Bovid Mammals and Ceratopsian Dinosaurs

A Dissertation Presented

by

Andrew Allen Farke

to

The Graduate School

in Partial Fulfillment of the

Requirements

for the Degree of

Doctor of Philosophy

in

Anatomical Sciences

Stony Brook University

May 2008

Stony Brook University

The Graduate School

Andrew Allen Farke

We, the dissertation committee for the above candidate for the

Doctor of Philosophy degree, hereby recommend acceptance of this dissertation.

Catherine A. Forster – Dissertation Advisor
Associate Professor, Department of Biological Sciences, The George Washington University

Brigitte Demes – Dissertation Co-advisor
Professor, Department of Anatomical Sciences

Nathan J. Kley – Chairperson of Defense
Assistant Professor, Department of Anatomical Sciences

James B. Rossie – Outside Member
Assistant Professor, Department of Anthropology

Stefan Judex – Outside Member
Associate Professor, Department of Biomedical Engineering

This dissertation is accepted by the Graduate School

Lawrence Martin
Dean of the Graduate School

Abstract of the Dissertation

Function and Evolution of the Cranial Sinuses in

Bovid Mammals and Ceratopsian Dinosaurs

by

Andrew Allen Farke

Doctor of Philosophy

in

Anatomical Sciences

Stony Brook University

2008

The paranasal sinuses, air-filled spaces within the skull originating as diverticula from the nasal cavity, are the object of numerous functional hypotheses. For instance, it has been hypothesized that enlarged frontal sinuses in bovids (the clade of horned artiodactyl mammals including goats, cattle, antelope and their relatives) and supracranial sinuses in ceratopsians (the clade of horned dinosaurs including *Triceratops*) function as shock absorbers to protect the brain during horn-to-horn combat. At present, the most commonly accepted hypothesis indicates that the sinuses in all terrestrial vertebrates are functionless structures resulting from the removal of mechanically unnecessary bone ("opportunistic pneumatization"). Yet, this and other hypotheses remain largely untested.

Finite element modeling (FEM) was used to examine the functional role of the frontal sinuses in domesticated goats. Models of the skull, with varying frontal bone and

sinus morphology, were loaded under simulated head-butting conditions. It was found that the sinuses are only moderately effective as shock absorbers, are poorly placed for protecting the brain from blows to the horns, and are located in areas of bone under low stress.

Frontal sinuses were measured and described for 63 species of Bovidae, in order to document the morphology and variation of the frontal sinus in this clade. Character optimization suggests that frontal sinuses were present at the origin of Bovidae, and secondarily reduced or lost at least six different times. No statistically significant link was found between head-butting behavior and sinus morphology (size or structural complexity). Partial correlations found a significant correlation between the volume of the frontal sinus and the size of the frontal bone, but not between the volume of the frontal sinus and horn or skull size. Both the FEM and comparative analyses were interpreted to be partially consistent with the hypothesis of frontal sinuses resulting from opportunistic pneumatization of structurally unnecessary bone.

Based on the results in bovids, the hypothesis that sinuses acted as shock absorbers in ceratopsians is weakened. In this clade, unlike in Bovidae, the sinuses form through a secondary roofing of the skull in conjunction with excavation of bone. The development of a closed sinus from an open depression was probably associated with an increase in skull and horn size in order to maintain the structural integrity of the skull, as well as an anatomical reorganization of the ceratopsian skull which resulted in a thickening of the skull roof. Although a pneumatic origin cannot be demonstrated irrefutably in ceratopsians, any air source would have had to enter the dorsum of the skull via the dorsotemporal fenestrae.

DEDICATION

To my parents, Greg and Joanne Farke

Table of Contents

List of Figures

List of Tables

Acknowledgments

First and foremost, I thank my advisor, Catherine Forster, and co-advisor, Brigitte Demes, for continually challenging me and pushing me to become the best researcher possible. I also thank my committee members, Stefan Judex, Nathan Kley, and James Rossie, for reading drafts of manuscripts, acting as sounding boards, and generally keeping me on task. I learned so much from all of you!

Next, thank you to all of the other faculty from the Department of Anatomical Sciences during my years at Stony Brook University. This includes John Fleagle, Bill Jungers, Dave Krause, Susan Larson, Maureen O'Leary, Callum Ross, Erik Seiffert, Jack Stern, and Randy Susman. You taught me how to be a researcher, a colleague, and a teacher.

My fellow graduate students from anatomy and IDPAS deserve no small credit. I could hardly list everyone here, but I wish to draw special attention to Doug Boyer, Sara Burch, Mark Coleman, Justin Georgi, Chris Gilbert, Ari Grossman, Justin Hall, Mitch Irwin, Keith Metzger, Danielle Royer, Karen Samonds, Justin Sipla, Matt Sisk, Liz St. Clair, Jacob McCartney, Sara Parent, Biren Patel, Joe Sertich, Gina Sorrentino, Anne Su, and Jesse Young. You (and all of the other students) were there when it counted, and I couldn't again find such a fun and challenging bunch if I tried.

For access to museum collections in their care, I thank Mike Brett-Surman and Matt Carrano (Smithsonian Institution), Jim Gardner (Royal Tyrrell Museum of Paleontology), Mark Goodwin (University of California Museum of Paleontology), Jack Horner (Museum of the Rockies), Walter Joyce (Yale Peabody Museum of Natural History), Bob McCord (Mesa Southwest Museum), Carl Mehling and Mark Norell (American Museum of Natural History), Kevin Seymour (Royal Ontario Museum),

Kieran Shepherd (Canadian Museum of Nature), Eileen Westwig (American Museum of Natural History), and Kristof Zyskowski (Yale Peabody Museum of Natural History). I owe a big debt of thanks to the Department of Radiology at the Stony Brook University Hospital, for access to CT scanning facilities. Michael Ryan and David Evans also generously provided access to some of their own CT scan data. John Shea was especially generous in his donation of the goat head used for the FEM portion of the dissertation.

Numerous other individuals, whether they realized it or not, contributed to the development of this dissertation through innumerable discussions. This includes Brenda Chinnery-Algeier, Peter Dodson, David Dufeau, Betsy Dumont, David Evans, Michael Farney, Mike Getty, Mark Goodwin, Casey Holliday, ReBecca Hunt, Peter Larson, Mark Loewen, Pat O'Connor, Kevin Padian, Rachel Racicot, Michael Ryan, Scott Sampson, David Strait, Darren Tanke, Jaime Tanner, Frank Varriale, Matt Wedel, Larry Witmer, and Ed Yoo.

This research was supported financially by grants from the Society of Integrative and Comparative Biology, Jurassic Foundation, Paleontological Society, and a National Science Foundation Graduate Research Fellowship.

Finally, I thank my long-suffering wife, Sarah Nichols. You have put up with long absences, bad-smelling clothing, weekends at the office, and shop talk at the most inopportune moments. In the midst of all of that, you've shared my love of science, and kept me well-grounded when it mattered most. Thank you!

Introduction and Background

Cranial pneumaticity, in which bone is replaced by air sacs derived from the nasal, tympanic, and pharyngeal cavities to create a system of air-filled cavities called sinuses, represents one of the more puzzling systems within the vertebrate head. Whereas the muscles of mastication, eyes, teeth, and other structures have rather obvious and well-documented functions, the cranial sinuses have a long and checkered history of explanatory hypotheses and debate. The variable presence and morphology of sinuses (Paulli, 1900a,b,c; Witmer, 1997), their apparent phylogenetic significance in some clades (e.g., Rae et al., 2002; Rossie, 2005), and their enigmatic function (Blaney, 1990; Blanton and Biggs, 1968) demand more detailed study. To what extent do genetic or epigenetic factors influence sinus morphology? Is sinus morphology correlated with behavior? Why do some clades have extensive cranial sinuses, and others lack them? Can the morphology of sinuses be used to infer the behavior of extinct animals?

On a physiological level, paranasal pneumaticity occurs when epithelium from the nasal cavity gains a position outside of the cartilaginous nasal capsule during development. Although the exact mechanism remain unclear (further elaborated upon below), Smith et al. (2005) documented the association of osteoclasts with this epithelium. As the osteoclasts remove trabecular bone, the sinus presumably expands behind them.

Hypotheses of pneumatic function are nearly innumerable, varying widely in plausibility, testability, and general applicability. These hypotheses include weight reduction, vocal resonance, shock absorption, and a number of others summarized elsewhere (Blaney, 1990; Blanton and Biggs, 1968; Witmer, 1997). At present, the most widely accepted hypothesis was popularized by Witmer (1997), as a unique spin upon

similar ideas proposed elsewhere (see below). Specifically, this is that the sinus spaces themselves are functionless structures, which result from the removal of "unnecessary" bone by osteoclast cells associated with air-filled diverticula from the nasal, pharyngeal, or tympanic cavities. The osteoclasts are able to "sense" whether or not bone is necessary, through the transduction processes hypothesized for bone modeling and remodeling (Currey, 2002). The idea of sinuses as functionless structures resulting from the removal of unneeded bone was not new (e.g., Moore, 1981; Weidenreich, 1924, 1941), but Witmer was particularly influential in moving the emphasis from the empty space itself to the epithelial lining of the space. Throughout this dissertation, that hypothesis will be referred to as the "opportunistic pneumatization" hypothesis, after Witmer's statement that "pneumatic diverticula are viewed simply as opportunistic pneumatizing machines, resorbing as much bone as possible within the constraints imposed by local biomechanical loading regimes" (Witmer, 1997, p. 64). In the ten years since its publication, "opportunistic pneumatization" has become the most accepted hypothesis on the origins of cranial pneumaticity (cited in 137 publications alone between 1997 and 2007, according to a search on ISI Web of Science).

Despite the appearance of a resolution regarding sinus function, much work remains. Support for the "opportunistic pneumatization" hypothesis primarily has been anecdotal, relying on case studies or isolated specimens. A recent histological study on callitrichid neonates was interpreted as offering support for this hypothesis (Smith et al., 2005), but little experimental work has been conducted on the problem of sinus function and development (with the exceptions of Hönig et al., 1999, 2002). The latter studies found that connection to a pneumatic diverticulum was not necessary for formation of a

frontal sinus in miniature pigs, a result at odds with most conventional understanding of sinus development, and one which deserves further scrutiny. Most quantitative studies have focused on examining allometry or intraspecific variation rather than function (e.g., Koppe et al., 2000, 2005, 1999; Koppe and Nagai, 1997, 1999; Rae et al., 2003, 2006; Rae and Koppe, 2000). The majority of these studies have concerned anthropoid primates, especially for their relevance to questions of primate evolution. Some of the studies indeed have addressed sinus function in one form or another, but not without shortcomings. These include a limited taxonomic focus, limited consideration of the effects of phylogeny, methodologies focusing on variables of debatable relevance to sinus morphology (e.g., basicranial length), and a near complete absence of work addressing the biomechanical significance of sinuses.

Opportunistic pneumatization implies that the structure of the skull is somehow optimized by the process of sinus formation. At first glance, the idea of sinuses as structural byproducts of bone remodeling is appealing in its universal applicability. Yet, the mechanism (if any) behind developmental optimization of a bony structure is unclear. How would osteoclasts "know" to remove bone to create a sinus? A great deal of recent work has focused on the mechanisms related to bone modeling and remodeling (recent reviews are given in Currey, 2002; Rubin et al., 2006), but no final verdict has emerged, and no work has focused on sinus development specifically (or even cranial bone instead of limb bones). A best guess would be that osteoclasts associated with the pneumatic diverticulum remove bone until a certain stress or strain threshold is crossed. Yet, for areas of the skull under impact loading (such as goats, discussed below), the impacts would induce high strains within the bone. This should inhibit osteoclast activity

and prevent removal of bone. Recent work also offers conflicting evidence on how well bone geometry matches its loading regime (e.g., Bouvier and Hylander, 1981; Lieberman et al., 2004). Additionally, other studies demonstrate that bones in the absence of mechanical stress have a basic shape that is probably determined genetically (e.g., Murray and Huxley, 1925). The opportunistic pneumatization hypothesis also implies that sinus growth should occur after bone growth (at least slightly), yet some research has indicated that the two processes occur virtually simultaneously for the maxillary sinus in primates (Smith et al., 2005). A great deal of work is needed to clarify the idea of "opportunistic pneumatization." Might there be more of a genetic component for sinus development than has been acknowledged in the recent literature (with the exception of Hönig et al., 2002, 1999)?

Thus, further research on sinus function and evolution is still sorely needed. In particular, 1) the taxonomic scope of intensive investigations should be broadened beyond primates; 2) focused quantitative methods should account both for cranial morphology and phylogeny; and 3) biomechanical studies should address the mechanical role, if any, that sinuses occupy. In order to address these issues, this dissertation adopts this multi-faceted approach to examining sinus evolution and functional morphology in two clades: Bovidae (Mammalia) and Ceratopsia (Dinosauria).

Bovidae is a clade of horned artiodactyls that arose during the Miocene and have since flourished in Africa, Asia, Europe, and North America. They are best known from their domesticated varieties, including sheep, goats, and cattle. Yet, these are only a small representation of a diverse clade numbering over 120 extant species, ranging in size from the 4 kg royal antelope to the 1,000 kg gaur (Silva and Downing, 1995). The

most striking feature of bovids is their diverse horn morphology, ranging from short, simple spikes in duiker antelope to spiraled horns measuring over 1 m in length in the greater kudu. This horn morphology is associated with a variety of behaviors (Estes, 1991). Perhaps best known is the role that horns play in intraspecific combat. The bighorn sheep and their relatives engage in spectacular head-ramming contests, and many African antelope (such as the oryx) lock their horns for sometimes quite lengthy wrestling matches. Recognition of these behaviors has led a number of workers to identify potential adaptations in the skull related to horn use, including specializations in horn shape, reorientation of the basicranium from an ancestral condition, and enlarged frontal sinuses (Jaslow, 1987; Kitchener, 1985, 1991; Lundrigan, 1996; Schaffer and Reed, 1972). The frontal sinuses of bovids are paranasal in origin, occupying space within the frontal bone and occasionally extending up into the horncores. Previously published phylogenetic hypotheses (Gentry, 1992; Vrba and Schaller, 2000) suggested that enlarged frontal sinuses (or even frontal sinuses of any size) evolved multiple times within Bovidae. Furthermore, several researchers have specifically identified the frontal sinuses of some bovids as an adaptation for shock absorption, to protect the brain and other cranial structures from the forces of impact (e.g., Schaffer and Reed, 1972).

Most previous studies of sinuses in primates have focused on the maxillary sinuses, which are caught between the competing spatial demands of the orbit, nasal cavity, and teeth. Thus, it is particularly difficult to separate the evolution of the maxillary sinuses from that of the adjacent structures. Although the frontal sinuses of bovids are certainly not completely independent structures (especially as related to the horn cores), it is inferred that their position makes them less likely to be affected by

nasal cavity, orbit, and teeth. This renders the frontal sinuses of even greater value for inferring function.

The frontal sinuses of bovids also are of interest as functional analogues for the sinuses of some extinct horned animals. Ceratopsia (horned dinosaurs) was a clade of herbivorous dinosaurs that lived in North America during the Late Cretaceous period. Their best-known member was the three-horned *Triceratops*, which had an estimated body mass of 4 to 5 tons (Henderson, 1999; Seebacher, 2001). Ceratopsids possess a unique system of hollow spaces, the supracranial sinuses, beneath their supraorbital horncores. The supracranial sinuses have been analogized with the frontal sinuses of bovids, and used thus to infer the presence of intraspecific horned combat in ceratopsids (Molnar, 1977). Hand-in-hand with inference of combat, a protective function for the sinuses of ceratopsids has also been hypothesized (Forster, 1996). Yet, in both bovids and ceratopsids, the alleged shock absorption potential of the sinuses never has been tested (Farke, 2006). Additionally, a pneumatic source for the supracranial sinuses never has been identified, and it is unknown whether these structures even were pneumatic in origin. Descriptions of the sinuses are incomplete, and as will be shown later in this dissertation, sometimes incorrect.

Bovidae and Ceratopsidae present ideal clades with which to better understand the evolution and function of cranial sinuses. They represent a considerable taxonomic departure from previous studies, permitting detailed investigation of sinus evolution in two non-primate clades. The multiple origins of enlarged frontal sinuses within Bovidae also allow detailed investigation of sinus evolution and its relevance to behavior within a quantitative and phylogenetic context (a combined approach, which effectively has been

absent in previous studies). Finally, a detailed analysis of bovid sinuses will allow a better understanding of sinus function, if any, in ceratopsids.

This dissertation is divided into three main chapters, each with a distinct focus. The first chapter investigates the mechanical significance of the frontal sinuses in the domesticated goat, *Capra hircus*. Finite element modeling is used to determine the effects of sinuses under various loads applied to the skull, in order to evaluate the role of the sinuses in head-butting and opportunistic pneumatization. The second chapter documents the evolution of the frontal sinuses across 63 species of bovids. Comparative statistical approaches are used to investigate the behavioral and anatomical factors most associated with sinus morphology, in an attempt to evaluate the "opportunistic pneumatization" hypothesis. The third and final chapter investigates the anatomy of the supracranial sinuses in Ceratopsidae, describing structural anatomy and evaluating potential functions in light of the data from bovids.

Frontal sinuses and head-butting in goats: a finite element analysis

ABSTRACT

Frontal sinuses in goats and other mammals have been hypothesized to function as shock absorbers, protecting the brain from blows during intraspecific combat. Furthermore, sinuses are thought to form through removal of 'structurally unnecessary' bone. These hypotheses were tested using finite element modeling. Three-dimensional models of domesticated goat (*Capra hircus*) skulls were constructed, with variable frontal bone and frontal sinus morphology, and loaded to simulate various head-butting behaviors. In general, models with sinuses experienced higher strain energy values (a proxy for shock absorption) than did models with unvaulted frontals, and the latter often had higher magnitudes than models with solid, vaulted frontals. Furthermore, vaulted frontals did not reduce magnitudes of principal strain on the surface of the endocranial cavity relative to models with unvaulted frontals under most loading conditions. Thus, these results were only partially consistent with sinuses, or the bone walling the sinuses, acting as shock absorbers. It is hypothesized that the keratinous horn sheaths and cranial sutures are probably more important for absorbing blows to the head. Models with sinuses did exhibit a more "efficient" distribution of stresses, as visualized by histograms in which models with solid frontals had numerous unloaded elements. This is consistent with the hypothesis that sinuses result at least in part from the removal of mechanically unnecessary bone.

INTRODUCTION

Head-to-head combat by sheep and goats is a spectacular event, both visually and mechanically. Rival males rear back and bang their horns together, and this event may be repeated several times in succession (e.g., Alvarez, 1990). In bighorn sheep (*Ovis canadensis*) the impact force may exceed 3,400 N, and the sudden deceleration of impact occurs over less than 300 ms (Kitchener, 1988). These intense impacts so near critical cranial organs have invited numerous lines of speculation on the structures that may be responsible for "shock absorption" during combat (e.g., Geist, 1966; Jaslow and Biewener, 1995; McDonald, 1981).

Shock absorbers dampen sudden accelerations by converting applied kinetic energy into another form (e.g., heat), through deformation over a period of time. These principles have been used to develop football helmets and other protective devices, which protect the human skull and brain by attenuating impact energy through deformation of the helmet in place of the head and reducing the force directly transmitted into the skull itself and/or spreading the force over a larger area (Levy et al., 2004). Similarly, an idealized biological shock absorber in the skull experiences elastic deformation (as opposed to brittle fracture or plastic deformation) and concentrates this deformation away from delicate cranial organs. A longer period of deformation, related to the elasticity of the deforming object, reduces strains (and hence potential damage) on brain tissue and blood vessels due to inertia. Several structures within a sheep or goat skull could contribute to shock absorption. For instance, the keratin sheath of the horns is considerably more elastic than bone, allowing a relatively greater amount of deformation (Kitchener, 1987, 1988), and the position of the sheaths localizes this

deformation away from the immediate area of the brain and other cranial organs. Several cranial sutures that are located near the horns (hence, near the area of impact), exhibit high strains during impact loads (Jaslow and Biewener, 1995), and thus may also function as a sort of "crumple zone" during impacts. Finally, the frontal sinus system is another candidate for shock absorbers.

The frontal sinuses of bovids (Fig. 2-1C-E) are air-filled spaces originating from the nasal cavity, located wholly within the vaulted (expanded) frontal bone. The sinuses are sandwiched between two layers of cortical bone—one at the outer table of the skull (hereafter referred to as the "external cortex") and one forming a portion of the surface of the endocranial cavity ("internal cortex")—and may extend into the horncores. Bony struts (usually numbering between four to six on each side in goats, with a typical thickness of a millimeter or less) may divide the sinuses into a series of interconnected chambers. The idea of frontal sinuses as "shock absorbers" is often repeated in the literature (e.g., Geist, 1966; Schaffer and Reed, 1972) and has even been used, by analogy, to infer the function of sinuses in extinct dinosaurs such as *Triceratops* (Molnar, 1977; Forster, 1996). Despite this, the idea of sinuses as protective structures remains completely untested.

Certainly, it is not the empty space of a sinus that absorbs shocks. As suggested by Schaffer and Reed (1972), the outer walls of the sinus or the struts within the sinus could deform during impact, in place of deformation of the endocranium. Thin walls of bone would be more deformable than solid bone. A related possibility is that the walls direct the forces away from biologically sensitive structures and towards sutures, where further deformation takes place.

Any discussion of sinus function must also consider the broadly accepted idea of the sinuses as a by-product of bony remodeling (e.g., Weidenreich, 1941; Edinger, 1950; Witmer, 1997). This mechanism follows models of bone adaptation discussed by Roux (1881) and others, in which the unpneumatized skull contains areas of bone that aren't necessary for mechanical support. Osteoclasts associated with pneumatic diverticula from the nasal cavity remove the structurally unnecessary bone, producing a sinus within a more "optimized" skull (Witmer, 1997). Under this hypothesis, the frontal bone that contains the sinus, and not the sinus itself, is the more important structure. The frontal could have its current morphology for any number of reasons, such as structural support of the horns, but the shape of the sinus itself only reflects the loads placed upon the skull (Preuschoft et al., 2002). Importantly, this concept is not mutually exclusive of other functions for the sinuses or the vaulted frontal, such as shock absorption.

The idea of sinuses as somehow producing "optimal" structures (greatest strength with least materials) remains extraordinarily difficult to test with conventional experimental methods. A similar problem plagues the shock absorption hypothesis. Thus, finite element modeling (FEM) was used in this study to test the effects of cranial sinuses in the domesticated goat, *Capra hircus*.

Hypotheses

Finite element models of variable morphology—including skulls with strutted sinuses, unstrutted sinuses, sinuses filled with trabecular or cortical bone, and skulls completely lacking sinuses and a vaulted frontal bone (Fig. 2-1A-E)—were constructed in order to test three (not mutually exclusive) hypotheses:

(1) Sinuses function as shock absorbers (Schaffer and Reed, 1972). Strain energy, used here as a proxy for shock absorption in static analysis (see Materials and Methods), should be elevated in the frontal for skulls with sinuses relative to skulls without, reflecting the fact that this energy then would not be transferred into the endocranial cavity. A second aspect of shock absorption could be effected by sinuses directing the strain resulting from forces placed on the horns away from the endocranial cavity (Schaffer and Reed, 1972). A skull with sinuses that is otherwise identical in shape to a skull that lacks sinuses (e.g., Fig 2-1E vs. 2-1B) should experience higher strains within the endocranial cavity, simply because the removal of bone reduces the overall stiffness of the frontal and results in greater overall deformation. But if the removal of bone to form a sinus results in a structure that directs the force of impact away from the endocranial cavity (or towards different regions), the skull with sinuses still should experience lower strains within the bone surrounding the endocranial cavity as well as exhibit a different spatial pattern of strain distribution. The struts within the sinus may also play a role in this regard, with similar predictions.

(2) The dorsally vaulted and thickened frontal, not the sinus, is important for protecting the brain. If this is true, it was expected that a skull without the normal vaulted frontal (Fig. 2-1A) would experience significantly higher stress, strain, deformation, and strain energy in the endocranial cortex or frontal bone than skulls with either a solid, vaulted frontal or a vaulted frontal with sinuses (Fig. 2-1B-1E).

(3) Frontal sinuses improve "structural efficiency" for skulls with vaulted frontals. This hypothesis was tested by comparing histograms of stress distribution within the frontal for models with solid and hollow frontals. It was predicted that a skull

with a completely solid frontal would have a significant population of unloaded bone segments in the area where the sinus would otherwise be located (using von Mises stress as a proxy for loading). Sinuses thus optimize the skull by removing unloaded bone.

List of Symbols and Abbreviations

Abbreviations used in the text and figures include: DHL, double horn loading case; E, modulus of elasticity; ec, endocranial cavity; ecx, external frontal cortex; fps, frontoparietal suture; fri, frontal region of interest; fs, frontal sinus; FL, frontal loading case; icx, internal frontal cortex; ifs, interfrontal suture; S.D., standard deviation; SFC, model with vaulted, cortical-bone filled frontals; SFT, model with vaulted, trabecular-bone filled frontals; SHF, single horn front loading case; SHL, single horn lateral loading case; SHT, single horn tip loading case; SS, model with strutted sinuses; UF, model with unvaulted frontals; US, model with unstrutted sinuses; ρ, density; ν, Poisson's ratio; ε_1, maximum principal strain; ε_2, minimum principal strain; $\mu\varepsilon$, microstrain; $\angle$, angle in degrees.

MATERIALS AND METHODS

The domesticated goat (*Capra hircus*) was chosen for this study because of the availability of experimental data on cranial impact for validation of the FE models (Jaslow and Biewener, 1995). Model geometry was based on CT scans of the skull of a young male goat, with an in-plane pixel resolution of 0.49 by 0.49 mm and interslice spacing of 2.5 mm. Visual inspection of renderings of the data indicated that this slice spacing adequately portrayed the cranial structures of interest in this study. The CT

slices were imported into the modeling package SolidWorks 2003 (SolidWorks Corporation, Concord, MA, USA), in which bone and keratinous horn sheath were traced manually on each slice, and the tracings were lofted into a three-dimensional solid model (Fig. 2-2A). In order to simplify the geometry of the model, the foramina of the basicranium (except for the foramen magnum) and the paroccipital and styloid processes were not incorporated into the model. Because the primary area of interest in the model was the cranial roof and not the cranial base, these simplifications were considered appropriate.

Numerous studies demonstrate that sutures exhibit elevated strain magnitudes relative to the surrounding bones and thus affect strain distribution across the skull (e.g., Behrents et al., 1978; Herring and Teng, 2000; Jaslow, 1990). Jaslow and Biewener (1995) even suggested that the sutures play a major role in shock absorption in goats. Thus, the models were constructed with lines of compliant elements for the interfrontal and fronto-parietal sutures. These sutures are closest to the sinuses (the area of interest) and the horncores (the area of primary loading) and thus are most likely to affect the results. It is important to note that the sutures themselves were not modeled here, but rather a sutural zone including both the suture and surrounding bone were modeled. For this reason, it was not appropriate to give the suture zones material properties for sutures as reported in the literature (e.g., Radhakrishnan and Mao, 2004). Instead, the suture zones were given properties intermediate between cortical bone and sutural material (E=0.400 GPa, ν=0.28, ρ=1.13 g/cm^3), reflecting the composite nature of the suture zone. These properties were adjusted over several iterations until a test model displayed strains across the sutures similar to those reported by Jaslow and Biewener (1995) for

their *in vitro* experiments on goat heads.

Four model geometries were constructed in order to test the functional effects of different morphologies of the frontal (Figs 2-1, 2-2). The first model ("unvaulted frontal") lacked sinuses, and the contour of the frontal was smoothed to a thickness approximately equal to that of the combined inner and outer tables of bone in the unmodified skull (Figs 2-1A). The resulting geometry was reminiscent of some bovids that lack enlarged frontal sinuses, such as members of the genus *Gazella*. The second model consisted of a skull completely lacking the frontal sinuses; the space within the vaulted frontal normally occupied by the sinuses was filled with bone (Fig. 2-1B,C). Two variants of this model were considered in the analysis, by setting the material properties of the bone occupying the location of the sinus to that of cortical bone ("vaulted cortical bone-filled frontal") or trabecular bone ("vaulted trabecular bone-filled frontal"; see below). The third model ("unstrutted sinus") comprised a skull with a simple, unstrutted sinus cavity (Fig. 2-1D). Here, the boundaries of the frontal sinuses were simplified to eliminate all struts within the sinus, except for the midline strut at the interfrontal suture. The final model incorporated a complex frontal sinus, with all struts included (Fig. 2-1E). This model ("strutted sinus") represented the original goat skull. All models were otherwise identical.

The model geometries were imported into the finite element modeling package ALGOR FEMPro (version 20.0; Algor, Inc., Pittsburgh, PA, USA). Within FEMPro, the model was meshed using mixed brick elements. Mesh density was set to allow for multiple element thickness across the regions of experimental interest, such as the cranial vault, to achieve a more realistic solution. Due to the size and complexity of the

models, it was not feasible to conduct convergence tests with varying mesh densities. The model with an unvaulted frontal had 152,750 nodes and 382,972 elements; the models with vaulted, solid frontals, 134,709 nodes and 363,407 elements; the model with unstrutted sinuses, 119,748 nodes and 309,790 elements; and the model with strutted sinuses, 119,436 nodes and 311,503 elements.

All models used identical material properties. Because properties for goat cranial bone have not been published, values were based on averages of measurements from primate cranial vaults (E=14.550 GPa, ν=0.28, ρ=1.725 g/cm^3; Wang et al., 2006). Properties of trabecular bone within the frontals (for models with vaulted, trabecular bone-filled frontals) were based on published measurements from human tibiae (E=0.637 GPa, ν=0.28, ρ=0.2634 g/cm^3; Ashman et al., 1989).With the exception of Poisson's ratio, to which an arbitrary value of 0.30 was applied, properties for the horn sheath were adapted from those published for other bovids (E=3.900 GPa, ν=0.30, ρ=1.3 g/cm^3; Kitchener, 1991). Linear isotropic material properties were assumed, but cranial bone may have a high degree of anisotropy, potentially affecting analysis results (Strait et al., 2005). However, the present study is largely focused on patterns, not precise values. Several studies have found that isotropic material properties, if properly selected, may be adequate for broadly characterizing most aspects of strain distribution within a skull (e.g., Metzger et al., 2005; Strait et al., 2005). Thus, anisotropic properties were not considered a major concern. For the same reasons, and because appropriate data are not available for goats, uniform material properties were used across the skull (except for the areas of trabecular or cortical bone within the frontal for certain models, keratin, and sutures).

Static versus Dynamic models, and Strain Energy

Shock absorption implies a dynamic component—deformation of a structure over time. Dynamic finite element analyses incorporating skull deceleration during impact are technically feasible, but require a set of data (duration of impact, motion of skull during impact, etc.) not currently available as well as massive computing power for the resolution of models considered here. Strain energy, which is the potential energy stored within a deformed material (Hibbeler, 1997), presents a relevant proxy for examining shock absorption in static models. Briefly, an object under load deforms and converts the kinetic energy of impact into strain energy. Strain energy stored in one portion of a structure (the walls of the frontal bone and frontal sinuses here) is not transferred elsewhere (e.g., as vibrations in the walls of the endocranial cavity).

Loading Conditions

The skulls were modeled at the moment of peak force during impact, as estimated from values provided in previous studies (Jaslow and Biewener, 1995). Five loading cases of equal total magnitude (1088 N) were tested here, in order to examine the effects of different locations and directions of loading upon the skull (Fig. 2-1F,G). In the first loading case (double horn loading), equal loads of 544 N were applied to the anterior surfaces of both horn sheaths at their proximal ends, for a total force of 1088 N. The forces were angled so that their combined vector passed through the center of the foramen magnum. Biologically, these loading conditions were considered a realistic representation of head-butting behavior in the goat (Jaslow and Biewener, 1995). Additionally, this loading condition was comparable to that used for *in vitro* experiments

on goat crania by Jaslow and Biewener (1995), allowing for comparison of the model with their data (Table 2-1). In the second loading case (single horn front loading), a load of 1088 N was applied to the anterior surface of the base of the right horn sheath only (at the same angle as in the double-horn loading condition). In the third loading case (single horn lateral loading), a medially-directed load of 1088 N was applied to the lateral surface of the base of the right horn sheath only. In the fourth loading case (single horn tip loading), a load of 1088 N was applied to the rostral surfaces of the right horn sheath approximately two-thirds of the way distally along its length. In the fifth and final loading case (frontal loading), a load of 1088 N was applied to the dorsal surface of the middle of the frontal bone, rostral to the base of the horncores. The angle relative to the base of the skull was identical to that used in double horn loading; the only difference was in the location of the load relative to the base of the horn.

Constraints

The models were constrained at the occipital condyles from translation and rotation in all planes. This followed an assumption of several previous studies, that the occipital region is held relatively steady by the vertebrae and cervical musculature during impact (Schaffer and Reed, 1972). All models had identical constraints.

Validation Methods

The FE models were validated through comparison with the results of Jaslow and Biewener (1995). Their study placed strain gauges on bone at several points across goat heads under *in vitro* impact loads. Strain gauge locations from the experimental study

that were comparable to the FE models included the anterior surface of the base of the horncore, posterior surface of the base of the horncore, and the external aspects of frontal and parietal bones. Due to inevitable differences in skull morphology and precise strain gauge placement as compared to the experimental results, strain gauge locations had to be approximated on the FE model. At each site of comparison, a set of nine nodes in a roughly rectangular pattern (three nodes in a triangular pattern for the posterior horncore, because of the limited exposed area) were selected for further analysis. Multiple nodes were sampled in order to mitigate the potential effects of poor-quality elements.

Strain gauges only measure strain in two dimensions at most, so the three dimensional strain vectors provided by FE models were not directly comparable. In order to measure the principal strains in the plane of the surface of the skull, the coordinate system was redefined separately for each area of the skull to coincide with the nodes sampled at each validation point. Then the normal and shear strain tensors in the plane of the sampling region were extracted, and the magnitude and direction of planar maximum and minimum principal strains were calculated using standard engineering equations (Hibbeler, 1997).

Jaslow and Biewener (1995) published average values and standard deviations for each strain gauge site; modeled strains and strain orientations were considered realistic if they fell within two standard deviations of the experimental values. Ratios for maximum and minimum principal strain were also compared, as another measure of model performance. Results were validated in the model with strutted sinuses (reflecting real-life skull geometry) for the condition of double-horn loading.

Comparison of Results

Results were extracted for two areas: 1) the bony surface of the endocranial cavity; and 2) the frontal bone, excluding the surface of the endocranial cavity (Fig. 2-3). In order to evaluate hypotheses related to the sinuses' role in protecting the brain and associated structures, values for principal strains were extracted for nodes of elements lining a portion of the bony surface of the endocranial cavity. These nodes were located in the dorsal half of the cavity, exclusive of the region of the cribriform plate, rostral to the frontoparietal suture, and excluding values from the interfrontal suture (Fig. 2-3B). This region was selected because it was closest to the frontal sinuses (hence most likely to be affected by any changes in their morphology) and furthest from the the occipital condyles (a region likely to have elevated values of stress and strain due to the constraints there). Graphical plots of strain were also generated, in order to visualize its distribution of across the surface of the endocranial cavity.

In order to evaluate hypotheses of how the sinuses affect the structural efficiency of the frontal, nodes were sampled from the entire frontal around and including the external cortex of the frontal sinus (exclusive of the free portion of the horncores, the bony surface of the endocranial cavity, and the sutures; see Fig. 2-3A). Values for von Mises stress (giving an estimate of overall stress magnitudes in the model) and strain energy (indicating how much energy is stored by the frontal) were extracted for all of the nodes in this region, for each model.

Interpretation of results for the frontals was complicated. For instance, it was expected *a priori* that average stress magnitudes should be greater throughout the model with sinuses than in the model with a solid vaulted frontal, because there was less bone

to dissipate forces. The relative distribution of the stresses was considered to be more informative. Thus, histograms were used to visualize the distribution of nodal magnitudes for von Mises stress within the frontal, as has been commonly done elsewhere in the modeling literature (e.g., Van Rietbergen et al., 2003). Because the models differed in the numbers of elements in the frontal (reflecting whether the frontal was filled with bone or struts, or unvaulted), the nodal results were downsampled to 100,000 nodal values each (by random sampling without replacement) in order to create comparable histograms. For the models with vaulted, bone-filled frontals, statistics and histograms for von Mises stress were calculated for the entire sampled frontal (including the bone occupying the space of the sinus), because this parameter was relevant to determining overall structural efficiency of the frontal bone.

Strain energy was a bulk measure for the entire frontal bone, so no further corrections were necessary. The value was calculated as the sum of the strain energies of all of the elements of the region of the frontal bone outlined in Fig. 2-3A (the same region used for the analysis of von Mises stress). Strain energy, rather than strain energy density, was considered appropriate because it measured the total energy stored within the frontal. Models were loaded identically (the same force vector for each loading case, regardless of model morphology), so the value allowed a direct evaluation of which models stored the most energy from the applied load within the frontal.

The 50^{th} (median) and 95^{th} percentile values were calculated for each of the above samples (except for strain energy); mean and maximum values were not determined directly, because of the occurrence of rare extreme outliers. These extreme values occurred at sharp steps in the model geometry (an occasional byproduct of the

process of generating the geometry from CT data in SolidWorks) or due to sharply shaped elements generated by the automated meshing routine. For instance, for the model with strutted sinuses under the double horn loading condition, the 95th percentile value for maximum principal strain within the body of the frontal bone was 858 N/m^2, whereas the maximum value was 24,454 N/m^2. Thus, the latter value could exert extreme leverage on the mean. Instead, interquantile means (referred to hereafter as "means," for simplicity) were calculated for all values between the 5th and 95th percentiles. All statistical calculations and histograms construction were completed in R (version 2.6, R Foundation for Statistical Computing, Vienna, Austria).

RESULTS

Validation Results

All principal strain magnitudes fell within two standard deviations of experimentally determined values, and most fell within one standard deviation (see Table 2-1). This suggests that the finite element models produced a realistic picture of strain magnitudes relative to *in vitro* loading conditions, at least at the external surfaces of the frontal, parietal, and horncores. Unfortunately, strain orientations in the models were less realistic (as commonly seen in finite element models of skulls; e.g., Metzger et al., 2005). Only two out of five sampled locations (on the left frontal and right parietal) produced angles of maximum principal strain within one standard deviation of experimental values (and the rest were greater than two standard deviations in difference). On a positive note, even the "noncomparable" angles were within at least 26 degrees or less of the average of the experimental values. Ratios of maximum principal

strain to minimum principal strain (reflecting the proportion of tensile strain to compressive strain) were quite similar across most locations. This indicated another broad level of similarity in the behavior of the computer model to *in vitro* experiments (regardless of differences in magnitude).

Differences between the experimental results and the finite element model may be due to subtle differences in shape or loading conditions between the model and experimental skulls. The material properties selected for the finite element model certainly affect results; a small alteration of the elastic modulus would close the gap of strain magnitudes from two standard deviations down to much less than one standard deviation. Application of anisotropic material properties also could bring the angles of principal strain closer to experimental observations.

Strain Energy

The results presented here and in the following sections focus on the models under the double horn and frontal loading conditions, except where indicated. As a reminder, strain energy was used as a proxy to gauge shock absorption potential for a structure. A higher magnitude of strain energy indicate more potential shock absorption.

Under the double horn loading condition (Table 2-2), the models with sinuses had the highest strain energy magnitudes within the frontal, followed by the model with unvaulted frontals (92 percent of the magnitude exhibited in the model with strutted sinuses), and models with vaulted, bone-filled frontals (69 percent of the magnitude in the model with strutted sinuses, whether the frontal bone was filled with trabecular or cortical bone). Results were dramatically different for a load applied to the frontals.

Here, the models with sinuses again had the greatest magnitudes of strain energy, but the model with vaulted, trabecular bone-filled frontals had the third rank (with 66 percent of the magnitude seen in the models with sinuses). The models with vaulted, cortical bone-filled frontals (18 percent of the magnitude for models with sinuses) and unvaulted frontals (14 percent of the magnitude) had much lower values than the other models.

Principal Strains on the Endocranial Surface

For models with vaulted frontals under double horn loading, the greatest magnitudes of principal strains (mean, median, and 95th percentile values) were seen in the models with sinuses, followed by the models with trabecular bone-filled frontals and then cortical bone-filled frontals (Tables 2-3, 2-4). The overall range of values across models typically spanned between 75 and 200 με. The model with an unvaulted frontal varied in rank relative to the other models, but typically had magnitudes less than or approximately equal to the models with sinuses.

Under a load applied to the frontal, a similar ranking of magnitudes of principal strains occurred for models with vaulted frontals (Tables 2-3, 2-4). Again, the model with an unvaulted frontal fell within the range exhibited for models with vaulted frontals (and had a smaller magnitude than the models with sinuses, except at the 95th percentile).

No major differences were found between models in the distribution patterns of strain across the bone lining the endocranial cavity (Fig. 2-4) under the double horn-loading condition. Sutural zones were under relatively high strain for both double horn and frontal loading conditions. Under the frontal loading condition, the model with an

unvaulted frontal was unique among the model geometries in the distribution of strain across the surface of the endocranial cavity (Fig. 2-4F,P). At the rostral end of the endocranial cavity, there was a zone of high principal strain magnitudes (Fig. 2-4F,P; note that this was primarily a difference in spatial distribution rather than overall magnitude; Tables 2-3, 2-4). This contrasted with the regions of lower strain immediately caudal to that zone. A very different pattern occurred in all four of the models with vaulted frontals, in which maximum principal strains were more evenly distributed across the surface of the endocranial cavity (Fig. 2-4G-J) and where greatest magnitudes of minimum principal strain were confined to the lateral edges of the region of interest (Fig. 2-4Q-T). The model with a cortical bone-filled frontal had consistently low magnitudes of strain across the endocranial region of interest for minimum principal strain, with a slight elevation of maximum principal strain at the caudal end (Fig. 2-4G,Q).

Von Mises Stress in the Frontal Bone

Von Mises stress within the external cortex of the frontal bone, exclusive of the nodes immediately lining the endocranial cavity and including the area of the sinus, was examined in order to test the hypotheses that sinuses remove "unnecessary" bone. Under the double horn loading condition (Fig. 2-5A-E), the model with unvaulted frontals and the model with cortical bone-filled, vaulted frontals showed a greater concentration of low-magnitude values than seen in the models with sinuses (Fig. 2-5A,B,D,E). A peak of low-stress elements in the model with trabecular bone corresponded to elements with material properties of trabecular bone (Fig. 2-5C). Under the frontal loading condition,

the models with solid, vaulted frontals and unvaulted frontals (Fig. 2-5F-H) all had prominent peaks of low stress elements in the frontal loading condition. Stress values were more evenly distributed in all models with sinuses (Fig. 2-5I-J).

Deformation

Overall deformation of the models was relatively consistent under loads applied to the horns. The bulk of the deformation occurred caudal to the base of the horncore, especially at the frontoparietal suture, regardless of frontal morphology. Most bony deformation occurred in the bone immediately rostral and immediately caudal to the suture, caused by the cranial vault warping outwards. Under the frontal loading condition, the models with vaulted frontals experienced little deformation of the endocranial cavity. Instead, the external cortex of the frontal exhibited the bulk of the deformation as the cortex was pushed inwards. Deformation in the model with the unvaulted frontal occurred as the bone at the front of the endocranial cavity was pushed inwards.

Results from Other Loading Conditions

Results for additional loading conditions are summarized here. Ranks of strain energy magnitude for loads applied to a single horn (regardless of direction) broadly followed those seen in the model under the double horn loading condition (Tables 2-5, 2-7). Models with sinuses always had greatest magnitude, and the model with a vaulted, cortical bone-filled frontal always had the least magnitude. The model with vaulted frontals had between 46 percent and 92 percent of the magnitude of strain energy seen in

the model with vaulted, strutted sinuses. For principal strain magnitudes in the surface of the endocranial cavity or within the external frontal cortex, the rank order of maximum, minimum or median values differed slightly in some cases, but there were few exceptions to the general patterns described above (Tables 2-6, 2-7). Generally, magnitudes of principal strain for the model with unvaulted frontals fell within the range seen for or occasionally slightly higher than (by no more than 120 με, but typically much less) seen in models with vaulted frontals.

Contrasting with the double horn loading condition, patterns of principal strain were not symmetrical across the endocranial cavity when the load was applied only to a single horn (Fig. 2-6). Strain magnitudes dropped greatly across the interfrontal suture in this case (consistent with the results of Jaslow and Biewener, 1995). Patterns of distribution were quite similar across model geometries within each loading condition.

Just as in the frontal loading condition (and the double horn loading condition, to a lesser extent), histograms of von Mises stress for the models with an unvaulted frontal and vaulted solid frontals showed prominent peaks of elements under low stress (Fig. 2-7).

DISCUSSION

Are Sinuses Shock Absorbers?

As discussed previously, sinuses or a vaulted frontal could absorb shocks to the brain by two general mechanisms: (1) dissipating the energy of impact before it reaches the endocranial cavity; and (2) directing strain (and stress) away from the bone lining the endocranial cavity. Evidence supporting such a protective function was mixed.

In this study, strain energy (a measure of energy storage within a structure) was used to test the frontal's shock absorption capacity. If sinuses (or a vaulted frontal) have a major role in storing energy, models with these structures should show elevated strain energy in the frontal relative to models without the sinuses or without vaulted frontals. This was generally true in that the models with sinuses always had the greatest magnitude of strain energy relative to other models. But a vaulted frontal did not always confer an advantage – under double horn loading in particular, models with vaulted frontals stored a much lower proportion of the strain energy within the frontal than did the model with unvaulted frontals. Thus, a sinus in combination with a vaulted frontal, rather than just a vaulted frontal, was needed to maximize the shock absorption potential of the frontal bone.

Additionally, sinuses did not reduce strains on the surface of the endocranial cavity during most loads applied to the horns relative to a model with unvaulted frontals. In nearly all cases of horn loading, the model with frontals filled with cortical bone had the lowest overall magnitudes of strains (as measured by the median values), and the model with strutted sinuses (similar in morphology to real goat skulls) had the highest magnitudes (Tables 2-3, 2-4, 2-6, 2-7). Most importantly, the overall patterns of strain distribution across the bone lining the surface of the endocranial cavity were quite similar across most models (Figs 2-4, 2-6; exceptions detailed below).

The model with trabecular bone-filled frontals generally behaved quite similarly to the models with sinuses (either strutted or unstrutted), when comparing the distribution of strains across the endocranial cavity. This was expected, in light of the fact that the elastic modulus for trabecular bone is much lower than that for cortical

bone.

The frontal loading case was the only situation in which sinuses or a vaulted frontal seemed to have a major beneficial effect on strains on the surface of the endocranial cavity or strain energy within the frontal bone, over the model with unvaulted frontals. Models with sinuses or a vaulted frontal distributed the load more evenly across the endocranial bone for loads to the frontal. The advantages of this are clear – by distributing deformation across a wide area, the risk of damage to dural sinuses or meningeal arteries (relatively delicate structures carrying blood to and from the brain) is minimized. Strains were highly concentrated at the rostral end of the endocranial cavity (beneath the point of load application) in the model with unvaulted frontals, and strain energy magnitudes were also much lower than for models with vaulted frontals (except for the model with a vaulted, cortical bone-filled frontal). Yet, frontal loading does not appear to be a particularly realistic loading condition for goats. Extensive behavioral observations on wild ibex (*Capra pyrenaica*, congeneric with the *Capra hircus* modeled here and also sharing its general frontal morphology) do not report any instances of blows applied to the frontals (Alvarez, 1990). Thus, the biological relevance of this loading condition is questionable for (although certainly important for animals with extensive frontal sinuses that do butt frontals, such as *Bison*).

In summary, sinuses (or more specifically, the bone surrounding the space of the sinuses) appeared at first glance to have shock absorbing potential under most loading conditions. This may be due to the fact that the thin walls of the sinus deform slightly during impact, creating a sort of "crumple zone," and morphologies without this thin wall (or a thin wall of cortical bone against a relatively deformable layer of trabecular

bone) do not allow this deformation. Yet, magnitudes of strain energy within the model with unvaulted frontals often approached magnitudes seen in models with sinuses, and patterns of principal strains also conflict with the idea of sinuses as shock absorbers.

The extra bone associated with sinuses or vaulted frontals seemingly would offer significant benefits for strain reduction. Why, then, don't these structures offer much greater shock absorption than seen in unvaulted frontals or a greater strain reduction in the walls of the endocranial cavity, especially when compared to dramatically different skull morphologies with unvaulted frontals? The most likely explanation is that the vaulted frontal and its sinuses are poorly placed to offer much protection from the typical dorso-ventral and rostro-caudal loads applied to the horns in life. Thus, the loads are directed away from the thickest part of the frontal, and directly into the thinner part of the braincase, where most of the deformation occurs. A biomechanically "better" design (at least in light of desired endocranial strains and deformation) would place the horns atop or in front of the vaulted frontal, instead of at the rear of this structure. Instead, the caudal placement of the horns in goats and many other bovids, along with reorientation of the basicranium and other structures, may serve to reduce torque about the foramen magnum during head-butting (Schaffer and Reed, 1972; Jaslow, 1987). The morphology of the goat skull is clearly a trade off between multiple structural considerations.

The Role of Struts

In goats, the struts within the sinuses did not appear to have a major role in absorbing shocks or distributing loads applied to the frontals. In comparing the model

with strutted sinuses to the model with unstrutted sinuses, very few differences were evident. The histogram distributions were virtually identical in most cases (Figs 2-5, 2-7). Similarly, there were no appreciable or consistent differences between the two models when considering patterns of endocranial strains (Figs 2-4, 2-6), or when considering strain energy within the frontal itself (Tables 2-2, 2-7).

Do the struts have any function, then? One possibility is that the struts are just a byproduct of sinus formation – bone that was "accidentally" left behind by osteoclasts. The midline strut separating the right and left frontal sinus (a structure that *was* included in all models) may be retained due to interactions between sutures (the interfrontal suture, in this case) and pneumatic epithelia (Farke, 2007). Another possibility is that the struts improve the overall strength of the frontal. However, given the extremely thin nature of some of these struts in *Capra*, this hypothesis appears doubtful. Additionally, many other bovids (e.g., *Alcelaphus* and *Damaliscus*) have sinuses with very few struts (Farke, 2007), with apparently little consequence. By contrast, bighorn sheep (*Ovis canadensis*), and Cape buffalo (*Syncerus caffer*) are notable for extensive strutting within their frontal sinuses (hundreds of struts, far beyond that seen in *Capra*; Schaffer and Reed, 1972; personal observation). These species, and many of their close relatives, engage in extremely vigorous head-butting. It is quite possible that the numerous struts of such taxa do play a role in structural support and shock absorption, whereas struts are less important in goats. Comparative quantitative analyses of sinus morphologies are necessary in order to determine if there is a correlation between the number of struts and behavior. Further finite element modeling may also prove useful.

Sinuses and 'Structural Efficiency'

Areas of bone that experience only low magnitude stresses are not used in load transmission or shock absorption, so such regions could be thought of as unnecessary for the structural support of the skull. Thus, an efficient structure eliminates such elements. The histograms of von Mises stress produced for these models were consistent with this hypothesis (Figs 2-5, 2-7). This was well-illustrated by models under the double horn loading condition (Fig. 2-5B-E). The model with cortical bone-filled frontals had a relatively larger peak of low-magnitude stresses (and fewer high magnitude stresses) as compared to the models with sinuses or the model with trabecular bone-filled frontals. Replacing the cortical bone in the center of the frontal with trabecular bone or a sinus eliminated this peak of elements under low stress.

Why a Vaulted Frontal?

Although "structural efficiency" and gains of shock absorption potential may explain the presence of a frontal sinus, it does little to explain why the frontal should be vaulted in the first place (when compared to other bovids, such as gazelles, that lack frontal vaulting). Certainly, as evidenced by ratios of strain energy, the vaulting does offer an advantage in shock absorption in some cases. Further study is needed to determine if this advantage is biologically meaningful or relevant on evolutionary time scales. A second possibility is that the vaulted frontal is needed as a base of support for the large horncores. The large base of support would increase the second moment of area, and hence strengthen the horns against applied loads. This is supported in part by the high proportion of frontal bone elements under low stress (Figs 2-5A,F, 2-7A,F,K) in

skulls with unvaulted frontals. This indicates that a small proportion of elements is bearing a significant portion of the load (especially considering that there is less bone volume when compared to any of the other skull morphologies). Alternatively, the enlarged frontals may increase the apparent "size" of the skull (useful for visual display). A whole host of possibilities exist, many of which are untestable with the current techniques.

CONCLUSIONS

The finite element models developed in this study highlight the usefulness of this technique for testing the effects of varying cranial morphologies on cranial function. Significantly, the analyses presented are some of the first to change one aspect of the skull while leaving the rest of the morphology otherwise identical. Most previous studies (e.g., Dumont et al., 2005; McHenry et al., 2006; Rayfield, 2005) have compared skulls of related animals with varying morphologies. Although a comparative taxonomic approach also may offer useful information (and be desirable for some questions), a clear interpretation of results may be muddied by disparate morphologies unrelated to the question at hand. Thus, digital manipulation of morphology is an often underutilized strength of finite element modeling for vertebrate skulls (e.g., Rayfield et al., 2007).

The present study finds mixed support for the frontal sinuses of the goat in protecting the skull against blows. Future work might investigate the shock-absorptive role of the keratinous sheaths of the horns. Although vaulted frontals with sinuses offer shock absorbing potential under certain loading conditions, skulls with unvaulted frontals often showed high shock absorption potential, too. Furthermore, frontal sinuses or even just a vaulted frontal bone do little to change the patterns of bone strain across

the endocranium for most loading conditions. All of these supposed “protective” structures are poorly placed for protecting the skull from most loads. Struts within the sinuses also seem to have little effect, at least for goats. Results are consistent, however, with the idea of sinuses removing “unnecessary” bone from the frontal.

Several questions remain. If vaulted frontals and frontal sinuses are so poorly placed to deal with blows to the horns, why do so many head-butting taxa have such morphologies? Are sinuses more important in taxa (such as bison) that butt frontals directly? Are these morphologies indeed correlated with head butting? What other factors lead to enlargement of the frontal bone? The static models considered here present only one proxy for investigating head-butting's effects upon the brain. How is the brain tissue itself affected during the dynamic motions of head-butting? Further experiments, modeling, and comparative anatomy may provide answers to such questions.

Figure 2-1. Schematics of models and loading conditions used in this study. (A-E) Schematics of hypothetical goat skulls in parasagittal section. (A) Unvaulted frontal (UF); (B) vaulted, cortical bone-filled frontal (SFC); (C) vaulted, trabecular bone-filled frontal (SFT); (D) vaulted frontal with unstrutted sinus (US); (E) vaulted frontal with strutted sinus (SS). The endocranial cavity (ec) and sinuses (fs) are indicated in black and trabecular bone is indicated in gray, along with the external cortex (ecx) and internal cortex (icx) of the frontal bone. Schematics of FE models in (F) dorsal and (G) left lateral views, with arrows indicating the location and direction of modeled loads for various loading cases.

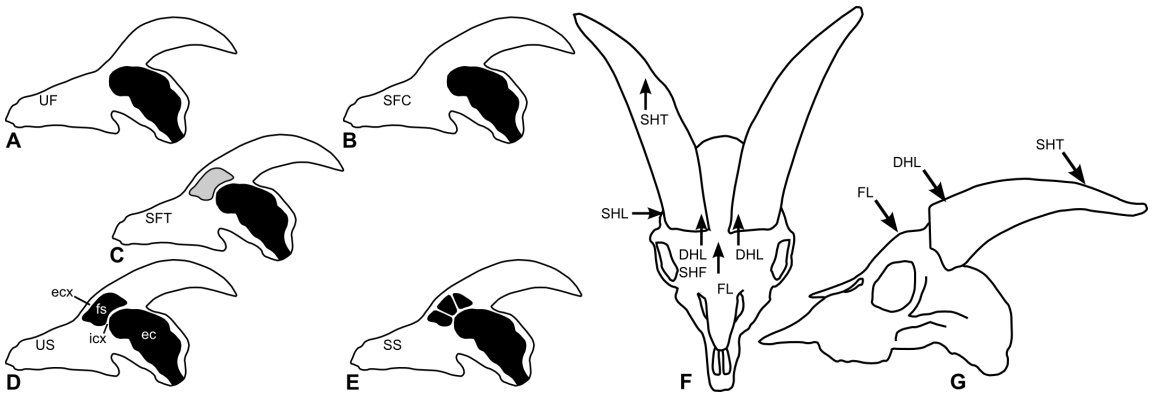
UF
A
SFC
B
SFT
C
ecx
fs
icx
ec
US
D
SS
E
SHT
SHL
DHL
SHF
DHL
FL
F
SHT
DHL
FL
G

Figure 2-2. Left lateral views of FE meshes for (A) the models with vaulted frontals (including the models with strutted and unstrutted sinuses and solid frontals) and (B) the model with unvaulted frontals. Scale bar equals 10 cm.

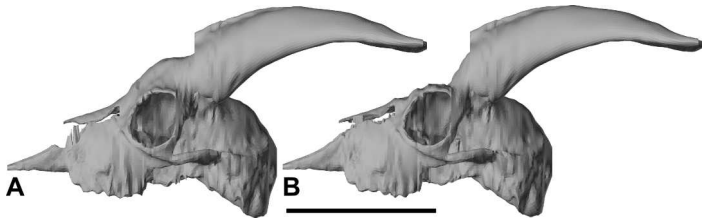
A
B

Figure 2-3. Schematic indicating the location of nodes sampled for further analysis. (A) Schematic in left lateral view, with the location at which nodes were sampled within the frontal bone indicated by the label "fri". This view also indicates the location of the plane across which the endocranium was "opened" in order to visualize principal strain patterns on the roof of the endocranial cavity. (B) View of the internal surface of the calvaria, with the dark gray area indicating the region of the endocranium that was sampled for the analyses presented in Tables 2-3 - 2-4 and 2-6 - 2-7 and illustrated in Figs 2-4 and 2-6. Abbreviations are given in the text.

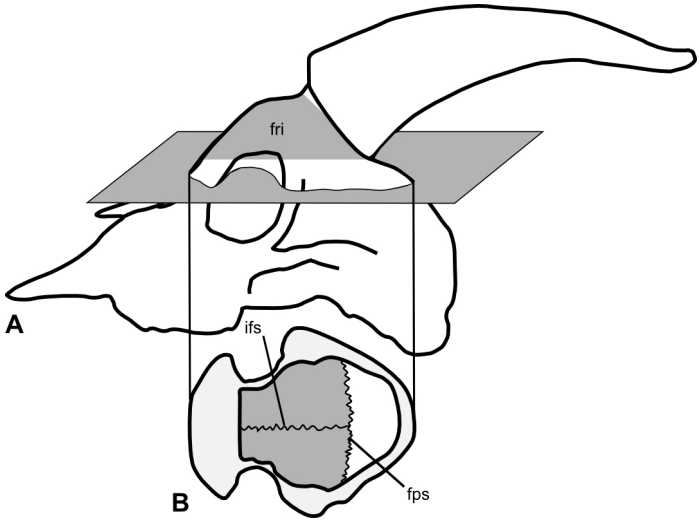
fri
A
ifs
fps
B

Figure 2-4. View of the internal surface of the rostral portion of the endocranial cavity, between the cribriform plate of the ethmoid (at the top of the images) and the frontoparietal sutures (at the bottom of the images), showing patterns of principal strains under the double horn (A-E, K-O) and frontal (F-J, P-T) loading conditions. The top two rows (A-J) show maximum principal strain; the bottom two rows show minimum principal strain (K-T). From left, the model geometries illustrated are unvaulted frontal (A, F, K, P), cortical bone-filled vaulted frontal (B, G, L, Q), trabecular bone-filled vaulted frontal (C, H, M, R), vaulted frontal with unstrutted sinus (D, I, N, S), and vaulted frontal with strutted sinus (E, J, O, T). The scale bar indicates principal strain magnitudes in microstrain.

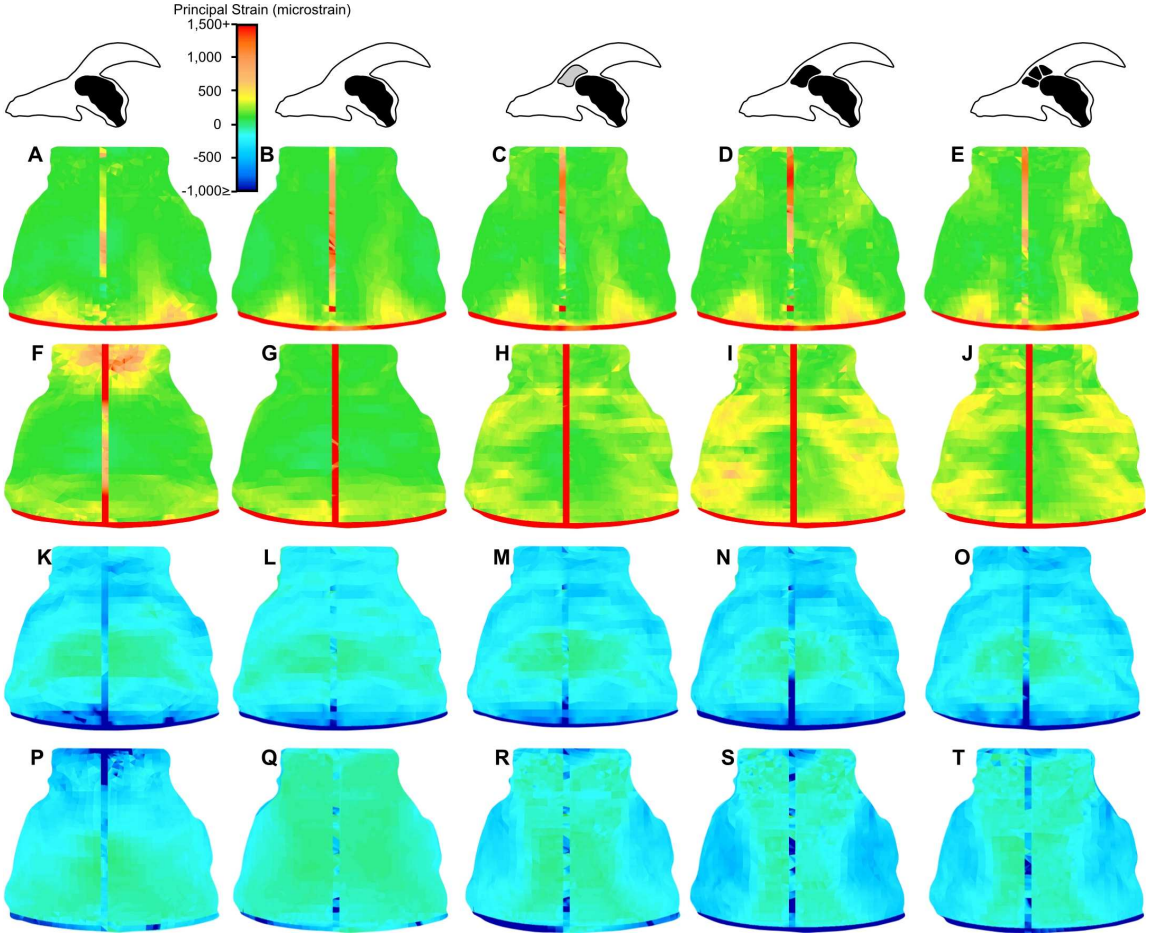
Principal Strain (microstrain)
1,500+
1,000
500
0
-500
-1,000≥
A
B
C
D
E
F
G
H
I
J
K
L
M
N
O
P
Q
R
S
T

Figure 2-5. Histograms of distributions of von Mises stress values within the frontal bone, exclusive of the surface of the endocranial cavity, for models under the double horn loading (A-E) and the frontal loading (F-J) conditions. The vertical axis indicates the number of nodes with that value (all models normalized to 100,000 nodal values). For some parts (C, F, H), the peak has been truncated in order to conserve space. Model geometries illustrated include the unvaulted frontal (A, F), vaulted cortical bone-filled frontal (B, G), vaulted trabecular bone-filled frontal (C, H), vaulted frontal with unstrutted sinus (D, I), and vaulted frontal with strutted sinus (E, J).

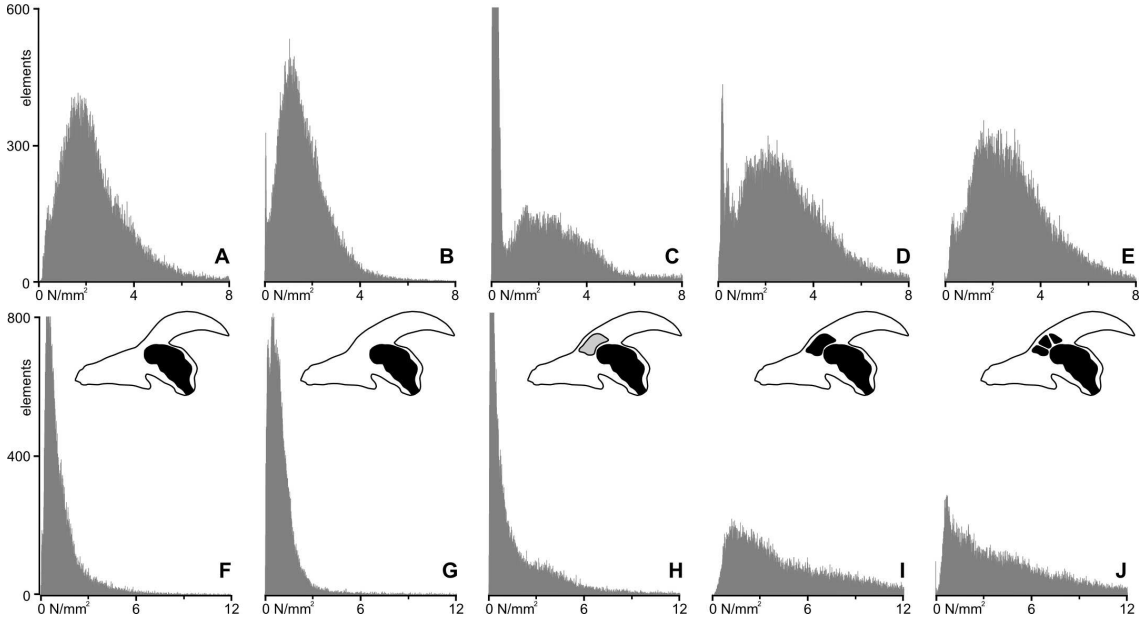
600
elements
300
0
A
B
C
D
E
0 N/mm²
4
8
800
400
F
G
H
I
J
6
12

Figure 2-6. View of the internal surface of the rostral portion of the endocranial cavity, between the cribriform plate of the ethmoid (at the top of the images) and the frontoparietal sutures (at the bottom of the images), showing patterns of principal strains. Maximum principal strains are shown in A-O and minimum principal strains are shown in P-DD. Model geometries illustrated include the unvaulted frontal (A, F, K, P, U, Z), vaulted cortical bone-filled frontal (B, G, L, Q, V, AA), vaulted trabecular bone-filled frontal (C, H, M, R, W, BB), vaulted frontal with unstrutted sinus (D, I, N, S, X, CC), and vaulted frontal with strutted sinus (E, J, O, T, Y, DD). Loading conditions include single horn front loading (A-E, P-T), single horn lateral loading (F-J, U-Y), and single horn tip loading (K-O, Z-DD). The scale bar indicates principal strain magnitudes in microstrain.

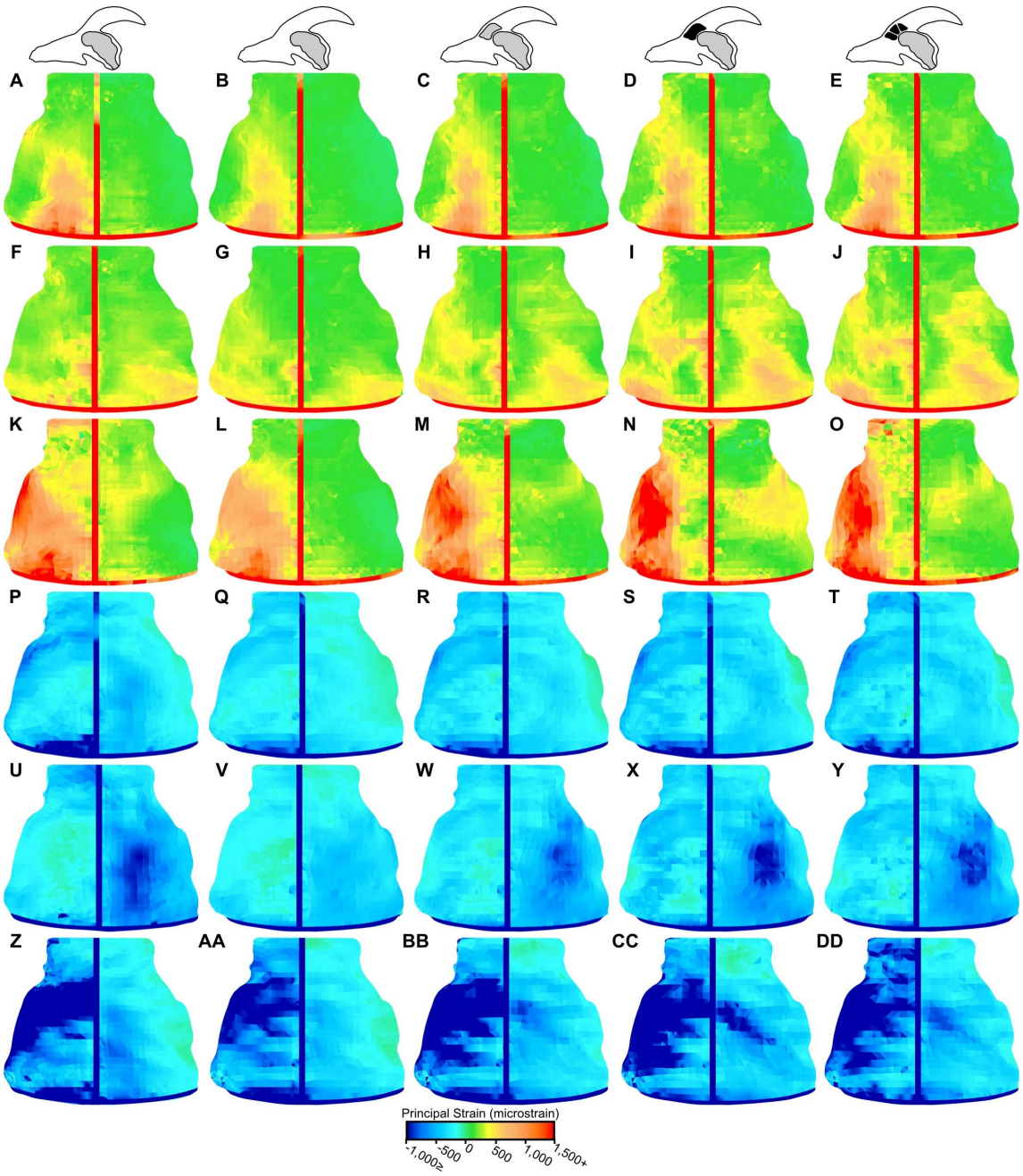
A
B
C
D
E
F
G
H
I
J
K
L
M
N
O
P
Q
R
S
T
U
V
W
X
Y
Z
AA
BB
CC
DD
Principal Strain (microstrain)
-1,000≥
-500
0
500
1,000
1,500+

Figure 2-7. Histograms of distributions of von Mises stress values within the frontal bone for models under the single horn front (A-E), single horn lateral (F-J), and single horn tip (K-O) loading conditions. The vertical axis indicates the number of nodes with that value (all models normalized to 100,000 nodal values). For some parts (B, C, H, M), the peak has been truncated in order to conserve space. Model geometries illustrated include the unvaulted frontal (A, F, K), vaulted cortical bone-filled frontal (B, G, L), vaulted trabecular bone-filled frontal (C, H, M), vaulted frontal with unstrutted sinus (D, I, N), and vaulted frontal with strutted sinus (E, J, O).

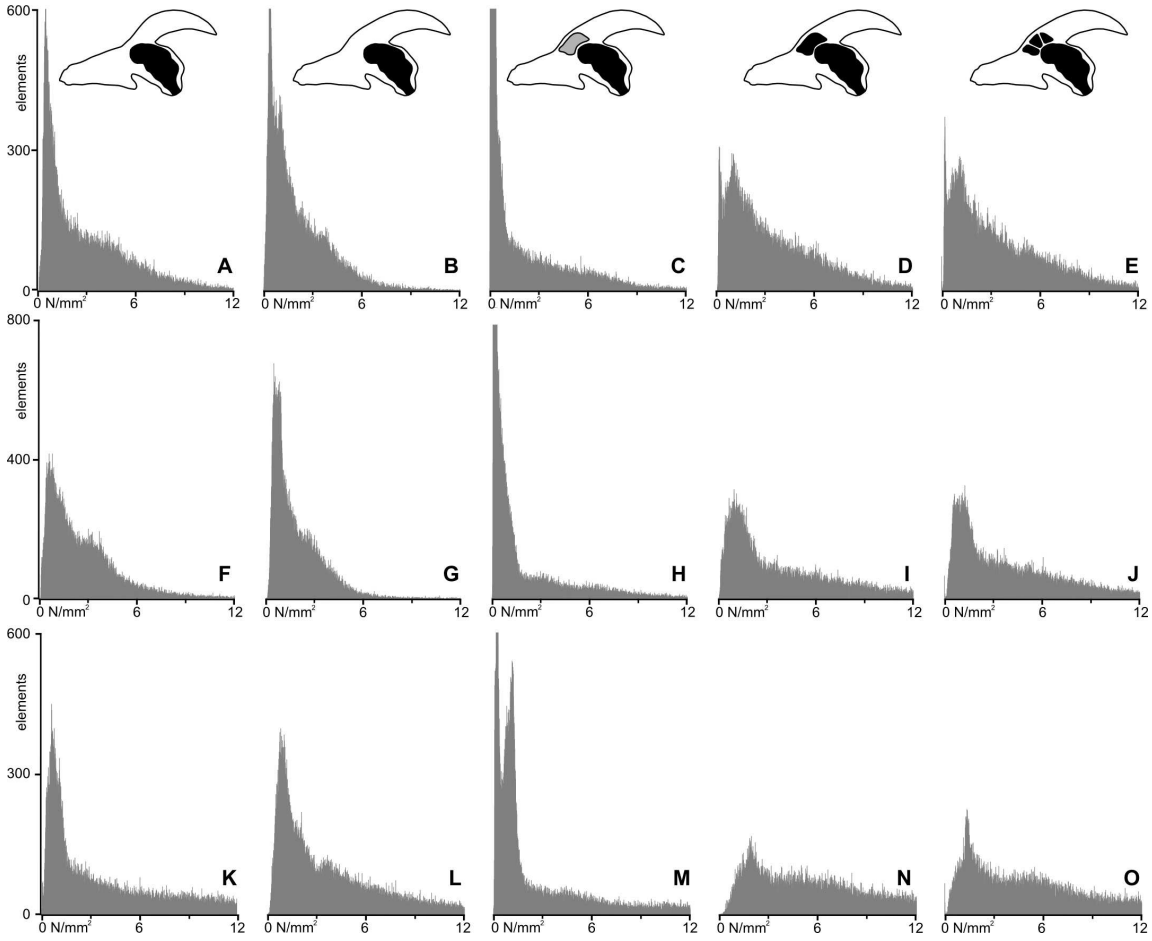
600
elements
300
0
A
B
C
D
E
0 N/mm²
6
12
800
400
F
G
H
I
J
K
L
M
N
O

Table 2-1. Results of validation analysis. *In vitro* data are taken from Jaslow and Biewener (1995). *indicates that the FE model values are within 1 standard deviation of the in vitro data; ** indicates that model values are within 2 standard deviations. All strain values are given in microstrain.

Location	Analysis	ε_1	S.D.	ε_2	S.D.	$\varepsilon_1/\varepsilon_2$	$\angle$	S.D.
Anterior horncore	FE model	344	**	-177	**	-1.94	-12º	
Anterior horncore	In vitro	721	385	-379	253	-1.90	10º	9
Posterior horncore	FE model	172	*	-668	*	-0.26	14º	
Posterior horncore	In vitro	551	314	-1985	1171	-0.28	-12º	10
Right frontal	FE model	130	*	-743	*	-0.17	-16º	
Right frontal	In vitro	348	142	-1146	376	-0.30	4º	10
Left frontal	FE model	147	*	-645	*	-0.23	9º	**
Left frontal	In vitro	384	142	-1167	378	-0.33	7º	7.5
Right parietal	FE model	9	*	-280	*	-0.03	21º	**
Right parietal	In vitro	223	107	-772	306	-0.29	18º	8.2

Table 2-2. Summary of strain energy values (in N•m) in the frontal. The number in parentheses indicates the ratio of magnitude to the magnitude for the model with strutted sinuses. All values are bulk values for the frontal bone.

	Model Geometry	
Load Case	**DHL**	**FL**
UF	7,870 (0.92)	6,630 (0.14)
SFC	5,974 (0.69)	9,047 (0.18)
SFT	5,898 (0.69)	32,387 (0.66)
US	8,215 (0.96)	48,925 (1.00)
SS	8,596 (1.00)	48,965 (1.00)

Table 2-3. Summary of maximum principal strain values (in microstrain) in the dorso-rostral portion of the surface of the endocranial cavity (rostral to the fronto-parietal suture).

		Model Geometry				
Load Case	**Percentile**	**UF**	**SFC**	**SFT**	**US**	**SS**
DHL	50%	107	94	114	122	124
FL	50%	176	121	221	273	258
DHL	95%	354	272	297	313	310
FL	95%	516	251	356	453	434
DHL	Mean	135	112	133	144	148
FL	Mean	186	127	214	268	252

Table 2-4. Summary of minimum principal strain values (in microstrain) in the dorso-rostral portion of the surface of the endocranial cavity (rostral to the fronto-parietal suture).

		Model Geometry				
Load Case	**Percentile**	**UF**	**SFC**	**SFT**	**US**	**SS**
DHL	50%	-244	-180	-236	-249	-255
FL	50%	-191	-95	-208	-234	-241
DHL	95%	-568	-396	-453	-461	-492
FL	95%	-528	-342	-441	-453	-500
DHL	Mean	-279	-203	-256	-268	-279
FL	Mean	-242	-136	-233	-258	-259

Table 2-5. Summary of strain energy values (in N•m) in the frontal. The number in parentheses indicates the ratio of magnitude to the magnitude for the model with strutted sinuses. All values are bulk values for the frontal bone.

	Model Geometry				
Load Case	**DHL**	**SHF**	**SHL**	**SHT**	**FL**
UF	7,870 (0.92)	15,974 (0.92)	10,436 (0.46)	62,458 (0.66)	6,630 (0.14)
SFC	5,974 (0.69)	11,254 (0.65)	8,709 (0.38)	56,638 (0.60)	9,047 (0.18)
SFT	5,898 (0.69)	15,530 (0.89)	18,975 (0.83)	86,733 (0.92)	32,387 (0.66)
US	8,215 (0.96)	16,177 (0.93)	24,324 (1.07)	105,686 (1.12)	48,925 (1.00)
SS	8,596 (1.00)	17,369 (1.00)	22,805 (1.00)	94,382 (1.00)	48,965 (1.00)

Table 2-6. Summary of maximum principal strain values (in microstrain) in the dorso-rostral portion of the surface of the endocranial cavity (rostral to the fronto-parietal suture).

		Model Geometry				
Load Case	**Percentile**	**UF**	**SFC**	**SFT**	**US**	**SS**
DHL	50%	107	94	114	122	124
SHF	50%	124	101	128	142	146
SHL	50%	219	179	248	255	257
SHT	50%	282	211	264	334	306
FL	50%	176	121	221	273	258
DHL	95%	354	272	297	313	310
SHF	95%	627	392	457	484	518
SHL	95%	457	424	492	581	571
SHT	95%	1285	803	1152	1299	1280
FL	95%	516	251	356	453	434
DHL	Mean	135	112	133	144	148
SHF	Mean	152	117	142	152	161
SHL	Mean	229	198	248	261	262
SHT	Mean	388	276	364	415	416
FL	Mean	186	127	214	268	252

Table 2-7. Summary of minimum principal strain values (in microstrain) in the dorso-rostral portion of the surface of the endocranial cavity (rostral to the fronto-parietal suture).

		Model Geometry				
Load Case	**Percentile**	**UF**	**SFC**	**SFT**	**US**	**SS**
DHL	50%	-244	-180	-236	-249	-255
SHF	50%	-256	-197	-260	-278	-276
SHL	50%	-334	-230	-295	-314	-319
SHT	50%	-344	-381	-397	-431	-415
FL	50%	-191	-95	-208	-234	-241
DHL	95%	-568	-396	-453	-461	-492
SHF	95%	-740	-457	-575	-614	-665
SHL	95%	-697	-458	-620	-681	-689
SHT	95%	-1588	-1154	-1615	-1647	-1593
FL	95%	-528	-342	-441	-453	-500
DHL	Mean	-279	-203	-256	-268	-279
SHF	Mean	-330	-231	-291	-303	-317
SHL	Mean	-377	-260	-336	-354	-364
SHT	Mean	-566	-499	-626	-663	-642
FL	Mean	-242	-136	-233	-258	-259

Evolution and functional morphology of the frontal sinuses in Bovidae (Mammalia: Artiodactyla), and implications for the evolution of cranial pneumaticity

ABSTRACT

The function and evolution of paranasal pneumaticity remains elusive, due in part to limited sampling and description in previous studies of vertebrate cranial morphology. Here, the frontal sinuses from 62 species of bovids (the clade of horned artiodactyls including sheep, goats, cattle, and antelope) were investigated using x-ray computed tomography. This survey revealed hitherto undescribed diversity in the morphology of this sinus, and suggests that it probably was present in the common ancestor of Bovidae. Among extant bovids, the frontal sinuses were lost or reduced to recesses at least six different times. Quantitative analyses, when accounting for phylogeny using phylogenetically independent contrasts, did not find any link between the size or complexity of the frontal sinus and head-to-head ramming behavior. Other analyses indicated that frontal sinus size was correlated most closely with the size of the frontal bone itself, rather than overall skull size or horn size. These results may be partially consistent with the hypothesis of sinuses being the result of "opportunistic pneumatization," in which sinus size was dependent on the amount of bone available for pneumatization as well as the mechanical demands placed on the skull. Additional evidence also indicates a strong phylogenetic correlation with sinus morphology, particularly as related to the presence of paranasal diverticula as well as the ability of sinuses to cross sutural boundaries.

INTRODUCTION

Cranial sinuses, air-filled chambers resulting from removal of bone by a pneumatic diverticulum, remain one of the most functionally enigmatic and debated structures within the vertebrate skull. Centuries of speculation have resulted in a host of functional hypotheses (see reviews in Blaney, 1990; Blanton and Biggs, 1968), although the current paradigm holds that the sinuses are simply functionless structures resulting from the interplay between bone resorption and deposition (e.g., Witmer, 1997; Edinger, 1950; Weidenreich, 1941). A number of descriptive studies have been published in support of one functional hypothesis or another, but quantitative and phylogenetically-informed analyses have been comparatively rare. Furthermore, most quantitative studies have focused on primates, and thus represent only a limited phylogenetic diversity. The most comprehensive quantitative analysis of sinus morphology to date, in terms of number of taxa, included only 14 closely-related species (Koppe and Nagai, 1999).

Hypotheses about sinus function are difficult to test without first obtaining information on sinus variation within and between species and higher level clades. With the exception of data for some primates, most information on variation in sinus form is purely qualitative or absent. In the present study, this situation will be addressed for the frontal sinuses of bovid mammals.

Bovidae, the clade of horned artiodactyls including cattle, sheep, goats, antelope, and their allies, is known to have extremely variable morphology of the frontal sinuses. These paranasal sinuses occupy the frontal bone and occasionally extend up into the horncores. Their presence, size, and internal complexity are extremely variable, and thus these attributes have been used as characters for cladistic analyses (e.g., Gentry, 1992;

Vrba and Schaller, 2000). Some authors (Schaffer, 1968; Schaffer and Reed, 1972) have suggested that the enlarged frontal sinuses of species such as bighorn sheep are an adaptation for head butting or ramming (common behaviors in many bovids), in order to protect the brain from impacts to the horns. Thus, the sinuses of bovids are a topic of considerable interest both from phylogenetic and functional viewpoints. However, morphological variability in the sinuses of bovids has been documented in only a handful of (mostly domesticated) taxa.

On a broader scale, the tremendous diversity of the frontal sinuses in bovids indicates their importance for understanding the evolution of paranasal pneumaticity. Numerous studies have documented the appearance or loss of certain paranasal sinuses, particularly for the maxillary sinus within cercopithecoid primates (e.g., Rae, 2008; Rae and Koppe, 2003). Yet hypotheses on factors contributing to the origin or loss of a sinus have been difficult to test, due to a lack of quantitative data as well as the limited taxonomic scope of most previous investigations.

If sinuses are primarily functionless structures, resulting as a byproduct of the removal of structurally unnecessary bone within the skull (Weidenreich, 1924; Witmer, 1997), it is predicted that a strong relationship should exist between the size of the frontal bone and the size of the frontal sinus in bovids. It is assumed that, with some variation due to the loads placed upon the skull, a relatively larger frontal (as compared to skull size) should have a greater proportion of "structurally unnecessary" bone. The relationship between the size of the frontal sinus and size of the skull and horns should be much less strong than that with the frontal bone itself. Farke (2007) found just such a relationship between frontal bone size and frontal sinus size in the hartebeest antelope,

Alcelaphus buselaphus, but, no large-scale statistical analysis has yet been undertaken. Bovidae is a clade particularly suited for testing hypotheses of sinus function and evolution for several reasons. First, bovids exhibit a wide range of adult body sizes—from 3 kg in *Madoqua* up to 1,200 kg in *Bubalus* (Silva and Downing, 1995). Second, bovids display a diversity of cranial morphologies with concomitant diversity of cranio-centric behaviors, including display, head-butting, and horn-rubbing. Finally, clade-wide phylogenies are available, allowing the use of phylogenetically-based analytical methods such as independent contrasts.

This contribution will describe frontal sinus anatomy across Bovidae, apply quantitative approaches to study the factors influencing frontal sinus morphology, and examine these data within a phylogenetic and behavioral context. It presents the largest quantitative examination of paranasal pneumaticity ever attempted.

PREVIOUS WORK ON BOVIDS

Descriptions of the frontal sinuses (and indeed, any of the cranial sinuses) of bovids are scattered sparsely throughout the literature. Most publications typically note only the presence or absence of frontal sinuses, with little or no comment on their form. With few exceptions, the frontal sinuses of bovid taxa are generally unillustrated, unquantified, and undescribed.

The morphology of the frontal sinuses has been well-described for domesticated taxa, including domesticated sheep (*Ovis aries*), goats *(Capra hircus),* and cattle (*Bos taurus*), from the early days of comparative study (Paulli, 1900b; Zuckerkandl, 1887). Heyne and Schumacher (1967) measured the volume of the cranial sinuses in a sample

of domesticated sheep, *Ovis aries*, by filling the sinuses with wax. Their study was one of only a handful to quantify sinus volume in non-primates. No significant correlation was found between the volume of the frontal sinus and various other cranial measurements.

One of the only comprehensive descriptions of frontal sinus morphology in non-domesticated bovids was undertaken by Schaffer and Reed (1972), for Caprinae, the clade including sheep and goats. Schaffer and Reed posited that enlarged frontal sinuses were associated with an "advanced" skull shape, in which the horncores were placed more caudally on the braincase relative to those animals which displayed a "primitive" skull shape. Also, it was noted that the complexity of the sinuses (i.e., the number of bony septa subdividing the sinuses) varied between taxa and sexes, and the extent of the cornual diverticulum of the frontal sinus varied similarly. Finally, Schaffer and Reed suggested that the morphology of the sinuses in caprines is an adaptation for protecting the skull from the forces of impact during fighting. Specifically, they inferred that a blow to the horns could be translated into deformation of the calvaria. This deformation results in shear within the brain tissue, with obvious deleterious effects. This built on an observation by Geist (1966), who noted that many animals engaging in head-butting or ramming behavior have a pneumatized skull roof. Alternatively, it might be suggested that thickened frontals are more important for protecting the brain, by separating the brain from forces applied to the skull, and the frontal sinuses are only coincidental. Kingdon (1982b, 1982a), who documented, at least in passing, the presence and extent of the frontal sinuses in a variety of African bovids, also hypothesized that the frontal sinuses buffer the brain and contents of the orbit from impact forces to the horns.

Jaslow (1987) analyzed a suite of measurements believed to be correlated with the mode of horn use (e.g., horn clashing vs. head butting) for sheep, goats, and their close relatives. The maximum cross-sectional area of the frontal sinus was measured in lateral view from radiographs. Jaslow found that sinus area (a proxy for total size of the sinus) was correlated neither with skull size nor calculated impact force to the horns. An alternative hypothesis was proposed, that "the size of the sinus is simply correlated with relative growth rates of the inner and outer tables of the frontal bone" (Jaslow, 1987, p. 43). Because brain size scales negatively with skull size, a thicker frontal bone was inferred to result, and thus there is more space for a frontal sinus. Another alternative hypothesis is that the thickness of the frontal bone was related to the dimensions of the horns; this was not tested. Additionally, no adjustments were made for phylogenetic effects. Although the results of Jaslow's study contradict the oft-cited hypothesis of Schaffer and Reed (1972), that increased frontal sinus size is associated with greater forces to the skull during horn use, the true meaning of the results is debatable given the shortcomings of the methodology available at the time of the study.

Frontal sinus occurrence and morphology are often used as characters for phylogenetic analyses of extant and extinct bovids. Vrba (1979) was one of the first to apply cladistic methods to bovids. In her analysis of alcelaphine taxa, she included a character for the frontal sinus, either as "absent to poorly developed" or "extensive (i.e., past supraorbital canals and into orbital rims) with a single large smooth-walled sinus which extends into basal horn core." She considered the latter condition to be autapomorphic for alcelaphines. Gentry (1992) scored the frontals as "(a) without, (b) with moderate or (c) with extensive internal sinuses." Vrba and Schaller's analysis

(2000) utilized two characters to describe frontal sinus morphology: frontal sinus extent and the presence of bony struts within the frontal sinuses. Although these analyses represent a useful first step, they do not completely describe the morphology observed within Bovidae, nor the full range of potential characters, as outlined later in this paper.

PREDICTIONS

Enlarged and/or complex frontal sinuses are associated with ramming behavior.

Previous workers (e.g., Schaffer and Reed, 1972) have suggested that taxa exhibiting ramming behavior may have enlarged or especially complex frontal sinuses to protect the brain by absorbing the energy of impact and maintaining structural integrity of the skull. If this is true, it is predicted that rammers should have sinuses that are larger, relatively more complex, and cover a greater proportion of the endocranial cavity. Ramming, rather than other bovid behaviors, such as horn clashing or stabbing, is the focus of this study, because it was assumed that this behavior would result in the highest accelerations and compressive forces applied to the skull, and hence the greatest chance of a structural manifestation in the bone of the skull and the strongest selection for enlarged or complex sinuses.

Frontal sinus volume most closely tracks the volume of the frontal bone, rather than skull size or horn size.

If sinuses are the result of "opportunistic pneumatization," the process by which osteoclasts associated with a pneumatic epithelium remove "unnecessary" bone, it is predicted that frontal sinus volume should more closely track the size of the frontal bone

itself, rather than overall skull size (Farke, 2007).

Phylogeny influences sinus morphology.

If phylogeny is more important than cranial architecture in determining the size of the sinus (or, alternatively, if phylogeny determines the architecture that in turn controls the sinus morphology), it is predicted that any correlations should be non-significant after accounting for the effects of phylogeny.

MATERIALS AND METHODS

Taxon Selection

Sixty-three of the over 120 currently recognized species of extant wild bovids were sampled in this study, in order to represent the full range of body size, skull size, cranial morphology, and taxonomic variability within this clade (Figures 3-1 and 3-2, Table 3-1). Skulls from individuals (wild shot whenever possible) were borrowed from collections at the American Museum of Natural History (AMNH, New York, New York, USA) and Yale Peabody Museum of Natural History (YPM, New Haven, Connecticut, USA). Only the skulls of adult males were considered, in order to control for effects of sexual dimorphism and ontogeny. Specimens were considered adult if the third molar was fully erupted. Samples for each species were limited to a single subspecies whenever possible. Most species were represented in the sample by two or three individuals.

Data Acquisition

All skulls were scanned on a GE Lightspeed 16 medical CT (computed tomography) scanner. Slice spacing depended on specimen size, but the main body of the skull (exclusive of the horns) typically was sampled with 400 to 600 slices. In-plane pixel resolution also varied by specimen; specimens were reconstructed at the minimal reconstruction diameter necessary to include the entire width of the skull exclusive of the unpneumatized portion of the horns. A lower resolution set of scans was reconstructed to include the entire extent of the horns along with the rest of the skull. Skulls were scanned in a coronal orientation when possible, but some skulls (e.g., those of *Syncerus caffer*) were too large to scan in this orientation and were scanned in the sagittal plane.

Volumetric Measurements

CT data were exported in DICOM format and reconstructed using 3D Slicer 2.7 (www.slicer.org). The bone surrounding the frontal sinuses was thresholded using a modified half maximum height protocol (Coleman and Colbert, 2007), with ten samples of the bone-air transition within the sinus measured on several slices from each specimen. After thresholding, the frontal sinuses were segmented by a combination of automatic and manual segmentation. Volumes of the reconstructed sinuses were measured to the nearest milliliter using the MeasureVol module in 3D Slicer 2.7 (Table 3-2). Additionally, the volume of the cornual diverticulum of the frontal sinus (the portion extending into the horncore) was measured separately from the rest of the sinus. The proximal end of the cornual diverticulum was delineated as coplanar with the burr (the prominent change of texture between the horncore and the rest of the skull) on the

external surface of the base of the core.

Although linear measurements of horn dimensions (e.g., basal length and width) may capture some aspects of horn size, they are not directly comparable across all taxa due to the range of variation in horn morphology. Thus, horn volume was used to represent horn size. The volume of the keratinous horn sheath also was defined, following a similar thresholding and segmentation protocol, and the volume of the horncore was estimated as the volume enclosed inside the hollow portion of the sheath. All volumetric measurements were converted to linear variables (in millimeters) by taking the cube roots of the original volumes.

Linear Cranial Measurements

A suite of external cranial measurements for each specimen was captured using digital calipers, to within .1 mm (see Table 3-2). Additional measurements related to the coverage of the endocranial cavity by the sinuses and horns were measured from the CT data (also see Table 3-2). All linear measurements were taken in millimeters.

Cranial size, instead of body mass, was the scaling variable used in this study, because skull size and not body mass was of most interest. As defined here, cranial size is the geometric mean of various cranial variables for each specimen. The variables selected focus on the dimensions of the tooth rows, calvaria, and splanchnocranium, excluding measurements on the horns and frontal. The horns and frontal were excluded from this geometric mean because they are the areas of focus in this study (following the recommendations of Coleman, 2008), and because of their extreme variability in size relative to the rest of the skull across taxa. Geometric means were used, rather than a

standard measurement such as skull length, because they should represent a better measure of overall size when examining a sample with variability in cranial proportions. For similar reasons, frontal size was described using a geometric mean of the frontal maximum length, width, and thickness.

Calculation of Sinus Complexity

The complexity, or number of struts subdividing the chamber of the frontal sinus, was calculated in a manner analogous to approaches used for quantifying the architecture of trabecular bone (e.g., Hildebrand et al., 1999; Hildebrand and Rüegsegger, 1997). Farke (2007) found that a direct measurement of strut number did not accurately represent the density of struts within the sinus, especially for specimens that have a relatively low density of struts (as seen in many bovids). Instead, he found that a sinus complexity index (SCI) provided a better estimate. This index is calculated as strut spacing divided by the cube root of sinus volume. Strut spacing (trabecular spacing, or Tb.S., of other authors) measures the average diameter of multiple spheres fitted into the empty spaces between struts of the sinus. A sinus with relatively large spacing between struts would have a relatively high SCI, and thus be considered non-complex. A sinus with relatively small spacing between struts would have a relatively low SCI, and be considered relatively complex. Strut spacing was calculated in the program CT Analyzer (version 1.7, SkyScan, Aartselaar, Belgium). Further details of this methodology are provided elsewhere (Farke, 2007).

Behavioral Data

Data on the presence or absence of ramming (head-butting) behavior were taken from the matrix published by Caro et al. (2003). Although data on the frequency of each behavior would be desirable, it is not available for most species.

Phylogenies and Character Mapping

Two alternative, but largely similar, phylogenies were used for calculations of contrasts and for mapping the evolution of sinus morphology (Figures 3-1 and 3-2). The first was based on a supertree published by Fernández and Vrba (2005), which was trimmed to include only the taxa used in this analysis. The second supertree was assembled based on a combined molecular and morphological analysis published by Gatesy and Arctander (2000), with additional data from other studies (Matthee and Davis, 2001; Rebholz and Harley, 1999; Schreiber et al., 1999; van Vuuren and Robinson, 2001; Willows-Munro et al., 2005; Lalueza-Fox et al., 2005; Buntjer et al., 2002; Pidancier et al., 2006). The latter tree was used in order to reflect the most recent phylogenetic hypotheses concerning bovids (i.e., those published in the past ten years), whereas the former relied on over thirty years worth of trees obtained through cladistic and non-cladistic methodology. Two trees were used instead of one in order to see how robust the results were in the face of competing phylogenies. Branch lengths were assigned using the method of Nee (cited in Purvis, 1995), which in the present dataset was found to best meet the assumption of no significant relationship between the contrast and the standard deviation (Garland et al., 1992). Branch lengths provided by Fernández and Vrba (2005) were initially used for that tree, but it was found that the data violated the aforementioned assumption.

Character history was traced on both trees in Mesquite (version 2.1) using parsimony ancestral state reconstruction.

Statistical Tests and Hypotheses

The influence of ramming behavior on SCI, relative sinus volume, and coverage of the endocranium was compared between taxa divided into ramming and non-ramming categories. For raw data, the two categories were compared using a Mann-Whitney U test. In order to account for the effects of phylogeny, data were analyzed using the BRUNCH algorithm in the program CAIC (version 2.6.9), with a sign test.

Because of the strong correlation between frontal size and skull size ($r>0.90$ in all data sets, regardless of phylogeny), partial correlation coefficients were calculated in order to better examine the relationships between skull size, frontal size, and frontal sinus size. Additionally, the relationship between sinus morphology and cranial morphology (skull size, frontal size, and horn size) was examined using reduced major axis regression (RMA). The RMA method was chosen in order to account for the fact that the variables were both measured with error. Each variable was tested for normality using an Anderson-Darling test, and the data were log-transformed to the base 10 in order to more closely approximate a normal distribution. Independent contrasts for this analysis were calculated in the PDAP module (version 1.11) of Mesquite. Statistical analyses were completed in R (version 2.6.2), using the SMATR module (version 2.1). A value of 1 was added to the sinus volumes, so that logarithms could be calculated for taxa with a sinus volume of 0. Plots of contrasts versus standard deviation did not uncover a significant relationship ($p>0.05$ for all variables). Additionally, a sign test was

used to determine if SCI was significantly associated with skull, horn, sinus, or frontal size.

Taxa were analyzed in two batches: one including all taxa and a second including only taxa with sinuses. This was done because regardless of the amount of bone available for pneumatization, no pneumatization should occur if a pneumatic recess from the nasal cavity is not present (outlined in greater detail in the discussion section). Thus, mixing taxa with and without sinuses could prevent a clear interpretation of the relationship between sinus size and the size of other cranial features. Therefore, it was desirable to exclude taxa without sinuses for some of the analyses.

Recognizing Sinuses

Previous authors have pointed out the difficulty in distinguishing between a paranasal sinus and a paranasal recess (e.g., Rossie, 2006). A recess is simply a concavity of the nasal cavity, not associated with active removal of bone. By contrast, the tissues associated with a paranasal sinus actively remove trabecular bone, thus resulting in an air-filled cavity placed between two layers of cortical bone. Identification of a sinus is comparatively easy for very large sinuses, but distinguishing between a sinus and a recess becomes more difficult for small sinuses or large recesses. Ideally, ontogenetic series or soft tissue histological sections would be needed in order to make this distinction. Unfortunately, such data either don't exist or were not practical to collect for this study. Sinuses were recognized as such in practice if they visibly and markedly impinged on the trabecular bone between the internal and external cortices of the frontal, and if they could be traced for at least a short extent between the two layers (i.e., the

space was separated from the main nasal cavity by a bony wall for at least a short distance; see Fig. 3-3C; Rae, 2008). Recesses were simply impressed into the internal layer of the cortex, perhaps creating a small depression, but not actually pneumatizing trabecular bone (see Fig. 3-3E).

QUANTITATIVE RESULTS

Behavior and Sinus Morphology

Species values for sinus volumes and sinus complexity are listed in Table 3-1. Results of statistical comparisons are given in detail in Table 3-3. Prior to accounting for the effects of phylogeny in the sample including only taxa with sinuses, ramming and non-ramming taxa differed in relative sinus volume and SCI, but not coverage of the endocranium. Regardless of which tree topology was used, none of these variables differed significantly between the two groups when accounting for phylogeny using the BRUNCH algorithm.

Prior to accounting for the effects of phylogeny in the entire sample (with and without sinuses), ramming and non-ramming taxa differed only in cornual sinus size. This correlation held only for PICs based on the composite tree (although the data violated the assumption that the nodal value versus the contrast slope was not significant; several attempts at branch length transformation or data transformation were unsuccessful in resolving this problem).

Sinus Morphology and Skull Morphology

For the sample including all taxa, the partial correlation coefficient of frontal

sinus size and frontal size was significant (i.e., the 95 percent confidence interval excluded 0) only for the raw sample. When calculated from phylogenetically independent contrasts, this correlation did not differ significantly from zero (Table 3-4).

Partial correlations between frontal sinus size and skull size or horn size, regardless of phylogeny, were never significant. For the sample including only taxa with sinuses, the partial correlation coefficients of sinus size and frontal size were always significantly different from 0, but never so for sinus size and skull size, regardless of phylogeny.

All regressions of frontal sinus volume onto frontal size, skull size, and horn size were significant, regardless of the scope of sample or phylogeny (Table 3-5). Of the three latter variables, frontal sinus volume was mostly highly correlated with frontal size, but never outside the 95 percent confidence interval for the correlation coefficients for the other variables (even after accounting for phylogenetic effects). Frontal sinus volume displays strong positive allometry relative to all of the other variables, and the 95 percent confidence intervals of the slopes for the PICs data all overlap.

A sign test on phylogenetically independent contrasts for SCI against sinus, skull, and frontal size indicates a significant relationship between these variables ($P<0.03$ in all cases, regardless of phylogeny). No such relationship exists between SCI and horn size, however ($P>0.18$ for both phylogenies).

MORPHOLOGY OF THE FRONTAL SINUSES

Frontal sinuses display considerable variation among bovid species in size relative to the skull, extent within the frontal bone, pneumatization of other cranial

bones, and extent within the horncore. In the following section, the frontal sinuses of bovids are described clade-by-clade. Where necessary, details for certain species are noted. The general classication scheme follows that of Gatesy and Arctander (2000), which is relatively consistent with clades recovered by most recent phylogenetic analyses and the tree topologies used in the present paper. Species of historically problematic affiliation (*Aepyceros melampus*, *Neotragus* spp., *Oreotragus oreotragus*, and *Pantholops hodgsonii*) are discussed within their own sections.

Terminology follows that previously proposed by Farke (2007). The midline strut is that formed between the left and right frontal sinuses, coinciding with the interfrontal suture. The supraorbital strut is that running from the bony supraorbital canal, usually towards the medial wall of the sinus. Finally, the cornual diverticulum of the frontal sinus is that portion extending into the bony horncore.

Alcelaphinae

The frontal sinuses of *Alcelaphus buselaphus* and *Sigmoceros lichtensteinii* were described recently in detail elsewhere (Farke, 2007), so they will not be considered further here (except as necessary for comparison). In general, the sinuses in *Damaliscus lunatus* (Fig. 3-4A,B) and *Connochaetes taurinus* are broadly similar to those of *A. buselaphus* and *S. lichtensteinii*. In all of these taxa, the strut containing the supraorbital canal joins the medial wall of the frontal sinus (along the midline strut) well rostral to the base of the horncore. In *D. lunatus*, the sinus extends up to the frontoparietal suture, but the parietal has no involvement in the sinus (contrasting with the condition in *A. buselaphus* and *S. lichtensteinii*, in which the parietal is involved, even if covered by a

veneer of frontal bone; Farke, 2007). In *C. taurinus* specimens in which the sutures are open (e.g., YPM unnumbered), the sinus clearly invades at least part of the parietal. In all of the taxa, the very base of the horncore is invaded by the sinus, but the cornual diverticulum is not extensive. Other struts within the sinus are relatively sparse, although they do occur consistently.

Antilopinae

Morphology of the sinus is quite variable within this clade, ranging from absent to extensive, so the sinuses are described by species or groups of species.

Antidorcas marsupialis.—This species has the largest and most extensive frontal sinuses of any antilopine, extending into the base of the horncores and to the very edge of the orbital margin (Fig. 3-4C,D). The supraorbital strut displays the typical bovid condition, extending from the caudal edge of the supraorbital canal and then trending caudomedially. It terminates on the wall of the midline strut just rostral to the base of the horn and its associated cornual diverticulum. Other struts are relatively widely spaced. The frontal sinus in this species is contained completely within the frontal bone.

Antilope cervicapra, Eudorcas thomsonii, Gazella subgutturosa, Litocranius walleri, Madoqua kirkii, Nanger granti, and Saiga tatarica.—The frontal sinuses in these taxa are relatively small and restricted rostrally, terminating rostral to the supraorbital canal in most cases (Fig. 3-3A,B). In *Saiga tatarica,* and one specimen of *E. thomsonii* (YPM 4042), the sinus extended up to the lateral portion of the supraorbital canal, within the supraorbital pits. Regardless, the canal is never surrounded completely by the sinuses as seen in some other bovids (e.g., *Alcelaphus buselaphus*). The sinus on

each side is restricted to the lateral portion of the frontal bone and separated from the lacrimal sinus by a thin lamina of bone. In nearly all individuals examined of these species, the sinus was completely unstrutted. The only exceptions were specimens of *A. cervicapra* (AMNH 54486) and *N. granti* (YPM 14579; Fig. 3-3B), which displayed a single strut at the middle of each sinus. In one specimen each of *L. walleri* (AMNH 81170) and *N. granti* (YPM 3865), only one of the two sinuses was strutted. One specimen of *M. kirkii* (YPM 3985) exhibited strong asymmetry in the shape and extent of the frontal sinuses. The left frontal sinus was quite well developed, extending to the lateral portion of the supraorbital canal, whereas the right frontal sinus was poorly developed and terminated rostral to its ipsilateral supraorbital canal. Similar, although less extreme, asymmetry in the frontal sinuses was observed in the other *M. kirkii* specimens, and two specimens of *N. granti* (YPM 3990 and 4039).

Other antelopines.—*Ourebia ourebi* lacks frontal sinuses as well as a distinct frontal recess on the internal surface of the frontal bone. *Gazella dorcas*, *Procapra gutturosa*, and *Raphicerus campestris* (Fig. 3-3E, G) also lack frontal sinuses but do have a distinct frontal recess in nearly all cases (although no distinct recess was observed in *P. gutturosa* specimen AMNH 85235). In some specimens the recess arguably borders on a true sinus in its degree of depression into the ventral surface of the frontal.

Boselaphini

Both extant boselaphines possess extensive frontal sinuses.

Boselaphus tragocamelus.—The frontal sinuses extend through the entire length and breadth of the frontal, up into the bases of the horncores and out to the lateral

margins of the orbital rim. The sinuses are extensively strutted throughout. The supraorbital strut heads nearly directly caudally, and can be traced only to the plane including the rostral ends of the horncores. The interfrontal suture is well-fused in all of the specimens examined here, and the midline strut has an undulating appearance in cross-section, perhaps due to extensive remodeling. However, the left and right frontal sinuses do not communicate at any point.

Tetracerus quadricornis.—The frontal sinuses of this taxon (Fig. 3-5C,D) are similar to those of *Boselaphus tragocamelus* in most morphological aspects, except as follows. The supraorbital strut is more distinct (unlike in *B. tragocamelus*), and trends caudomedially from the caudal end of the supraorbital canal towards the midline strut. The bases of both the rostral pair of horncores as well as the caudal pair of horncores are pneumatized. The left and right sinuses are well-separated along the caudal third of their length (without the thin midline strut), concomitant with the lateral placement of the horncores. The portion of the sinus in the base of the caudal horncores is unstrutted in all of the specimens studied here.

Bovini

All bovines have relatively large frontal sinuses, differing somewhat in their extent and complexity.

Bison bison.—The frontal sinuses (Fig. 3-5E-F) pneumatize the entire frontal bone in this taxon as well as the entire parietal. The sinus extends immediately up to the suture between the squamous temporal and the parietal. The occipital receives a pneumatic diverticulum from the parietal portion of the frontal sinus in some specimens,

although most of this bone remains unpneumatized in ontogenetically younger specimens (YPM 3405). In the oldest specimens (YPM 3406, as indicated by the degree of sutural fusion), the frontal sinus extends up to the foramen magnum and the base of the paroccipital process, but not into the occipital condyles. The midline strut may be heavily remodeled and indistinct caudally. This condition apparently is associated with fusion of the interfrontal suture. No distinct supraorbital strut exists beyond the immediate area of the supraorbital canal. The sinus extends to the distal tip of the horncores in the specimens examined here and is heavily strutted throughout.

Bos javanicus.—The extent and morphology of the sinuses in this taxon are quite similar to those seen in *Bison bison*. The occipital sutures were not fused completely in the specimen that was studied here (AMNH 113755, although it did have complete eruption of the third molar), indicating that the supraoccipital, but not the exoccipital portion of the occipital bone, was pneumatized in this individual.

Bubalus.—*Bubalus depressicornis* (Fig. 3-5A-B) and *B. mindorensis* both have frontal sinuses of variable extent, possibly depending on age. The supraorbital canal is entirely enclosed by bone, but the supraorbital strut is not traceable for a great distance before it merges with a number of other, unrelated struts. Variability was seen in the pneumatization of the parietal and the extent of pneumatization of the horncore in *B. mindorensis*. In one specimen (AMNH 40046), only the basal portion of the horncore was pneumatized, and the sinus did not cross the frontoparietal suture into the parietal. In the other specimen (AMNH 99339), over two-thirds of the length of the horncore and the rostralmost portion of the parietal were pneumatized. The frontoparietal suture was somewhat less distinct in the latter specimen, as visualized through CT and on the

original specimen. In *B. depressicornis*, the sinus extended right up to the suture (Fig. 3-5B), but it did not pneumatize the parietal in either of the specimens observed here.

Syncerus caffer.—The frontal sinuses are quite extensive in this taxon, pneumatizing the parietal and potentially the occipital (sutures were nearly completely fused on the specimen examined here, so it cannot be determined for certain). The basal third of the horncores are pneumatized. The midline strut remains sharply defined along most of its length, up until the former location of the frontoparietal suture. A distinct, enclosed supraorbital canal is present, but a discrete supraorbital strut cannot be identified due to the abundance of other struts within the sinus.

Caprinae

All taxa within this clade possess a frontal sinus. Tremendous variation in the morphology of this structure necessitates a taxon-by-taxon description.

Budorcas taxicolor.—The entire extent of the frontal is pneumatized, up to the basal portion of the horncores (Fig. 3-5G-H). The sinus crosses the frontoparietal suture (which is still patent in both specimens examined here) to pneumatize the proximal portion of the parietal bone, but not the occipital bone. Numerous struts subdivide the sinus, and, consequently, a distinct supraorbital strut cannot be traced away from the supraorbital canal.

Capra.—The morphology of the frontal sinus is relatively uniform across the four species of *Capra* that were studied here (*C. aegagrus*, *C. falconeri*, C. *nubiana*, and *C. sibirica*). The entire extent of the frontal is pneumatized, nearly up to the frontoparietal suture. A discrete supraorbital strut is not always present, although when it

can be traced it trends medially for a short distance before joining the medial wall of the sinus. In *C. falconeri*, there is no distinct supraorbital strut. The horncores are pneumatized for their entire length in the oldest individuals (e.g., *C. sibirica*, AMNH 54906; Fig. 3-6A-B), although in younger adults, only the basal half is pneumatized (e.g., *C. sibirica*, AMNH 57317). The sinuses are strutted, but less prominently than seen in *Ovis*.

Capricornis sumatraensis and Naemorhedus goral.—These two species (which are closely related) are similar in most details of the sinus, and are described together. The frontal is pneumatized along nearly its entire extent (not quite to the frontoparietal suture; Fig. 3-6E-F), with no pneumatization of the parietal, but only the basal third of the horncore is pneumatized. A supraorbital strut extends caudal to the supraorbital canal for a short distance, ending on the medial wall of the sinus rostral to the horncore. Relatively thin struts occur throughout the rest of the sinus.

Hemitragus hylocrius.—The entire frontal is pneumatized in this taxon, up to (but not across) the frontoparietal suture and through at least three-quarters of the length of the horncore. The sinus is well-strutted, as a consequence of which a discrete supraorbital strut cannot be traced beyond the supraorbital canal.

Oreamnos americana.—The frontal sinus fills the body of the frontal bone, but ends at the bases of the horncores well before reaching the frontoparietal suture (Fig. 3-6G-H). Only the base of the horncores is pneumatized. The strutting within the sinus is relatively infrequent, particularly as compared to *Ovis.* A distinct supraorbital strut can be traced running from the caudal edge of the supraorbital canal back to the medial surface of the sinus, terminating approximately at the base of the horncore.

Ovibos moschatus.—The frontals are pneumatized entirely in this taxon, but only the very base of the horncore contains a sinus. In one specimen (AMNH 80095), both halves of the parietal and the portion of the occipital bordering the frontoparietal suture (unilaterally) are pneumatized. In the other (AMNH 29949), the parietal is not pneumatized. One major difference between the specimens appears to be the degree of fusion between the sutures – in AMNH 80095, the sutures are much more fused in this region than in AMNH 29949. A distinct supraorbital canal is present within the sinus, but no supraorbital strut is discernible due to the high number of other struts.

Ovis.—An extensive frontal sinus occupies the entire frontal bone in both species of *Ovis* examined here (*O. ammon* and *O. canadensis*), with some differences between the two. A cornual diverticulum extends to the very tip in *O. canadensis* (Fig. 3-6C-D) but only along half to three quarters of the length of the horncore in *O. ammon.* The sinuses are subdivided into a large number of small chambers by numerous bony struts. Some of these struts contain neurovascular canals that communicate with foramina on the external surface of the horncore and dorsum of the skull. The origin of most of these canals cannot be traced, due to structural discontinuities. The midline strut is well defined, although it is not perfectly flat in the sagittal plane. A "wavy" surface is effected by occasional pneumatic diverticula excavated into the side of the septum. The supraorbital canal is fully contained within a strut, but the strut is not traceable for any great distance due to the numerous septa within the sinus.

The parietal is pneumatized by the frontal sinus in all individuals of *Ovis canadensis* examined here (but not in *O. ammon*), and the sinus clearly crosses sutural boundaries even in specimens in which the sutures are not completely ossified (e.g.,

YPM 183, *O. canadensis*). In YPM 183, the one specimen of *O. canadensis* for which the sutures could be traced reasonably well on CT scans, the frontal portion of the sinus is separated from the parietal portion of the sinus by a strut that seems to conform to the contours of the frontoparietal suture. On one side in this specimen, the strut is completely continuous (i.e., there is no communication between the frontal and parietal portions of the sinus). On the other side, there is a wide communication between these portions of the sinus. Thus, it appears that the pneumatic diverticulum that pneumatized the parietal entered only on one side. In other specimens, the pneumatic diverticulum appears to be bilateral. By comparison with external landmarks on the skulls with fused sutures, it is apparent that the parietal is pneumatized in all specimens considered here. The sinus does not invade the occipital. Unlike the condition seen in the frontal, no midline strut divides the parietal portion of the frontal sinus into left and right halves (perhaps corresponding to the early fusion of the parietal in bovids). In tracing the structural continuity of the parietal portion, it has no relation to any pneumatic diverticula from the middle ear.

Pseudois nayaur.—The sinuses of *Pseudois nayaur* are similar in morphology and extent to those seen in *Ovis*. Although sutures are fused on the specimens examined here, topological relationships indicate that the parietal is pneumatized. The horncore is pneumatized along approximately three-fourths of its length.

Rupicapra rupicapra.—In this species, the sinuses occupy the frontal bone exclusively, extending slightly behind the base of the horncore but not up to the frontoparietal suture. The base of the horncore is pneumatized, also. The sinuses are relatively undivided, but no supraorbital strut is associated with the supraorbital canal in

either specimen examined here.

Cephalophinae

This clade (including *Cephalophus*, *Philantomba*, and *Sylvicapra*) is remarkable in its consistent lack of frontal sinuses or apparently even a frontal recess (no well-developed depression is evident at any point on the ventral surface of the frontals; Fig. 3-3D). This morphology is invariant, whether in the smallest (e.g., *P. maxwelli*) or largest (*C. sylvicultor*) species examined here.

Hippotraginae

The sinuses of *Hippotragus niger* and *H. equinus* are quite similar in all respects, so they are described together. Based on examination of a skull of *H. niger* in which the sutures are not completely fused (AMNH 83606; Fig. 3-7A-B), the sinus is contained exclusively within the frontal bone. Caudally, it extends up to the frontoparietal suture and into the base of the horncore. The strut coincident with the supraorbital canal continues for some distance caudomedially past the termination of the canal, ending at the medial base of the horncore but not entering the horncore itself. The sinus is subdivided by bony struts, although the chamber leading into the base of the horncore is relatively open.

In *Oryx gazella*, the extent of the frontal sinus is similar to that seen in *Hippotragus*. The sinuses of *O. gazella* have comparatively more struts, and the supraorbital strut does not continue caudally beyond the end of the supraorbital canal.

Reduncinae

None of the specimens of *Pelea capreolus* displayed frontal sinuses, although one (AMNH 80920) displayed a clear frontal recess. The occurrence of a frontal sinus is variable within other reduncines, but the sinus is small even when present.

Kobus.—In the single specimen of *Kobus leche* examined here (YPM 14577), the frontal sinuses are present and strongly asymmetrical. The left sinus extends to the rostral end of the supraorbital canal, and the right sinus extends around the lateral margin of the canal, nearly to the caudal end of the orbit. Similar asymmetry was seen in a specimen of *K. ellipsyprymnus* (YPM 3484; Fig. 3-7C-D). In other specimens of *K. ellipsiprymnus*, the sinuses extend to the lateral margin of the supraorbital canal. In *K. kob*, the sinuses extend to the rostral ends of the supraorbital canals. The sinuses in all of these species typically have a few struts within them. *K. vardonii* lacks a frontal sinus but does have a frontal recess.

Redunca.—The presence of a sinus was highly variable within both species examined, although at least a recess was present in all cases. Two out of three specimens of *Redunca arundinum* had frontal sinuses, and one out of three specimens of *R. fulvorufula* had them. In *R. arundinum*, the sinuses are extremely small, unstrutted and restricted to the lateral- and rostralmost portions of the frontal bone. The single specimen of *R. fulvorufula* with a sinus had similar morphology, but the sinus was developed only on one side.

Tragelaphini

Of the three taxa examined from this clade, only one (*Taurotragus oryx*; Fig.

3-8A-B) displayed evidence of a true frontal sinus. In this taxon, the frontal sinus is extremely restricted in size and extent. It originates from a large recess in the caudo-dorsal portion of the nasal cavity, is bordered by a distinct bony wall, and excavates a small volume of trabecular bone. The sinus does not extend to even the rostral border of the supraorbital canal and is situated medial to the parasagittal plane containing the canal. The right and left sinuses do not meet along the midline. *Tragelaphus strepsiceros* shows a small recess in the equivalent region, but *T. scriptus* lacks even this feature.

Tragelaphines are unique in the presence of a separate "cornual sinus" within the very base of the horncores, extending only as far forward as the caudal margin of the orbits. All individuals of all three taxa examined for this study preserved this feature, which was observed both in CT scans and in sectioned horns. This sinus is not connected to the nasal cavities, and thus was almost certainly not pneumatic in origin. Instead, it may have been filled with fat or marrow in life. Rostrally, the cavities are lined by relatively smooth bone, but the bone surface becomes trabecular towards the caudal end. This contrasts sharply with the completely smooth bone lining of the pneumatic frontal sinus in other bovids.

Taxa of Uncertain Affinity

Aepyceros melampus.—In this taxon (Fig. 3-8C-D), the frontal sinus is contained strictly within the frontal and extends only into the most basal portion of the horncores. The cornual diverticulum has a peaked distal end, with struts running parallel to the long axis of the horncore. In all specimens examined, the supraorbital strut runs from the caudal border of the supraorbital canal to the very base of the cornual diverticulum.

Unlike the condition in other bovids, the strut trends caudolaterally to terminate on the lateral wall of the sinus, rather than caudomedially to terminate on the midline strut. The dorsal and caudodorsal margins of the orbit are pneumatized by the frontal sinus. The main body of the sinus is subdivided into numerous chambers by a series of bony struts.

Neotragus spp.—Neither of the species of *Neotragus* examined here (*N. batesi* and *N. moschatus*) exhibited frontal sinuses, or even a prominent recess along the internal surface of the frontal bone.

Oreotragus oreotragus.—All specimens of this taxon possessed a small, unstrutted frontal sinus, which is restricted to the frontal bone well rostral to the supraorbital canal (Fig. 3-8E-F). The frontal sinus is immediately adjacent to the lacrimal sinus and separated from it by a thin lamina of bone.

Pantholops hodgsonii.—The frontal sinuses extend into the bases of the horncores, but not to the frontoparietal suture (Fig. 3-8G-H). Relatively few struts occur within the sinus, and the most prominent is a supraorbital strut that extends from the supraorbital canal medially and caudally, back to the very base of the horncore.

EVOLUTION OF THE FRONTAL SINUSES

As optimized on the two phylogenetic hypotheses used here, the presence of a frontal sinus was the ancestral condition for Bovidae. Depending on the tree topology, frontal sinuses were lost or reduced to a recess independently at least six times (Figures 3-1 and 3-2). These instances were within tragelaphines, reduncines (*Kobus* and *Pelea*), antilopines (*Raphicerus* and *Procapra*), *Neotragus*, and cephalophines.

DISCUSSION

Sinuses and Behavior

After accounting for phylogenetic effects, the analyses do not support the claim that enlarged frontal sinuses or bony struts within the sinuses are an adaptation for head-butting. Although use of the BRUNCH algorithm greatly reduces the effective sample size (down to 12 data points, in some cases), and hence the power of the statistical tests, *P*-values are well above 0.05 in all cases (Table 3-3). So, it is probably not simply a case of significance masked by small sample size. Instead, the analysis indicated that variables such as relative frontal sinus size or complexity, as well as ramming behavior, have a strong phylogenetic component. In the raw sample, much of the pattern may be driven by caprines (sheep, goats, and their allies) and bovines (cattle and their allies). As a whole, these two groups have the lowest SCI (indicating greatest complexity) and the largest relative sinus volumes of any of the groups considered (even though not all members butt heads). Furthermore, frontal sinuses are completely absent in cephalophines, which do butt heads (Estes, 1991). Outside of Bovidae, frontal sinuses are absent in a number of taxa which also use cranial appendages (horns or antlers) for vigorous combat behavior. Examination of CT scans of various cervids (*Alces alces*, *Odocoileus virginianus*) and *Antilocapra americana* (pers. obs.) indicates that the frontal sinuses are extremely restricted or absent in these taxa. Paulli (1900b) presented further data in agreement with this observation. Although these taxa do not necessarily butt heads, such observations do indicate that enlarged frontal sinuses are not absolutely necessary to protect the brain from forces applied to the horns or antlers.

The statistical results indicating no link between sinus morphology and head

butting behavior are consistent with results from finite element modeling of a goat skull under loads to the horns (see Dissertation Chapter 2). These simulations varied the morphology of a goat skull, including filling the frontal sinuses with bone or removing the sinuses and altering the overall morphology of the frontal bone, and examined the effects on shock absorption (as measured through strain energy density and principal strains). In general, it was found that the frontal sinuses only had a minor role in protecting the endocranial cavity and its contents from blows to the horns. Thus, the results of the comparative analysis are consistent with these modeling results.

Sinuses and Cranial Morphology

The results of the partial correlations are at least partially consistent with the "opportunistic pneumatization" hypothesis, which implies that paranasal sinuses are primarily functionless, resulting from the removal of structurally unnecessary bone (although because correlation and causation cannot be separated here, the results are not definitive). This hypothesis predicts that among frontal size, horn size, and skull size, sinus size logically should be most correlated with the first. Here, it was found that frontal sinus size was only significantly correlated with frontal size (but not with skull or horn size), when considering partial correlations. No previous interspecific comparisons have so directly examined the relationship between a sinus and the bone it occupies. Thus, no previously published analysis is completely comparable with the present study, either in terms of variables considered, number of species, or types of statistical analyses.

Koppe and Nagai (1999) published regressions for maxillary sinus volume on

skull length for hominoid primates (six species) and *Macaca* (eight species). The two clades were analyzed separately, specimen data points rather than species means were used to calculate the regressions, and no confidence intervals are given, so it cannot be compared with the results presented here. A similar analysis of anthropoid primates (five genera) found an isometric relationship between maxillary sinus volume and facial volume or geometric mean, strong allometry relative to basicranial length, and similar correlation coefficients between all of those variables with maxillary sinus volume (Rae and Koppe, 2000). The isometric relationship between facial volume and maxillary sinus volume is interesting, but it cannot be compared directly to the strongly allometric relationship between frontal sinus size and frontal size for two reasons. First, "facial volume" included not only the size of the maxilla, but also the size of the nasal cavity. Nasal cavity size previously has been recognized to have an effect on maxillary sinus size in some taxa (Rae et al., 2003; Shea, 1977). An alternative analysis might subtract out the size of the nasal cavity from facial volume in order to examine more directly the relationship between sinus volume and maxilla volume. A more important departure preventing direct comparison between the present study and the previous ones is the use of specimen data points, rather than species means. Particularly because of the unequal sample numbers between genera (between 6 and 11) and the lack of information on the number of species represented in each genus of the sample, it is difficult to determine if the pattern of isometry is genuine or driven by the choice of specimens.

The inference of "opportunistic pneumatization" also is consistent with finite element modeling of goat skulls mentioned above (see Chapter 2). In these models, it was found that the bone removed by the sinuses was generally unloaded.

The statistical analysis also indicates that a complex sinus is associated with large skull size (and its accompanying large frontal and frontal sinuses). Regardless of behavior, a large sinus would need more struts within it in order to maintain structural integrity.

It is important to note that significant correlations between frontal sinus size and frontal size were not found for the samples including all taxa (with and without sinuses) and accounting for phylogeny. This may indicate phylogenetic influence upon the presence or absence of a recess capable of pneumatizing the frontal, as well as a detrimental statistical effect of including a large number of taxa with sinus volumes of "0". Such a phylogenetic effect may counter the conclusion that pneumatization proceeds only within areas of unloaded bone (delimited in turn by the location, strength and frequency of loads placed on the skull).

The strong positive allometry of sinus size relative to skull size (and frontal size) also is consistent with the role of the sinuses as weight-reducing structures in larger members of this group. It is expected that weight reduction would be a much more important factor at large body sizes; thus, large bovids should have proportionately larger sinuses. However, it does not yet explain the ultimate factors behind the origin of skeletal pneumaticity.

Prerequisites for Sinuses

Witmer (1997) emphasized the necessity of air-filled epithelial diverticula for the formation of a sinus. However, he also noted that many taxa possess extracapsular epithelial diverticula but lack cranial sinuses (e.g., *Varanus*). No explanation has been

offered for this yet. Based on the results of the present study, two conditions are hypothesized as prerequisites for paranasal sinus development: 1) presence of an extracapsular epithelial diverticulum of the nasal cavity; and 2) presence of bone that can be pneumatized by the diverticulum without structural compromise of the skull. If either condition is not met, a bony sinus will not develop. It is important to note here that bone development and sinus development proceed simultaneously (Koppe et al., 2000). A similar hypothesis, although not explicitly stated, was implied by Rossie (2006), who also noted the importance of close spatial proximity between the diverticulum and the bone to be pneumatized.

The best support for the above hypothesis lies in groups that fulfill only one of the two above criteria, and thus lack sinuses. Among bovids, Cephalophinae perhaps represent one such clade. Here, the frontal bone is quite thick in some taxa, but there is no paranasal diverticulum associated with this bone, so the frontal is not pneumatized (Fig. 3-3D). Further examples are found in cercopithecoid primates, the Old World monkeys. All extant members of this clade, except for *Macaca*, lack maxillary sinuses. Rae et al. (2002) demonstrated that the loss of maxillary sinuses occurred near the origin of this clade. However, they could offer no explanation for why this group lost them. Rae and Koppe proposed that the development of sinuses was "suppressed" in cercopithecoids, but there is currently no good evidence of the precise mechanism by which this suppression would occur (Rae, 2008; Rae and Koppe, 2003). Detailed comparative histological studies of cercopithecoid nasal cavities are necessary to evaluate this hypothesis.

Other examples exist among bovids (e.g., *Gazella* and *Procapra*) in which there

is apparently a diverticulum, but no pneumatization of the trabecular bone within the frontal (criterion one but not two). Rossie (2006) noted a similar lack of bone in the platyrrhine primates *Cacajao* and *Saimiri*, which both lack maxillary sinuses but possess maxillary recesses. The condition in these genera contrasts with that of closely related platyrrhines, which have a relatively deeper maxilla with more trabecular bone, more potential space for a sinus to occupy, and thus a sinus.

Sinus Evolution in Bovids

Although molecular phylogenies have played an increased role in reconstructing bovid evolution, identification of valid morphological characters is necessary for placing most extinct taxa within a phylogenetic framework. The present study indicates that some characters are probably more useful than others and also identifies previously unrecognized characters of potential importance. For instance, the presence or frequency of bony struts within the sinus has been used as a character (Vrba and Schaller, 2000). The data here found that although some taxa have many struts within their sinuses and others have very few, there is no discrete cut-off between the two states. The most common character relating to the frontal sinuses concerns relative size. Many workers have simply specified whether the sinuses are large or small (e.g., Gentry, 1992). The approach taken by Vrba (1979), specifying the extent of the sinus relative to the supraorbital canal, seems to be most tractable in light of the data presented here. For a single character related to sinus extent, the most logical states would include 0) complete absence of frontal recess; 1) frontal recess present but no sinus; 2) frontal sinus present but does not extend caudal to supraorbital canal; and 3) frontal sinus present and extends

caudal to supraorbital canal. An additional, hitherto undocumented character, concerns pneumatization of the parietal and occipital bones by the frontal sinus. This character appears to be age-dependent in at least some taxa (only appearing in relatively old individuals), but it nonetheless may be quite informative.

The data are partially consistent with opportunistic pneumatization as an influence upon sinus morphology in bovids. Yet, some aspects of the sinuses, such as sinus complexity or the absence of a frontal recess, apparently are correlated with phylogeny. Is this a direct link, in which a gene or set of genes directly influences sinus morphology? Or is it an indirect link, in which frontal architecture is determined genetically and the sinus morphology follows? The present study cannot address this. Further work is needed, for instance, on the factors that cause some taxa to completely lose a pneumatic recess associated with the frontal bone, or the factors that lead to pneumatization of the parietal and occipital. Is this development under genetic control or epigenetic control? More developmental and histological studies (along the lines of Hönig et al., 2002; Smith et al., 2005) are needed in order to answer this question.

Rather than indicating multiple origins of the frontal sinuses within Bovidae, the present data for bovids strongly suggest multiple losses instead. The factors behind these losses are uncertain, but two possibilities exist. As suggested for the maxillary sinuses of *Cacajao* (in which the lateral recess of the nasal cavity is well separated from trabecular bone within the maxilla; Rossie, 2006), issues of spatial packing may have led to a loss of the frontal sinus in some bovids. In cephalophines, the nasal cavity is narrowed drastically internally, in association with an extremely enlarged preorbital gland on the external aspect of the skull. The spatial constraints imposed by this condition may have

led to the loss of a recess capable of pneumatizing the frontal bone or the positioning of such a recess well away from the frontal. Alternatively, an extreme reduction in overall skull size may also explain the loss of a sinus, if sufficient bone is not then available for pneumatization (as proposed for bats; Moore, 1981). If the ancestor of a clade went through a "dwarf" phase that resulted in the loss of a sinus, even descendants that became larger would also lack this sinus. However, some taxa with very small body size and skull size still exhibit frontal sinuses (such as *Madoqua*, with a maximum adult body mass of 5.5 kg, one of the smallest within Bovidae; Silva and Downing, 1995). Paleontological data are needed for other clades in order to support or refute this hypothesis.

Sinuses and Sutures

Farke (2007) documented apparent but not direct pneumatization of the parietal by the frontal sinus in hartebeest (*Alcelaphus* and *Sigmoceros*). In these taxa, a thin "veneer" of frontal bone was adhered to the parietal portion of the sinus, in at least some individuals. With age, this veneer was lost. Regardless of whether or not a thin portion of the frontal remained against the parietal, the internal morphology of the parietal was affected by the pneumatization. Based on this evidence, it was suggested that cranial sutures may have a role in restricting or influencing pneumatization.

The results of the present study are mixed in this regard. In at least some taxa, the frontal sinus extends up to the frontoparietal suture, and even conforms to its morphology in part, but does not cross the suture. The interfrontal suture also appears to be maintained relatively consistently across taxa, even when well-fused.

In other taxa (e.g., *Bos javanicus*), the sinus crosses multiple patent sutures to pneumatize the parietal and occasionally even the occipital bone. Thus, sutures may have a role in restricting the expansion of sinuses, but some taxa appear to circumvent this supposed restriction. Again, genetic factors, rather than the purely structural factors indicated by "opportunistic pneumatization" may be more important here. Clearly, additional work is needed on the interactions between the pneumatic epithelium of the sinus and surrounding tissues. Why do the sutures apparently restrict sinus growth in some taxa but not others?

Sinuses and Asymmetry

Strong asymmetry was observed between the left and right sinuses in several taxa (e.g., Fig. 3-7D). This manifested as marked development on one side and minimal development or absence on the other. This is not attributable to asymmetry in the frontal bone itself, as the frontals in these individuals seem to be symmetrical in cross-section. Neither can it be attributed to pathology such as atelectasis, as no abnormal bone morphology is visible in the CT scans (Koppe et al., 2006). This marked asymmetry only occurred in taxa with relatively small sinuses. Unfortunately, the sample size at present is too small to determine if this can be classified as fluctuating asymmetry or some other process.

Ontogenetic Factors

Although documentation of ontogenetic variation was not a central aim of this study, some differences were observed among adult specimens that may be due to

ontogenetic effects. This is due to the fact that adult status was judged by molar eruption, and sinus expansion apparently continued after the eruption of the third molar in some taxa. In particular, this was noted in *Capra sibiricus* and *Bison bison*. By contrast, relatively little change in frontal sinus extent occurs within *Alcelaphus buselaphus* and *Sigmoceros lichtensteinii* after eruption of the third molar (Farke, 2007). Additional research, using large specimen samples, is needed in order to determine just how much change, if any, occurs in sinus morphology during adulthood (or throughout ontogeny in general).

CONCLUSIONS

This study presents the broadest and most comprehensive quantitative analysis of sinus morphology ever attempted. It was found that the frontal sinuses are closely tied to the size of the frontal bone, but less tied to overall cranial size or horn size. This is perhaps consistent with the "opportunistic pneumatization" hypothesis, yet phylogenetic effects are also implicated in some cases. Thus, opportunistic pneumatization, or a purely structural role for the sinuses, cannot be the only factor determining the morphology of the sinuses. Furthermore, the data integrating behavior and relative sinus volume or complexity do not strongly support the role of the frontal sinuses as shock absorbers within Bovidae.

Within Bovidae, the sinuses hold clear promise as characters for morphological phylogenetic analysis. On a broader level, bovids offer an ideal opportunity for further study of the mechanisms behind cranial pneumatization. What genetic or epigenetic factors lead to sinus loss? Or is sinus loss purely a structural phenomenon? Are all

portions of the sinus within bovids derived from homologous nasal recesses? Ontogenetic, and particularly soft tissue-based studies, are needed to clarify these issues.

Although the two-part criteria outlined above offer a framework in which to understand the range of morphologies observed in paranasal sinuses, they do not necessarily provide a prediction of the selective pressures (if any) leading to paranasal recesses and sinuses. In the end, bovids provide a case study in multiple losses of a sinus, and an evolutionary test of sinus origins still remains. Much work is necessary in this regard, especially including fossil taxa.

Figure 3-1. Phylogeny of Bovidae based on a supertree published by Fernández and Vrba (2005). Taxa with sinuses are indicated in black on the phylogeny, and taxa without are in white. States between nodes were inferred using ancestral parsimony state reconstruction. Asterisks indicate taxa that engage in ramming behavior (data from Caro et al. 2003).


Tragelaphini
Bovini
Boselaphini
Antilopinae
Caprinae
Hippotraginae
Alcelaphinae
Cephalophinae
Reduncinae
Taurotragus oryx*
Tragelaphus strepsiceros
Tragelaphus scriptus
Bison bison*
Bos javanicus
Syncerus caffer*
Bubalus depressicornis*
Bubalus mindorensis*
Tetracerus quadricornis*
Boselaphus tragocamelus
Raphicerus campestris
Ourebia ourebi*
Madoqua kirkii
Procapra gutturosa
Saiga tatarica*
Litocranius walleri
Antidorcas marsupialis
Antilope cervicapra
Eudorcas thomsonii*
Nanger granti*
Gazella dorcas
Gazella subgutturosa
Aepyceros melampus*
Pantholops hodgsonii*
Rupicapra rupicapra
Oreamnos americanus
Ovibos moschatus*
Capricornis sumatraensis
Naemorhedus goral*
Budorcas taxicolor*
Ovis canadensis*
Ovis ammon*
Pseudois nayaur*
Hemitragus hylocrius*
Capra aegagrus*
Capra falconeri*
Capra nubiana*
Capra sibirica*
Hippotragus equinus
Hippotragus niger
Oryx gazella
Connochaetes taurinus*
Damaliscus lunatus*
Alcelaphus buselaphus*
Sigmoceros lichtensteinii
Cephalophus dorsalis*
Cephalophus silvicultor*
Cephalophus niger*
Cephalophus natalensis*
Cephalophus nigrifrons*
Cephalophus leucogaster*
Philantomba maxwellii*
Sylvicapra grimmia
Pelea capreolus
Redunca fulvorufula
Redunca arundinum*
Kobus leche
Kobus ellipsiprymnus*
Kobus vardoni*
Kobus kob*
Oreotragus oreotragus
Neotragus moschatus
Neotragus batesi

Figure 3-2. Phylogeny of Bovidae based on a composite supertree constructed as indicated in the text. Taxa with sinuses are indicated in black on the phylogeny, and taxa without are in white. States between nodes were inferred using ancestral parsimony state reconstruction. Asterisks indicate taxa that engage in ramming behavior (data from Caro et al. 2003).

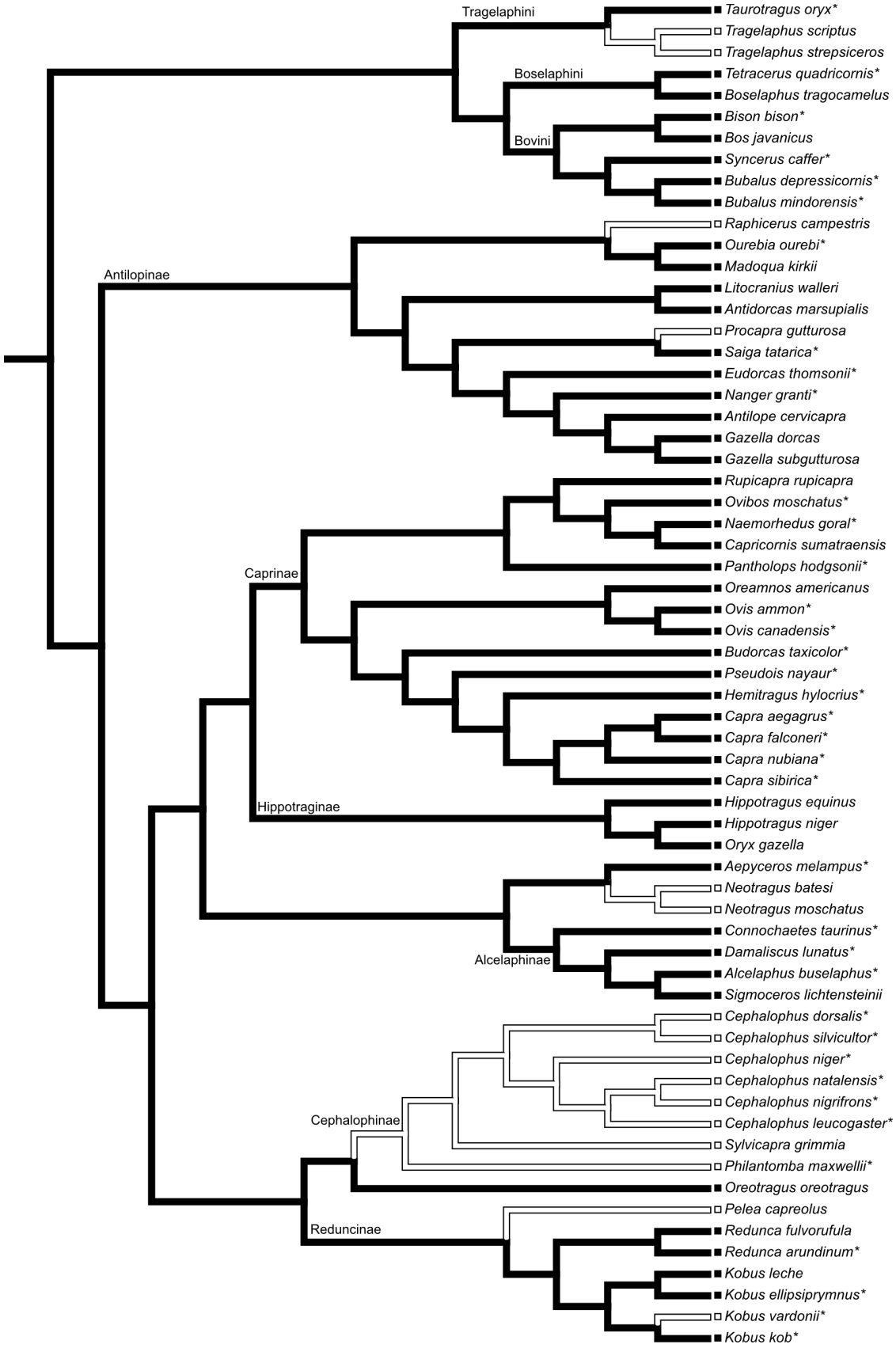
Tragelaphini
Taurotragus oryx*
Tragelaphus scriptus
Tragelaphus strepsiceros
Boselaphini
Tetracerus quadricornis*
Boselaphus tragocamelus
Bovini
Bison bison*
Bos javanicus
Syncerus caffer*
Bubalus depressicornis*
Bubalus mindorensis*
Antilopinae
Raphicerus campestris
Ourebia ourebi*
Madoqua kirkii
Litocranius walleri
Antidorcas marsupialis
Procapra gutturosa
Saiga tatarica*
Eudorcas thomsonii*
Nanger granti*
Antilope cervicapra
Gazella dorcas
Gazella subgutturosa
Rupicapra rupicapra
Ovibos moschatus*
Naemorhedus goral*
Capricornis sumatraensis
Caprinae
Pantholops hodgsonii*
Oreamnos americanus
Ovis ammon*
Ovis canadensis*
Budorcas taxicolor*
Pseudois nayaur*
Hemitragus hylocrius*
Capra aegagrus*
Capra falconeri*
Capra nubiana*
Capra sibirica*
Hippotraginae
Hippotragus equinus
Hippotragus niger
Oryx gazella
Aepyceros melampus*
Neotragus batesi
Neotragus moschatus
Connochaetes taurinus*
Alcelaphinae
Damaliscus lunatus*
Alcelaphus buselaphus*
Sigmoceros lichtensteinii
Cephalophus dorsalis*
Cephalophus silvicultor*
Cephalophus niger*
Cephalophus natalensis*
Cephalophus nigrifrons*
Cephalophinae
Cephalophus leucogaster*
Sylvicapra grimmia
Philantomba maxwellii*
Oreotragus oreotragus
Pelea capreolus
Reduncinae
Redunca fulvorufula
Redunca arundinum*
Kobus leche
Kobus ellipsiprymnus*
Kobus vardonii*
Kobus kob*

Figure 3-3. Digital reconstructions and CT slices of bovid skulls, illustrating frontal sinuses and related anatomy, in *Nanger granti* (A-C; YPM 14579), *Cephalophus leucogaster* (D, F; AMNH 52802), and *Raphicerus campestris* (E, G; YPM 5113). In C, note the distinct frontal sinus that invades the trabecular bone, is bounded by cortical bone on all sides, and distinctly separated from the olfactory turbinals below. This contrasts with the condition in E, in which a distinct recess above the olfactory turbinals is pressed into the frontal bone, but does not actually invade the trabecular bone. In D, no recess exists at all, and the space beneath the frontals is entirely occupied by turbinals. The dashed lines in A, F, and G indicate the approximate positions of the coronal CT slices in C, D, and E, respectively. The boxed areas in A and B indicate the region of the skull that has been rendered partially transparent in order to visualize the anatomy of the frontal sinuses. Abbreviations: fr, frontal recess; fs, frontal sinus; ls, lacrimal sinus; ms, maxillary sinus; o, orbit. Scale bars equal 5 cm.

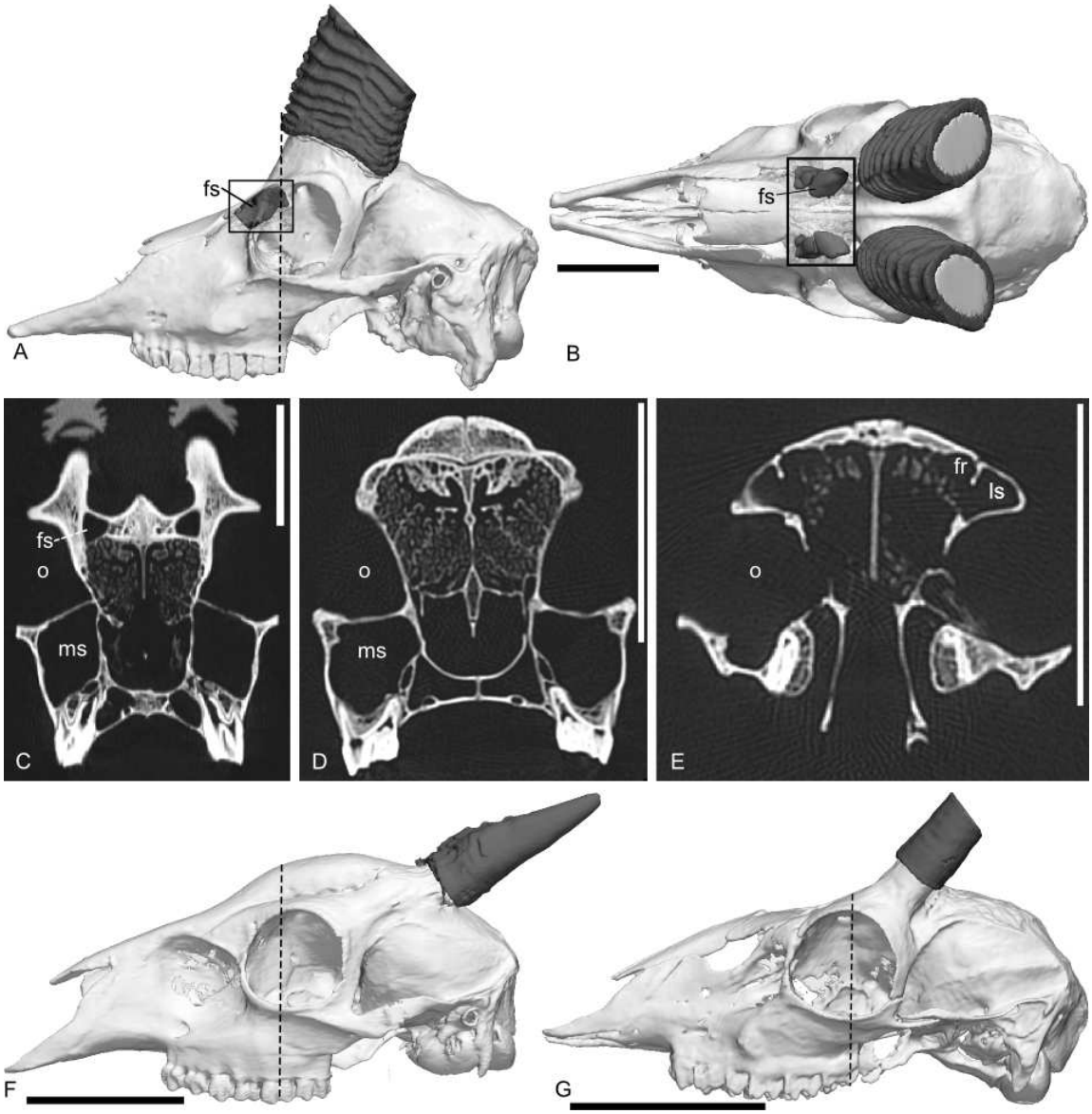
fs
A
fs
B
fs
o
ms
C
o
ms
D
fr
ls
o
E
F
G

Figure 3-4. Digital reconstructions from CT scan data of the skulls of *Damaliscus lunatus* (A-B; YPM 3971) and *Antidorcas marsupialis* (C-D; AMNH 233055), illustrating frontal sinuses and related anatomy. Skulls are shown in lateral (A, C) and dorsal (B, D) views. The boxed areas indicate the region of the skull that has been rendered partially transparent in order to visualize the anatomy of the frontal sinuses. The horns have been truncated in C and D. Abbreviations: cd, cornual diverticulum; fs, frontal sinus; ms, midline strut; ss, supraorbital strut. Scale bars equal 5 cm.

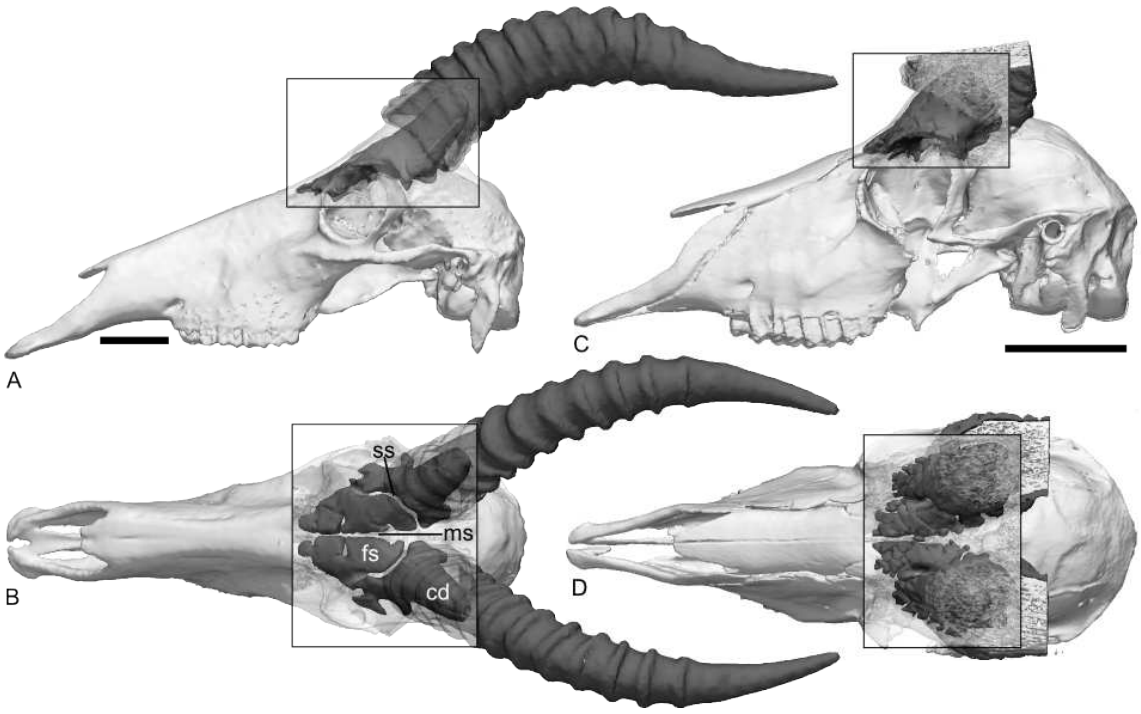
A
B
C
D
ss
ms
fs
cd

Figure 3-5. Digital reconstructions from CT scan data of the skulls of *Bubalus depressicornis* (A-B; AMNH 152684)*, Tetracerus quadricornis* (C-D; YPM 1509)*, Bison bison* (E-F; YPM 3406)*,* and *Budorcas taxicolor* (G-H; AMNH 110476), illustrating frontal sinuses and related anatomy. Skulls are shown in lateral (A, C, E, G) and dorsal (B, D, F, H) views. The boxed areas indicate the region of the skull that has been rendered partially transparent in order to visualize the anatomy of the frontal sinuses. The horns have been truncated in E-H. Scale bars equal 5 cm.

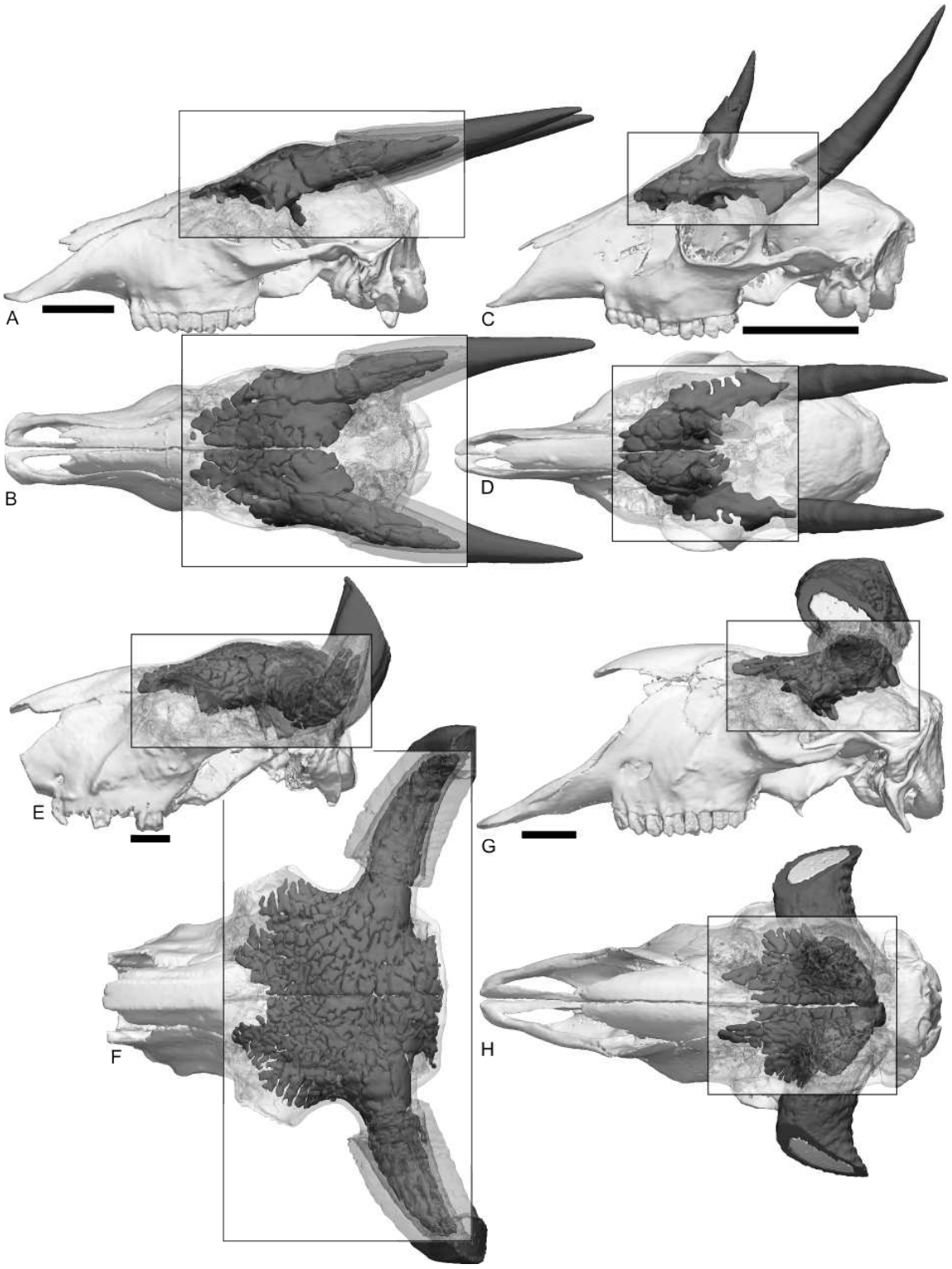
A
C
B
D
E
G
F
H

Figure 3-6. Digital reconstructions from CT scan data of the skulls of *Capra sibirica* (A-B; AMNH 54906)*, Ovis canadensis* (C-D; YPM 1489)*, Nemorhaedus goral* (E-F; AMNH 43033)*,* and *Oreamnos americanus* (G-H; AMNH 128105), illustrating frontal sinuses and related anatomy. Skulls are shown in lateral (A, C, E, G) and dorsal (B, D, F, H) views. The boxed areas indicate the region of the skull that has been rendered partially transparent in order to visualize the anatomy of the frontal sinuses. The horn sheaths have not been rendered in A-D and G-H. Scale bars equal 5 cm.

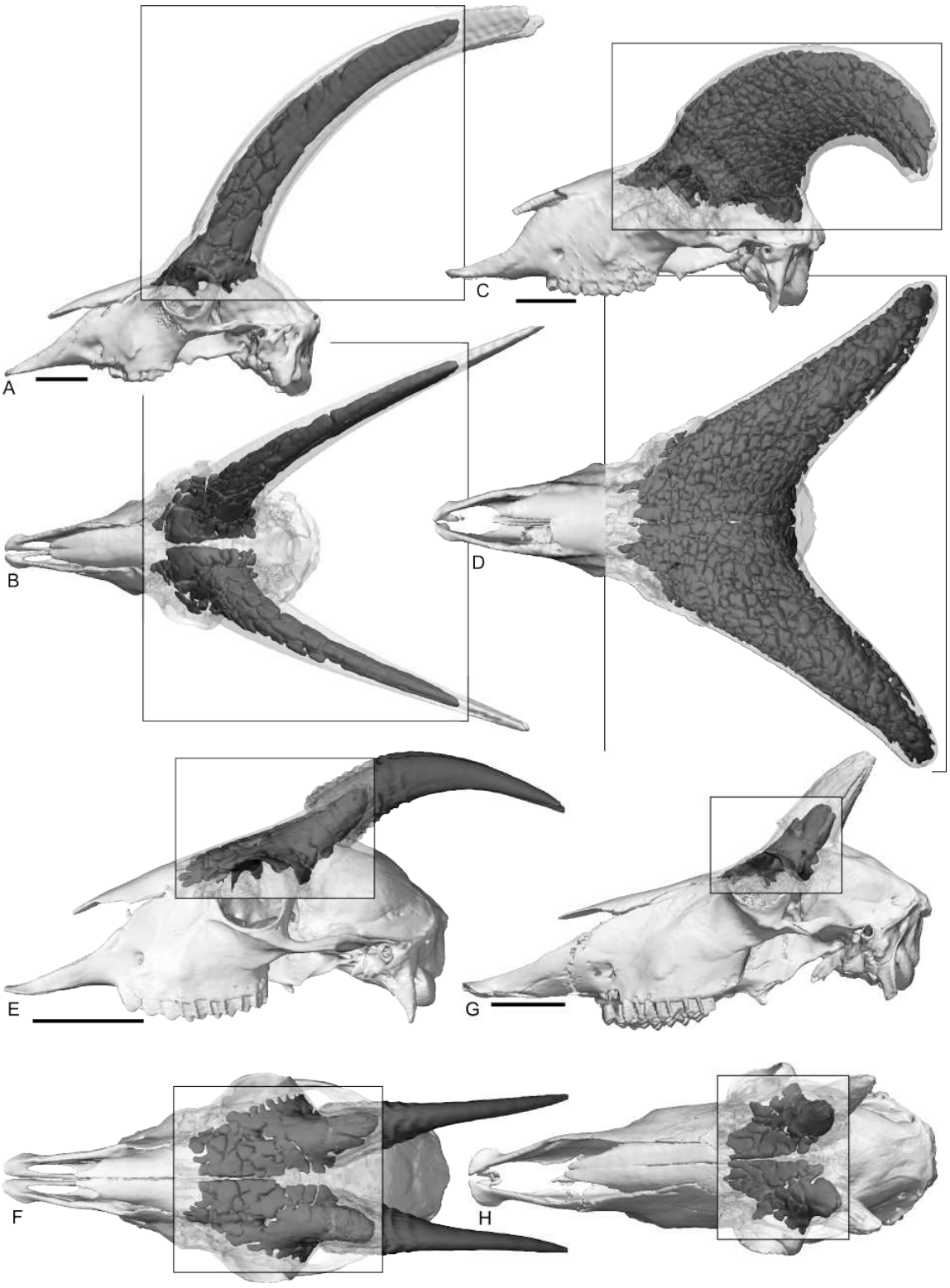
A
B
C
D
E
F
G
H

Figure 3-7. Digital reconstructions from CT scan data of the skulls of *Hippotragus niger* (A-B; AMNH 83606) and *Kobus ellipsyprymnus* (C-D; YPM 3484), illustrating frontal sinuses and related anatomy. Skulls are shown in lateral (A, C) and dorsal (B, D) views. The boxed areas indicate the region of the skull that has been rendered partially transparent in order to visualize the anatomy of the frontal sinuses. The horn sheaths have not been rendered on A-B, and the horns were truncated on all images. Scale bars equal 5 cm.

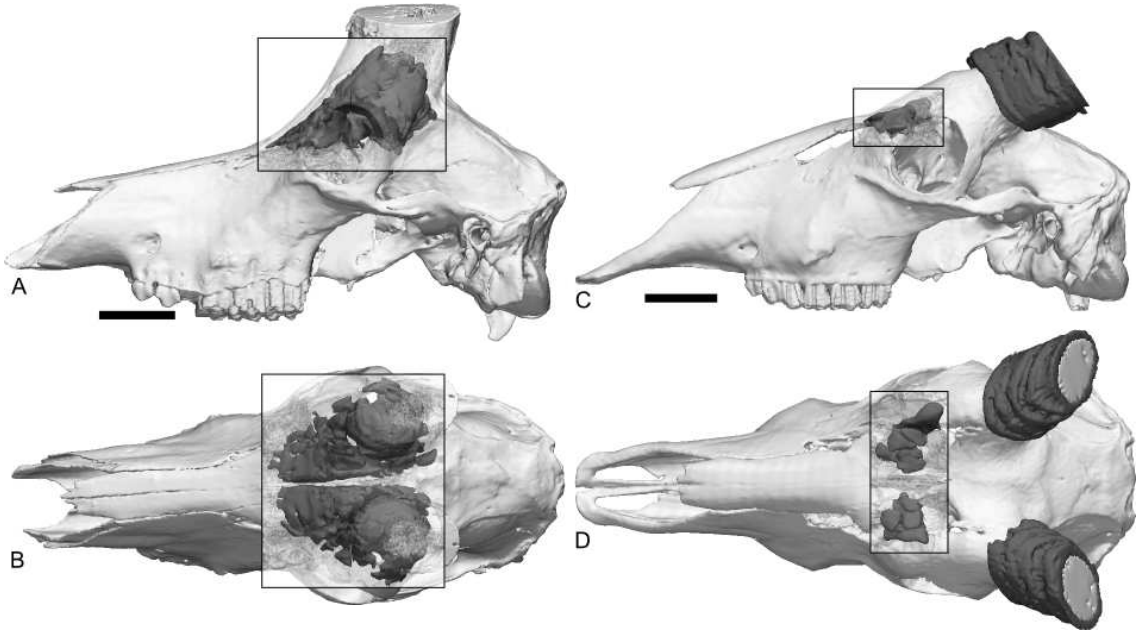
A
B
C
D

Figure 3-8. Digital reconstructions from CT scan data of the skulls of *Taurotragus oryx* (A-B; YPM 6059)*, Aepyceros melampus* (C-D; YPM 3982)*, Oreotragus oreotragus* (E-F; AMNH 27827)*,* and *Pantholops hodgsonii* (G-H; AMNH 55819), illustrating frontal sinuses and related anatomy. Skulls are shown in lateral (A, C, E, G) and dorsal (B, D, F, H) views. The boxed areas indicate the region of the skull that has been rendered partially transparent in order to visualize the anatomy of the frontal sinuses. The horn sheaths have not been rendered in A-B, and they are truncated in C-H. Scale bars equal 5 cm.

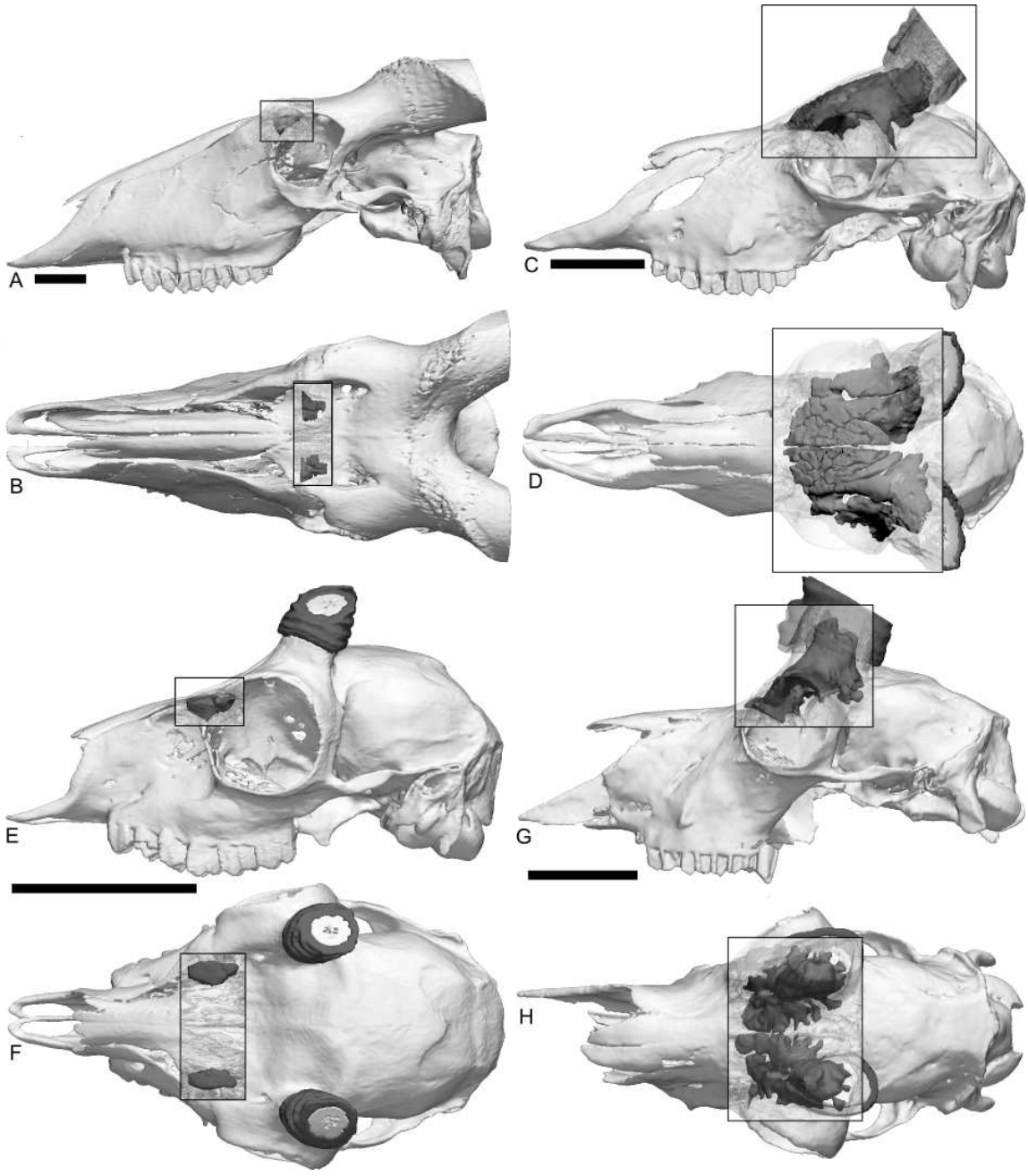
A
B
C
D
E
F
G
H

Table 3-1. List of taxa, specimens and measurements used in this study. Abbreviations: N=number of specimens; SV, sinus volume in milliliters; SE, standard error; SCI, sinus complexity index.

Taxon	Specimen	N	SV (ml)	SE	SCI	SE
Aepyceros melampus	YPM 9192, 9597, 11525	3	58.9	5.3	0.27	0.02
Alcelaphus buselaphus	YPM 7393, 9127, 9131, 9174, 9177, 9185, 10281, 10473, 11519, 11542	10	393.5	118.2	0.48	0.02
Antidorcas marsupialis	AMNH 165078, 165080, 233055	3	47.1	6.5	0.44	0.04
Antilope cervicapra	AMNH 19613, 54485, 54486	3	1.7	0.8	0.43	0.03
Bison bison	YPM 3404, 3405, 3406	3	2530.1	356.9	0.17	0.01
Bos javanicus	AMNH 113755	1	1626.0		0.21	
Boselaphus tragocamelus	AMNH 22842, 35520	2	104.3	5.8	0.21	0.00
Bubalus depressicornis	AMNH 61146, 152856, 152864	3	150.8	36.1	0.23	0.02
Bubalus mindorensis	AMNH 40046, 99339	2	499.6	316.6	0.21	0.03
Budorcas taxicolor	AMNH 110476, 110477	2	331.5	102.8	0.15	0.00
Capra aegagrus	AMNH 88691, 88697	2	302.2	113.5	0.21	0.04
Capra falconeri	AMNH 54610	1	451.3		0.16	
Capra nubiana	AMNH 82264	1	338.4		0.20	
Capra sibirica	AMNH 54906, 57317, 57318	3	364.1	211.5	0.25	0.08
Capricornis sumatraensis	AMNH 45348, 56981; YPM 7398	3	134.0	20.6	0.24	0.03
Cephalophus dorsalis	AMNH 52917, 52924, 52987	3	0.0	0.0		
Cephalophus leucogaster	AMNH 52799, 52802, 52804, 52843	4	0.0	0.0		
Cephalophus natalensis	AMNH 216376	1	0.0			
Cephalophus niger	AMNH 89402	1	0.0			
Cephalophus nigrifrons	AMNH 52949, 52989	2	0.0	0.0		
Cephalophus silvicultor	AMNH 55382, 55383, 170368	3	0.0	0.0		

Table 3-1 (continued).

Taxon	Specimen	N	SV (ml)	SE	SCI	SE
Connochaetes taurinus	YPM 9537, 9585, 10282, unnumbered	4	357.1	73.2	0.33	0.03
Damaliscus lunatus	YPM 9482, 9586	2	156.9	15.8	0.38	0.01
Eudorcas thomsonii	YPM 9246, 9651, 10480	3	0.8	0.5	0.46	0.03
Gazella dorcas	AMNH 82283, 82285, 82288	3	0.2	0.4	0.47	
Gazella subgutturosa	AMNH 57263, 57272	2	0.6	0.7	0.48	0.01
Hemitragus hylocrius	AMNH 54755; YPM 7391	2	244.3	49.3	0.15	0.00
Hippotragus equinus	YPM 9141	1	220.9		0.28	
Hippotragus niger	AMNH 83606; YPM 9140	2	216.2	8.9	0.31	0.04
Kobus ellipsiprymnus	YPM 9101, 9183, 9193	3	15.6	9.4	0.32	0.06
Kobus kob	YPM 9164	1	3.4		0.30	
Kobus leche	YPM 11524	1	12.2		0.44	
Kobus vardonii	YPM 8975	1	0.0			
Litocranius walleri	AMNH 81170; YPM 9602, 10278	3	0.9	0.3	0.43	0.02
Madoqua kirkii	YPM 9600, 10561, 10563	3	0.1	0.1	0.50	0.03
Naemorhedus goral	AMNH 43033, 110485	2	34.6	5.9	0.26	0.00
Nanger granti	YPM 9480, 9605, 11526	3	2.6	1.9	0.44	0.03
Neotragus batesi	AMNH 53169, 53192, 53202	3	0.0	0.0		
Neotragus moschatus	YPM 3129	1	0.0			
Oreamnos americanus	AMNH 60793, 128105; YPM 11552	3	45.2	11.4	0.32	0.02
Oreotragus oreotragus	AMNH 27827; YPM 8399, 10275	3	0.2	0.2	0.43	0.12
Oryx gazella	AMNH 233035	1	227.8		0.24	
Ourebia ourebi	AMNH 90163, 118450; YPM 7389	3	0.0	0.0	0.00	
Ovibos moschatus	AMNH 29949, 80095	2	568.8	118.3	0.16	0.02

Table 3-1 (continued).

Taxon	Specimen	N	SV (ml)	SE	SCI	SE
Ovis ammon	YPM 4295, 54885	2	973.4	10.1	0.11	0.02
Ovis canadensis	YPM 6682, 7376, 7377	3	1374.9	131.6	0.09	0.01
Pantholops hodgsonii	AMNH 55818, 55819; YPM 9554	3	27.8	1.5	0.34	0.02
Pelea capreolus	AMNH 80919, 80920; YPM 7386	3	0.0	0.0		
Philantomba maxwellii	AMNH 89432, 89625	2	0.0	0.0		
Procapra gutturosa	AMNH 57252, 57260, 85235	3	0.0	0.0		
Pseudois nayaur	AMNH 110494, 117401	2	645.4	380.5	0.12	0.03
Raphicerus campestris	AMNH 54186, 54193; YPM 10276	3	0.0	0.0		
Redunca arundinum	YPM 9180, 9186, 11545	3	0.1	0.1	0.46	0.09
Redunca fulvorufula	AMNH 54257; YPM 9594, 10277	3	0.0	0.0	0.56	
Rupicapra rupicapra	AMNH 90235, 90237	2	38.0	14.8	0.25	0.01
Saiga tatarica	AMNH 85301; YPM 7397	2	2.5	0.6	0.45	0.04
Sigmoceros lichtensteinii	YPM 8952, 8955, 8968, 9106, 11535	5	491.0	71.0	0.36	0.02
Sylvicapra grimmia	YPM 10523, 10524, 10525	3	0.0	0.0		
Syncerus caffer	YPM 11649	1	4461.8		0.12	
Taurotragus oryx	YPM 9549, 10471, 11549	3	10.3	4.3	0.38	0.02
Tetracerus quadricornis	AMNH 54941, 54983; YPM 7396	3	18.0	4.4	0.25	0.01
Tragelaphus scriptus	YPM unnumbered (3)	3	0.0	0.0		
Tragelaphus strepsiceros	YPM 8957, unnumbered	2	0.0	0.0		

Table 3-2. Measurements used in this study.

Measurements used in geometric mean for skull size

1 Greatest width across nasals
2 Greatest breadth across maxillae
3 Distance between orbits, caudal end
4 Shortest distance between supratemporal lines
5 Greatest breadth across external surface of braincase
6 Greatest distance between lateral edge of occipital condyles
7 Greatest distance between lateral edge of bases of paroccipital processes
8 Medio-lateral diameter of foramen magnum
9 Distance from rostral end of tooth row to rostral limit of premaxillae
10 Rostro-caudal length of tooth row
11 Greatest medio-lateral breadth across maxillary tooth row
12 Length of skull, from caudal end of occipital condyles to rostral limit of premaxillae
13 Distance from rostral border of orbit to rostral limit of premaxillae
14 Rostro-caudal diameter of orbit
15 Maximum depth of upper jaw, alveolus to top of lacrimal
16 Width across premaxillae at rostral end

Measurements used in geometric mean for frontal size

17 Greatest mediolateral width across frontals at base of horncores
18 Rostrocaudal length of frontal along midline, from bregma to fronto-nasal suture
19 Greatest thickness of frontal perpendicular to endocranial cavity at midline

Measurements used in calculating horn size

20 Volume of horncore
21 Volume of horn sheath
22 Distance from caudal margin of horncore to dorsal border of foramen magnum
23 Length along dorsal surface of endocranium, from dorsal margin of cribriform plate to dorsal border of foramen magnum
24 Length of endocranium covered by frontal sinus
25 Greatest thickness of frontal
26 Volume of frontal sinuses
27 Average size of chambers within sinus (average trabecular spacing)
28 Volume of sinus within horncore
29 Volume of horncore
30 Volume of horn sheath

Table 3-2 (continued).

Derived measurements

31 Skull size (geometric mean of 1-16)
32 Frontal size (geometric mean of 17-19)
33 Horn size (cube root of sum of 20 and 21)
34 Frontal sinus size (cube root of 26 minus 29)
35 Sinus complexity index (SCI; 27 divided by 26)
36 Relative sinus volume (34 divided by 31)
37 Sinus coverage of endocranial cavity (24 divided by 23)

Table 3-3. Results of analyses comparing relative sinus volume (normalized for skull size) and coverage of the endocranium by the frontal sinus in ramming and non-ramming bovids. For analyses without PICs, the mean for each category is given. Under the phylogeny column, "none" refers to analyses on the raw data, "C" refers to analyses calculated using the composite phylogeny, and "F&V" refers to analyses calculated using the phylogeny from Fernández and Vrba 1995. Under the sample column, "all" refers to the analyses in which all taxa were used (regardless of sinus presence or absence) and "SO" refers to the analyses using taxa with sinuses only. Note that the latter category is not included for SCI, because this required a sinus in order to be calculated. *indicates significance at $P<0.05$.

Phylogeny	Sample	Variable	Mean (rammers, non-rammers)	N	*P*
None	All	Relative Sinus Volume	0.45, 0.29	63	0.053
None	SO	Relative Sinus Volume	0.57, 0.42	47	*0.040
C	All	Relative Sinus Volume		19	0.153
C	SO	Relative Sinus Volume		13	0.390
F&V	All	Relative Sinus Volume		15	0.147
F&V	SO	Relative Sinus Volume		12	0.525
None	All	Endocranial Coverage	0.26, 0.15	63	0.067
None	SO	Endocranial Coverage	0.33, 0.21	47	0.080
C	All	Endocranial Coverage		19	0.286
C	SO	Endocranial Coverage		13	0.546
F&V	All	Endocranial Coverage		15	0.431
F&V	SO	Endocranial Coverage		12	0.908
None	SO	SCI	0.27, 0.35	47	*0.022
C	SO	SCI		13	0.367
F&V	SO	SCI		12	0.890

Table 3-4. Partial correlation coefficients for frontal sinus size on several variables. All data were logged prior to analysis. The final column presents the partial correlation coefficient between the first two variables (v_1 and v_2) while holding the second two variables (v_3 and v_4) constant. *indicates significance at P=0.05. Refer to Table 3-3 legend for phylogeny and sample conventions.

Phylogeny	Sample	v_1	v_2	v_3	v_4	$r_{12\cdot34}$
None	All	sinus	frontal	skull	horn	*0.38
None	SO	sinus	frontal	skull	horn	*0.59
C	All	sinus	frontal	skull	horn	0.09
C	SO	sinus	frontal	skull	horn	*0.35
F&V	All	sinus	frontal	skull	horn	0.19
F&V	SO	sinus	frontal	skull	horn	*0.38
None	All	sinus	horn	skull	frontal	0.14
None	SO	sinus	horn	skull	frontal	-0.16
C	All	sinus	horn	skull	frontal	0.09
C	SO	sinus	horn	skull	frontal	-0.07
F&V	All	sinus	horn	skull	frontal	-0.06
F&V	SO	sinus	horn	skull	frontal	0.00
None	All	sinus	skull	frontal	horn	-0.19
None	SO	sinus	skull	frontal	horn	-0.12
C	SO	sinus	skull	frontal	horn	0.11
C	All	sinus	skull	frontal	horn	0.04
F&V	SO	sinus	skull	frontal	horn	0.09
F&V	All	sinus	skull	frontal	horn	0.06

Table 3-5. Results of RMA regressions for frontal sinus size on several variables. All data were logged prior to regression. The numbers in parentheses indicate 95 percent confidence intervals. Refer to Table 3-3 legend for phylogeny and sample conventions.

Phylogeny	Sample	Y	X	Slope	Intercept	r^2	N
None	All	sinus	frontal	2.82 (2.41 - 3.31)	-8.54 (-10.33 - -6.75)	0.61	63
None	SO	sinus	frontal	1.90 (1.63 - 2.21)	-4.41 (1.63 - -3.21)	0.74	47
C	All	sinus	frontal	2.64 (2.14 - 3.25)	0	0.33	62
C	SO	sinus	frontal	1.58 (1.28 - 1.94)	0	0.51	46
F&V	All	sinus	frontal	2.67 (2.16 - 3.30)	0	0.31	62
F&V	SO	sinus	frontal	1.66 (1.37 - 2.01)	0	0.58	46
None	All	sinus	horn	2.27 (1.92 - 2.69)	-6.42 (-7.98 - -4.86)	0.56	63
None	SO	sinus	horn	1.81 (1.46 - 2.24)	-4.21 (1.46 - -2.57)	0.49	47
C	All	sinus	horn	2.00 (1.62 - 2.47)	0	0.31	62
C	SO	sinus	horn	1.26 (1.00 - 1.59)	0	0.39	46
F&V	All	sinus	horn	2.08 (1.66 - 2.60)	0	0.23	62
F&V	SO	sinus	horn	1.34 (1.08 - 1.66)	0	0.47	46
None	All	sinus	skull	4.44 (3.70 - 5.32)	-15.94 (-19.34 - -12.54)	0.49	63
None	SO	sinus	skull	2.94 (2.43 - 3.55)	-9.12 (2.43 - -6.72)	0.59	47
C	All	sinus	skull	3.74 (3.03 - 4.63)	0	0.31	62
C	SO	sinus	skull	2.18 (1.73 - 2.73)	0	0.42	46
F&V	All	sinus	skull	3.72 (3.00 - 4.61)	0	0.29	62
F&V	SO	sinus	skull	2.25 (1.81 - 2.80)	0	0.47	46

Evolution, homology, and function of the supracranial sinuses in ceratopsian dinosaurs

ABSTRACT

Ceratopsians, or horned dinosaurs, display a spectrum of variation in the system of depressions or sinuses on the dorsum of the skull. Derived neoceratopsians such as *Protoceratops* and *Zuniceratops* variably possess a frontoparietal depression rostral to the dorsotemporal fenestrae. In ceratopsids, such as *Triceratops*, the depression is roofed secondarily by bone to form a supracranial sinus. The sinuses vary in their lateral extent, with the most restricted condition found in *Centrosaurus* and *Styracosaurus*. The sinuses are inferred to be pneumatic structures, although it cannot be determined if they are paranasal, paratympanic, or pharyngeal in origin. The pneumatic diverticula that supplied the sinus ran from the dorsotemporal fenestrae into the sinus via a pair of channels on the dorsum of the skull. Ontogenetically, the sinus began as a shallow depression on the roof of the skull, that was enclosed by excavation into the cranial bone and overgrowth of bone. After accounting for phylogenetic effects, sinus extent was not correlated with skull length or horn length. Sinus morphology in bovid mammals, frequently invoked analogues for ceratopsids, is not correlated with behaviors such as head butting, but differences in sinus placement and anatomy between the groups temper the use of bovid sinuses as an analogy for ceratopsid sinuses. The development of a closed sinus in ceratopsids from an open depression was probably associated with an increase in skull size and the accompanying relatively greater loads applied to the horns (in order to maintain the structural integrity of the skull), as well as an anatomical reorganization of the ceratopsian skull.

INTRODUCTION

Ceratopsia (horned dinosaurs) is a clade of herbivorous ornithischian dinosaurs that encompassed an enormous amount of cranial diversity throughout their evolution. The earliest forms, such as *Yinlong downsi* from the Late Jurassic of China and *Psittacosaurus* spp. from the Early Cretaceous of Asia, were characterized by relatively unadorned skulls measuring no more than 30 cm in length. Many of the more derived neoceratopsians, such as *Protoceratops andrewsi* from the Late Cretaceous of Mongolia, sported a bony frill over the neck, and some reached total cranial lengths of nearly a meter. Finally, ceratopsids from the Late Cretaceous of western North America took cranial size and ornamentation to an extreme. This clade, with members such as *Triceratops horridus*, had skulls bristling with nasal horns and brow horns, an elongate bony frill over the neck, and occasionally even spikes protruding from this frill (as seen in *Styracosaurus albertensis*). Some ceratopsids, such as *Torosaurus latus*, are particularly notable for their immense skull size, exceeding over 3.5 meters in length for some individuals.

Understandably then, anatomical, functional, and phylogenetic studies of the ceratopsians typically emphasize the bony frills, horns and beaks that ornament the skulls of these animals. Ceratopsians, with their spectrum of cranial morphologies and high taxonomic diversity, represent an ideal clade in which to document major changes in cranial architecture and inferred function, and a number of studies have done just that (e.g., Dodson, 1993; Ostrom, 1966).

Yet, the skulls of ceratopsians are marked by a number of other unusual structures that are less frequently studied. One such structural complex is a system of

supracranial sinuses (also known as the frontal sinuses), hollow spaces in the skull roof situated between the orbits, over the endocranial cavity, and often underlying the brow horns (Fig. 4-1). These spaces typically are hidden by a bony secondary skull roof, and hence are often undetected and undescribed. Their function remains enigmatic (but not without speculation), anatomical terminology for the sinuses varies from paper to paper, and homologies of structures within the sinuses are uncertain. Finally, although it is commonly assumed that the sinuses were pneumatic (air-filled), no origin for the pneumatic source has ever been confirmed (Forster, 1996; Sampson et al., 1997; Witmer, 1997). This is a particularly vexing problem, in that it limits comparisons of the ceratopsian sinuses with those in other archosaurs.

From nearly the first discoveries of ceratopsians such as *Triceratops*, cavities in the bases of the postorbital horncores were recognized and analogized with the frontal sinuses (of paranasal origin) seen in bovid mammals such as cattle, sheep, and goats (Hatcher et al., 1907). This "bovid paradigm" has colored subsequent descriptions and functional interpretations of ceratopsian anatomy. Several authors have hypothesized that the sinuses in at least some bovids may act as shock absorbers against forces applied to the horns (Schaffer, 1968; Schaffer and Reed, 1972). This hypothesis has been extended to ceratopsians (Forster, 1996; Molnar, 1977; Sampson et al., 1997; Tyson, 1977), although Farke (2006) disputed the appropriateness of the analogy. In particular, Farke highlighted differences between the sinuses of ceratopsids and bovids, such as the lack of strutting within the ceratopsid sinus, suggesting a diminished shock absorbing capacity in ceratopsids. Lehman (1998) presented an alternative interpretation, positing that much of the variation in the sinuses was associated with variation in skull size.

Finally, Brown and Schlaikjer (1940) noted similarities between the supracranial sinuses of ceratopsids and the frontal depression of *Protoceratops*, and hypothesized that the sinuses developed from the depression in order to strengthen the skull against loads to the frill and the horns.

The supracranial sinuses figure, at least in passing, in many treatments of ceratopsian anatomy. Most descriptions of sinuses have focused on *Triceratops* (e.g., Forster, 1996; Gilmore, 1919; Hatcher et al., 1907; Lull, 1903), especially the specimen USNM 5740. Primarily based upon this specimen, Forster (1996) presented an explicit hypothesis of the cranial bones that contribute to the margins of the sinus (parietal, frontal, laterosphenoid, postorbital, supraoccipital, and exoccipital), building upon previous hypotheses presented at least implicitly in figures by others (e.g., Gilmore, 1919; Hatcher et al., 1907). Less detailed descriptions have been published for other chasmosaurine and some centrosaurine ceratopsids (e.g., Gilmore, 1917; Lehman, 1990; Sampson, 1995; Sampson et al., 1997). Farke (2006) described and illustrated in detail the morphology of the cornual diverticulum of the supracranial sinus within chasmosaurines. Numerous cladistic analyses have used the supracranial sinuses or some aspect of them as characters (e.g., Forster, 1990; Lehman, 1996).

The supracranial sinuses are thus of interest from the perspectives of cranial function, comparative anatomy, and phylogenetic relationships. Yet, as alluded to above, a number of issues cloud our understanding of the supracranial sinuses. First, the sinuses are frequently treated as a distinct and discrete unit within the skull, with many descriptions downplaying or ignoring their integration into the greater cranial whole. As will be discussed below, the relationships to the sinus of some structures, such as the

dorsotemporal channels, are critical for interpreting sinus development, homology, and soft tissue associations. The extent of the sinus is often described, but important details such as topological relationships are almost never noted. Similarly, *Triceratops*, the taxon on which most hypotheses of sinus function have been based, is highly derived within Ceratopsidae, and is not necessarily representative of the group. A broader evolutionary context is sorely needed.

Fortunately, a number of new ceratopsian specimens have been described in recent years, and nearly complete ontogenetic series are now known for several taxa. These new discoveries allow a more complete reassessment of the supracranial sinuses in ceratopsians. This paper provides comprehensive descriptions of the supracranial sinuses across ceratopsians, in both an ontogenetic and evolutionary context. Anatomical terminology is standardized, and homologies are identified for the sinuses and related cranial structures across ceratopsians. Recent reassessments of frontal sinus evolution in Bovidae will also be used to provide insight into the function and evolution of the supracranial sinuses in ceratopsids. This information has implications not only for ceratopsian phylogenetics and functional interpretations, but also provides important new information on the evolution and diversity of the archosaur skull.

Institutional abbreviations—AMNH, American Museum of Natural History, New York, New York; **CMN**, Canadian Museum of Nature, Ottawa, Ontario; **IGM**, Mongolian Institute of Geology, Ulan Baatar; **MNHCM**, Mokpo Natural History and Culture Museum, Korea; **MOR,** Museum of the Rockies, Bozeman, Montana; **ROM**, Royal Ontario Museum, Toronto; **TMP**, Royal Tyrrell Museum of Palaeontology,

Drumheller, Alberta; **UCMP**, University of California Museum of Paleontology, Berkeley; **USNM**, National Museum of Natural History, Washington, D.C.; **UW**, University of Wyoming, Laramie; **YPM**, Yale Peabody Museum, New Haven, Connecticut.

MATERIALS AND METHODS

This study is divided into a descriptive and an analytical portion. The supracranial sinuses are described from a number of prepared museum specimens representing taxa across the clade Ceratopsia (Table 4-1). Descriptions are based primarily on first-hand physical examination of specimens. Some were subjected to computed tomographic (CT) scanning on medical scanners, in order to resolve details of internal morphology obscured by bone or matrix. Specimens were selected by preservation of the relevant areas and by physical size (so that they could be fit through a scanner). The digital data were imported into the program 3D Slicer, in which aspects of the sinuses, endocranium, and related structures were then reconstructed.

The quantitative analysis examined the interplay between sinus morphology, skull and horn length, and phylogeny. Measurements were taken to the nearest millimeter using digital calipers. For some specimens, sinus volume was estimated by pouring sand into the sinus or from the digitally reconstructed models. In cases where neither of these procedures was possible, sinus volume was estimated from linear measurements taken directly on the sinus. Unfortunately, sinus volume could not be measured directly for more than a handful of specimens due to issues of preservation and preparation. So, the degree of secondary closure of the sinus and its extent relative to the

postorbital in adults was used as a proxy for sinus volume: taxa without any development of a sinus or frontoparietal depression were scored as 0, 1 for a frontoparietal depression, 2 for a sinus with no invasion of the postorbital, 3 for invasion of the postorbital but not the postorbital ornamentation, and 4 for invasion of the postorbital and the postorbital ornamentation (Table 4-2).

Basal skull length (the distance from the tip of the rostral bone to the caudal end of the occipital condyles) was used as a proxy for skull size. Although a geometric mean of several skull measurements might be more desirable, incomplete preservation or crushing of skulls in many taxa prevented this. In some cases, no complete skulls are known and basal skull length was estimated from a reconstruction or a closely related taxon. Horn length, measured from the dorsal margin of the orbit to the distal end of the horncore, was standardized by dividing it by basal skull length to produce a ratio. For taxa where measurements from multiple specimens were available, the largest specimen from the sample was utilized in order to exclude juveniles or subadults that had not yet reached full adult size. All measurements are presented in Table 4-2. A proxy for frontal thickness, frontal size, or a similar metric, as in Farke (2007), could not be used in this study, due to the incomplete preservation or preparation in a majority of the taxa as well as the extensive sutural fusion that prevented an adequate delineation of landmarks for measurement.

Spearman's correlation coefficients were calculated in order to determine factors potentially related to sinus development, for sinus extent versus skull length and relative horn length. This test was chosen because an Anderson-Darling test for normality found that none of the variables were normally distributed ($P<0.05$). In order to compensate for

the effects of shared ancestry upon the dataset, correlations were also calculated for phylogenetically independent contrasts in the PDAP module of Mesquite. A composite phylogenetic tree of Ceratopsia (Fig. 4-2) was compiled from previously published analyses (Chinnery and Horner, 2007; Makovicky and Norell, 2006; Ryan and Russell, 2005; Ryan, 2007; Xu et al., 2006; Wu et al., 2007). This approach was necessary because none of the currently published analyses include all ceratopsian taxa within a single analysis. The broad level of agreement in phylogenetic placement among recent analyses supports the validity of this approach. For calculation of independent contrasts, all branch lengths were set to one (a simplification that best met the assumption of no significant relationship between the contrasts and their standard deviations; Garland et al., 1992). Two analyses were run, on all ceratopsians and only ceratopsoids (*Zuniceratops* plus Ceratopsidae) for correlations between skull size and sinus development, in order to examine trends at different phylogenetic levels, and on ceratopsoids alone for correlations between sinus development and skull size (because only these taxa have recognizable supraorbital ornamentation among the taxa considered here).

DESCRIPTION OF THE SINUSES AND ASSOCIATED STRUCTURES

Terminology for the sinuses as a whole is quite variable and often inaccurate relative to the anatomical components of the structure. A standardized terminology, including both previously designated and novel terms, is proposed here (Table 4-3) and explained in detail in the text. The supracranial sinuses differ from the frontoparietal

depression in that the former is at least partially enclosed by a secondary roof of bone, whereas the latter is completely open along its dorsal border.

Basal Ceratopsia

No evidence of supracranial sinuses or a frontoparietal depression exists in the most basal ceratopsians considered here, *Psittacosaurus* and *Yinlong*. In the adult condition for both taxa, a shallow, well-defined depression surrounds much of the dorsotemporal fenestrae. This depression incorporates both the frontal and parietal at the rostral ends. The left and right dorsotemporal depressions, and the dorsotemporal fenestrae, are separated by a sharp, midline ridge of parietal along their entire length. This is the same condition seen in most other non-avian archosaurs, including basal ornithopods. The morphology differs from the frontoparietal depression in that it often surrounds the entire dorsotemporal fenestra, and the depressions are not conjoined rostrally.

Non-Ceratopsoid Neoceratopsians

This group, including *Leptoceratops*, *Protoceratops*, and others, also lacks a true supracranial sinus. However, many of its taxa are characterized by a deep midline frontoparietal depression comprising the rostral end of the parietals and the caudal end of the frontals (Fig. 4-3), rostral to the dorsotemporal fenestrae. It differs from the structures seen in ceratopsids by the comparative restriction of the depression as well as the lack of a bony roof.

A deep depression occupies the caudal third of the dorsal surface of the frontals in all known specimens from all known ontogenetic stages of *Prenoceratops* and *Cerasinops* (Chinnery, 2004; Chinnery and Horner, 2007). This depression is floored by smooth bone and is separated from the main dorsal surface of the frontal by a distinct ridge at the rostral end of the depression. *Cerasinops* is unique in that a low, yet sharp, ridge between the two frontals separates the left and right halves of the depression (Chinnery and Horner, 2007). The relevant portions of the parietal are not well preserved for either taxon, so the extent of the parietal's contribution to the depression (if any) is not known. Neither of the two skulls of *Leptoceratops gracilis* (CMN 8887, 8889) with the frontals preserved exhibit evidence of a frontoparietal depression.

In *Bagaceratops*, the frontoparietal depression is variably developed, and it seems to occur only in the oldest individuals when it is present (Maryanska and Osmólska, 1975). A similar pattern is also seen in *Protoceratops* (Brown and Schlaikjer, 1940). In the largest individuals of this taxon, a prominent depression occupies the dorsal surface of the caudal third of the frontals and the rostral-most portion of the parietal (Fig. 4-3). A poorly defined ridge may mark the sutural contact between the frontals, but otherwise the right and left halves of the depression are completely continuous. Caudally, a more defined midline ridge in the depression grades into the prominent sagittal crest (between the two dorsotemporal fenestrae) along the midline of the parietal. The parietal forms the caudal boundary of the depression, at which point it drops into the dorsotemporal fenestrae. In smaller individuals (e.g., AMNH 6429), the right and left frontoparietal depressions are not conjoined, and the smallest individuals lack any sign of a depression (Brown and Schlaikjer, 1940).

Zuniceratops

Zuniceratops christopheri has a frontoparietal depression, but not a supracranial sinus, in that the depression is not roofed over. Unfortunately, the relevant material (MSM P2102, P3812) is disarticulated, crushed, and from fully adult individuals, so all relevant sutures are fused. MSM P3812, a right postorbital horn and associated elements, is the best preserved of the specimens, so the description focuses on this specimen, with supplementary information from MSM P2102 (a left postorbital, which may or may not pertain to the same individual). Because the sutures are fully fused, it cannot be determined which elements are invaded by the depression. It is assumed, but not certainly known, that the frontal but not the postorbital was involved. None of the parietal fragments known from *Zuniceratops* preserve the relevant region. The depression is located caudal and medial to the base of the horncore, but relationships to the laterosphenoid cannot be determined. The rostral end of the depression terminates roughly in the same plane as the caudal third of the orbit. The depression is completely open to the dorsal roof of the skull, with no secondary roofing, and is lined by smooth bone, contrasting sharply with the roughened, vascularized texture present on the rest of the dorsum of the element. The floor of the depression is also divided into a rostral and a caudal half by a transversely running, smoothly-rounded ridge of bone. In MSM P3812, as preserved, the depression measures 53 mm long, 36 mm wide, and approximately15 mm deep. In MSM P2102, as preserved, the structure measures 51 mm long, 30 mm wide, and approximately 10 mm deep.

An isolated postorbital from a juvenile *Zuniceratops* (MSM P2101) shows no evidence of a sinus or depression. Contrary to previous reports (Wolfe, 2000), the postorbital horncore itself is not invaded by a sinus in any specimens of *Zuniceratops*.

Ceratopsidae

General anatomy—Ceratopsids are broadly similar to each other in many aspects of their supracranial sinuses. Thus, the generalized anatomy of the sinus is described first, and variations by taxon are discussed as necessary. The sinus can be divided into two major sections: the supracranial sinus proper (typically divided into a rostral and caudal chamber by a bilateral transverse buttress) and a pair of dorsotemporal channels leading into the caudal aspect of the sinuses.

Dorsotemporal channels—The dorsotemporal channels are bilaterally symmetric structures incised into the rostral end of the parietal, running between the dorsotemporal fenestrae and the caudal chamber of the supracranial sinuses (Figures 4-5). The term "parietal sulci" has previously been applied to these structures (Forster, 1996), but this term does not distinguish the structures from the abundant neurovascular sulci extending from the caudal margin of the dorsotemporal fenestrae up onto the parietal. In all specimens examined, the floor of the channels was perfectly smooth, lacking the prominent neurovascular impressions seen running into the caudal end of the dorsotemporal fenestrae from the caudal portion of the parietal (described briefly in Forster, 1996) or occasionally seen within the supracranial sinus itself. The channels are inset several millimeters below the dorsal surface of the parietal, and occasionally the channels are excavated so as to create an "overhang" of the dorsal surface of the parietal

over the channels. At their rostral ends, the channels proceed rostromedially and either join to form a single channel that communicates with the caudal chamber of the supracranial sinuses via the frontoparietal fontanelle (e.g., *Centrosaurus brinkmani*, TMP 2002.68.130; *Diceratops hatcheri*, USNM 2412; Fig. 4-4, Fig. 4-5A) or enter the caudal chamber of the sinus individually (e.g., *Centrosaurus apertus*, AMNH 5259, ROM 767; Fig. 4-5B). A tab of bone from the dorsal surface of the parietal, which may be comparatively narrow or broad, or a raised ridge of bone from within the sinus, separates the two channels in the latter condition (or only partially separates the channels in the former). The character shows intraspecific variation in some taxa (e.g., *Anchiceratops ornatus*, in AMNH 5251 and ROM 802 show a single channel entering the caudal chamber, or UW 2419, in which the channels remain separate).

In at least some specimens (e.g., *Torosaurus latus*, MOR 1122; *Triceratops horridus*, USNM 2100, Fig. 4-5B), the caudal ends of the dorsotemporal channels do not visibly communicate with the dorsotemporal fenestrae (as noted by Forster, 1996). In these cases, the distal ends of the channels terminate at bone with the vascularized surface texture typical for the dorsal surface of the frill. However, it cannot be determined in any of these specimens (due to plaster or matrix) if the dorsotemporal channel is indeed obstructed by bone, or if it continues beneath the surface of the parietal. The latter case seems especially plausible for USNM 2100, because the channel deepens considerably just before it reaches the "obstructing" bone. Some ceratopsid specimens (e.g., *Arrhinoceratops brachyops*, ROM 796; *Torosaurus latus*, ANSP 15192; *Triceratops prorsus*, YPM 1822) completely lack dorsotemporal channels, and the frontal fontanelle is closed over. It is speculated that the supracranial sinuses and

dorsotemporal channels still exist in these taxa, but are buried beneath a roof of bone. Unfortunately, it was not possible to subject these specimens to CT scanning in order to confirm this.

The dorsotemporal channels of *Diceratops hatcheri* (USNM 2412, Fig. 4-5A) and one specimen of *Torosaurus latus* (YPM 1831) have received special attention in the literature, due to the supposed presence of an "anterior temporal foramen" (Hatcher et al., 1907), an accessory opening at the caudal end of the channels that terminates medial to the dorsotemporal fenestrae. Unfortunately, the relevant areas in both specimens have been heavily reconstructed with plaster, so it is impossible at present to determine if this morphology is genuine. All that can be said is that the channels in these specimens are unique among ceratopsids in that the channels trend towards the medial border of the dorsotemporal fenestrae, rather than the rostral border (as is most typical).

The rostral parietal from the type specimen of *Torosaurus utahensis*, USNM 15583 (Fig. 4-6) preserves additional unusual morphology in this region. The dorsotemporal channels communicate with the dorsotemporal fenestrae, as is typical, but the left channel has a small diverticulum that heads medially, for about 15 mm (the equivalent area is not preserved on the right side). The channel communicates at its caudal end with the dorsotemporal fenestra, floored by smooth bone. A sharp, low crest separates the fenestra from the dorsal surface of the parietal (which has the usual rugose, vascularized texture). At the anterior end of the dorsotemporal fenestra, on its medial side, is an "accessory" foramen, similar in morphology and position to the "anterior temporal foramina" described above. A thin shelf of parietal (9 mm medially, to about 5 mm laterally, at its thinnest) overhangs this. At the rostral end of the foramen, two small

pillars of bone are present—one directly adjacent to the foramen, and then another right at a "lip" of rounded bone leading to the dorsotemporal channels. These pillars are joined by a floor of smooth bone. Due to plaster reconstruction, it cannot be determined if the accessory foramen pierced the floor of the parietal, or if it was floored by bone.

Transverse buttress—The supracranial sinuses in adult individuals are typically (but not always) divided into a rostral and a caudal chamber by a transverse buttress (Forster, 1996). This buttress runs from the ventral floor of the sinus up to the roof. It may run vertically, or be slightly inclined rostrally or caudally. The relative thickness of the buttress also varies, but it is relatively robust in most specimens. The transverse buttress varies slightly in its position relative to the base of the horncore, even within species. In *Centrosaurus brinkmani* (e.g., TMP 2002.68.21, 2002.68.32; Fig. 4-7A), for instance, the buttress may approximately bisect the coronal plane containing the midpoint of the horn's base, or sit slightly caudal to the midpoint of the base (TMP 2002.68.18). Regardless, in centrosaurines or chasmosaurines, the buttress predominantly sits beneath the middle portion of the horncore and never occurs completely rostral or caudal to it. The buttress also contrasts with the condition in *Zuniceratops* in that this taxon has a much broader and less distinct swelling on the floor of the frontoparietal depression.

Accessory buttresses occur in some specimens of *Pachyrhinosaurus* n. sp. (TMP 89.55.21), *Centrosaurus brinkmani* (e.g., TMP 2002.68.12), and *Triceratops* sp. (USNM 2416), rostral to the transverse buttress. These buttresses further subdivide the rostral chamber of the sinus.

Caudal chamber—The caudal chamber of the supracranial sinuses is generally the deeper of the two primary chambers, but it varies drastically in depth across its extent in many species. The caudal chamber communicates with the dorsotemporal channels at their rostral ends, and may excavate under a portion of the dorsal surface of the parietal in some individuals of some taxa (e.g., *Anchiceratops ornatus*, UW 2419; *Triceratops* sp., USNM 5420). The caudal chamber is often the most laterally expanded of the two chambers; in *Triceratops* and other chasmosaurines, the chamber expands up and into the bases of the postorbital horncores (e.g., *Triceratops* sp., USNM 2416, 5420), forming a cornual diverticulum. In *Pachyrhinosaurus* n. sp., this cornual diverticulum is formed by both the rostral and caudal chamber of the sinus, which excavate the postorbital so completely in some individuals (e.g., TMP 89.55.21) so as to open on the lateral surface of the skull through a small foramen. A similar contribution from both chambers of the sinus occurs in *Einiosaurus procurvicornis* (e.g., MOR 456-8-9-6-1) and *Achelousaurus horneri* (MOR 485). At least some adult or near-adult specimens of *E. procurvicornis* (e.g., MOR 373-6-26-6-13) do not have excavation beneath the area of the horncores, demonstrating variability in this feature within that taxon.

Interfrontal foramen—Numerous authors have identified multiple specimens with a foramen ("pineal foramen" or "frontoparietal foramen") caudal to the transverse buttress, allowing communication between the endocranial cavity and the supracranial sinuses (Forster, 1996; Gilmore, 1919; Sampson et al., 1997; Ryan et al., 2007). A definitive foramen was observed only in one specimen of *Triceratops,* CMN 8528. Here, a small portion of smooth, unbroken bony margin on the foramen indicates that the

structure is not taphonomic artifact. Based on the location of the structure, it likely did not include the parietal bone, and so the foramen is properly termed the interfrontal foramen (rather than the frontoparietal foramen of Sampson et al., 1997). As indicated by Forster (1996), the margins of the foramen are broken on other specimens of *Triceratops*, suggesting that it may have been bridged by a thin layer of bone (or the preserved morphology is a genuine, but broken, foramen). Direct examination uncovered little evidence for the existence of such a structure at an equivalent position in other taxa. Some taxa clearly lack an interfrontal foramen (e.g., *Pachyrhinosaurus* n.sp., TMP 1989.55.1243; *Albertaceratops nesmoi*, TMP 2002.69.1), and the relevant area is simply poorly preserved or broken post mortem (often during collection or preparation) in other cases. A foramen was observed by previous authors (Forster, 1996; Ryan et al., 2007; Sampson et al., 1997) for specimens of *Centrosaurus apertus* (CMN 8790, 8798), *Chasmosaurus russelli* (CMN 2280), and *Styracosaurus albertensis* (CMN 344), but was not found in the present study. In specimens of *Chasmosaurus russelli* (CMN 2280, 8800) and one specimen of *C. apertus* (CMN 8790), the floor of the sinus is smooth and unperforated where matrix has been cleared away. In other centrosaurine specimens the portion of the sinus where the foramen should be is either poorly preserved (CMN 8798) or obscured by glue (CMN 344). A smooth-bordered foramen does occur at the very caudal end of the sinus (and may thus be a true "fronto-parietal foramen") in CMN 344. However, this foramen opens to the cervical region caudal to the foramen magnum and consequently did not communicate with the endocranial cavity. Thus, it cannot be homologized with the structure seen in *Triceratops*.

Rostral chamber—The rostral chamber is typically the smaller and more restricted of the two chambers. As described above, it may contribute to the cornual diverticulum in some centrosaurines, but does not do so in any chasmosaurines. Rostrally, the chamber ends in a rounded, blind pocket, approximately in the same plane as the anterior portion of the orbit (although the precise extent varies). Examination of disarticulated specimens and CT scans (AMNH 5342, TMP 79.11.147) failed to find any evidence of a connection to the nasal cavity from the rostral chamber. This chamber may have accessory cavities in some specimens (e.g., *Triceratops* sp., USNM 5420).

Well-preserved specimens of *Centrosaurus brinkmani* (e.g., TMP 2002.68.18, 2002.68.21, 2002.68.32; Fig. 4-7B-C) display a rostral extension of the rostral chamber of the supracranial sinuses onto the dorsum of the skull. This extension is lined by smooth, unvascularized bone, distinguishing it from the more typical vascularized texture in the surrounding bone. This rostral extension extends to the same plane as the antorbital buttress of the orbital margin.

Frontoparietal fontanelle—In ceratopsids, the frontoparietal fontanelle results from incomplete closure of the secondary roof over the supracranial sinuses. Equivalent terms used in the literature are rejected because they misidentify the nature of the fontanelle (Marsh, 1891), misidentify the bones surrounding the fontanelle (Lambe, 1913), or do not recognize the contribution of the parietal to the secondary roof (Sternberg, 1927). The dorsal portion of the supracranial sinus is open in most specimens through a frontoparietal fontanelle, although it is closed (presumably secondarily, based on ontogenetic series) in some specimens of some taxa (e.g., *Triceratops prorsus*, YPM 1822; *Torosaurus latus*, MOR 1122). The bone leading up to the edge of the fontanelle

is generally quite thin (<10 mm), and tapers gently up to the fontanelle's margins. In some specimens (e.g., *Centrosaurus brinkmani*, TMP 2002.68.30), the fontanelle extends up nearly to the rostral end of the sinus, straddling both chambers. In other specimens, (e.g., *Triceratops horridus*, USNM 2100, Fig. 4-5B), the fontanelle is restricted and apparently opens only into the caudal chamber of the sinus.

Pachyrhinosaurus n. sp. (e.g., TMP 89.55.1131) is distinctive in that the margin of the fontanelle is squared-off and thickened, rather than thin and tapering. This margin measures between 23 and 32 mm in thickness in most specimens, and displays a smooth bone texture similar to that in the sinus itself.

Vasculature of the supracranial sinus—All of the specimens observed in this study were consistent in the complete lack of neurovascular canals within the dorsotemporal channels. Many, but not all, of the specimens preserved neurovascular impressions in the walls of the supracranial sinuses themselves. However, matrix or lack of preparation obscures the full pathway in many cases. Two specimens, then, are particularly informative in tracing the path of bloodflow into and through the sinus.

An isolated postorbital referrable to *Chasmosaurus* sp., ROM 12789 (Fig. 4-8A), preserves neurovascular grooves on the wall of the sinus. The impressions are relatively numerous rostrally, but disappear completely caudal to the caudal-most fold in the lateral wall of the sinus. The grooves in the space between the two folds are visibly continuous with neurovascular foramina in the dorso-medial wall of the orbit. The grooves terminate in a canal that passes rostrally into the postorbital horncore, and some go into the bone on the dorsal roof of the skull. Thus, blood could have flowed from the orbit into the

wall of the frontal sinus and then into the horncore or dorsal roof of the skull (or vice versa).

Nearly identical morphology is seen in an isolated postorbital from a centrosaurine ceratopsid, ROM 12787 (Fig. 4-8B). Only four or five neurovascular grooves trend dorso-ventrally in the sinus. One is broken open to show that it opens through a foramen into the orbit. The proximal end of this groove appears to continue onto the dorsum of the skull.

In TMP 2002.69.01, a braincase referred to *Albertaceratops nesmoi*, two neurovascular canals open into the rostral chamber of the sinus, just posterior and dorsal to the space for the olfactory bulbs. The foramina occur only on the left side and pass up through bone immediately around the endocranial cavity.

TMP 79.11.147—This specimen from the Dinosaur Park Formation of Alberta, Canada, is referable to *Chasmosaurus* sp., based on the morphology of the postorbital and nasal horns (which distinguish it from centrosaurines occurring in the same formation). It is briefly described here because it is the first specimen of *Chasmosaurus* for which nearly the entire sinus can be described for a single individual (Fig. 4-9). The sinus is relatively completely preserved in this specimen and was studied through first-hand examination and CT scanning. *Chasmosaurus* is unusual among ceratopsids in its lack of a transverse buttress (also seen in CMN 2280, 8800, 41357). The sinus chamber is broadest at its rostral end, with two expansions partly projecting under the base of the postorbital horncore (Fig. 4-9B). A slight swelling on the floor of the sinus marks its very rostral extremity. The sinus is of remarkably uniform depth along its entire length, of approximately 68 mm. The dorsotemporal channels do not merge before entering the

supracranial sinus. Due to breakage, the presence of an interfrontal foramen cannot be determined, and the morphology of the frontoparietal fontanelle is unknown. The rostral end of the sinus is completely solid, with no evidence of a connection to the nasal cavity visible first-hand or on CT scans. The volume of the sinus is estimated based on CT reconstruction at 932 ml, with a maximum length of 131 mm and a maximum width of 202 mm..

Ontogenetic Series

"Brachyceratops montanus"—Gilmore (1917) described the skull of the type specimen of *Brachyceratops montanus* (USNM 7951, probably a specimen of *Achelousaurus horneri*, *Einiosaurus procurvicornis*, or *Styracosaurus ovatus*; Sampson et al., 1997) in great detail but made very little mention of the morphology of the supracranial sinuses or their relevance to understanding the ontogeny of these structures. Other workers (e.g., Sampson et al. 1997) have offered further comment, but little additional description (and, as detailed below, some commonly reproduced illustrations are simply incorrect). The material of "*Brachyceratops"* is extremely well preserved and displays a subadult onotogenetic stage. Thus, the sinuses of "*Brachyceratops*" are described here.

The specimen (USNM 7951, frontals, and USNM 7950, parietal; Fig. 4-10) was disarticulated and part of a bonebed with at least five other individuals. Gilmore (1917) hypothesized that the majority of the cranial material pertained to a single individual, based on the tight degree to which the bones could be articulated. This view is accepted

here; regardless, the conclusions and descriptions would not be greatly affected if it were shown that the cranial material indeed pertains to multiple individuals.

The supracranial sinus comprises space within the paired frontals rostrally (approximately three-quarters of the overall area, in dorsal view) and the fused parietals caudally (the remaining one quarter). The three elements meet at a "triple junction" at the caudal third of the sinus (Fig. 4-10), with the frontals wrapping around the lateral surface of the rostral end of the parietal. In dorsal view, the supracranial sinus itself is approximately diamond-shaped, with its broadest (58 mm) and deepest (33 mm) point approximately in the same coronal plane as the triple-junction suture. In sagittal section, the sinus gradually gets shallower towards its rostral end. The rostral end of the sinus is co-planar with the rostral quarter of the orbit.

The frontal portion of the supracranial sinus lacks the neurovascular impressions and transverse buttresses typical of adult ceratopsids. It is recessed within the dorsal surface of the frontal, with no secondary roofing. The structure of the parietal portion of the sinus is more complex, with two major sections – a rostral component within the sinus proper and paired parietal channels on either side of the midline. Rostrally, the portion of the parietal that floors the main body of the sinus is smooth, and a "tab" of bone from the dorsal surface of the parietal (i.e., that portion at the rostral midline, outside of the sinus) slightly overhangs the sinus. This portion of the sinus communicates with the paired parietal channels. Each channel is approximately 9 mm wide and recessed approximately 5 to 7 mm below the dorsal surface of the parietal. The channels are contained exclusively within the parietal itself, with no contribution from other cranial elements. The medial borders of the channels are recessed medially against

the midline of the parietal, but the lateral borders are only recessed dorsally. The channels are extremely short and terminate directly into the dorsotemporal fenestrae.

Despite numerous claims (e.g., Sampson et al., 1997; Gilmore, 1917) and illustrations (Gilmore, 1917, fig. 3; Sampson et al., 1997, fig. 3) to the contrary, there is no evidence of an interfrontal foramen in USNM 7951. The parietal and frontals articulate tightly at the "triple junction" which is recessed as the deepest point in the sinus, but no foramen communicates with the endocranial cavity (Fig. 4-10). The reason for this departure between the original specimen and the illustrations cannot be determined.

***Centrosaurus* spp.**—Despite numerous "baby" specimens referrable to *Centrosaurus* spp. from bonebeds and isolated occurrences (e.g., TMP 82.16.11; Dodson and Currie, 1988), none of these include the frontals or the rostral-most portion of the parietal. However, juvenile and subadult specimens of postorbitals do offer information on the lateral expansion of the sinus through ontogeny.

In the very smallest known postorbitals of *Centrosaurus apertus* (e.g., TMP 79.11.157, with a horncore height of 13.77 mm), there is no indication of a sinus occupying the postorbital. This character state is maintained in all of the subadult specimens with open sutures that were examined (e.g., TMP 79.11.20, 82.18.19). In adult *Centrosaurus brinkmani* (e.g., TMP 2002.68.1) and *Centrosaurus apertus* (e.g., ROM 43214), the sinuses may extend laterally up to the very medial base of the postorbital horncore. Because there is no evidence of pneumatization actually crossing into the base of the horn core, and judging by the relationship between the postorbital-frontal sutures and the postorbital horncore in subadults (in which the suture is at the

very medial edge of the horncore), the postorbital is not pneumatized in *Centrosaurus* spp.

***Chasmosaurus* spp.—**Isolated and disarticulated postorbitals from *Chasmosaurus* spp., from the Dinosaur Park Formation of Alberta, indicate the development of a portion of the supracranial sinus in later ontogenetic stages for this taxon. Unfortunately, the very smallest stages are not preserved, so it is not known when the sinus invaded the postorbital. TMP 88.36.50 is a left postorbital in which the suture with the postorbital is open, suggesting that it is not a full or old adult individual. This specimen preserves the postorbital portion of the supracranial sinus, just rostral to the laterosphenoid cotylus and separated from it by a ridge of bone. The sinus is just caudal to a preserved portion of the frontopostorbital suture and only slightly invaginates the base of the horncore. Fully adult specimens (e.g., TMP 67.8.17, 79.11.147, 85.36.227; ROM 12789) also demonstrate a partial invagination of the base of the horncore, although no specimen indicates a full cornual diverticulum. It is interesting to note that all of the specimens described here preserve the "long-horned" condition, contrasting with the extremely abbreviated horns seen in other individuals of *Chasmosaurus* spp.

***Triceratops* sp.—**Goodwin et al. (2006) described the skull of a baby *Triceratops* sp. (UCMP 15442) from the Hell Creek Formation of Montana. Some details of this material, not noted in the original description, offer additional information on the ontogeny of the frontal sinus in this taxon. Farke (2006) presents additional details on the ontogeny of the cornual diverticulum of the supracranial sinus in this taxon.

The rostral-most portion of the parietal is preserved, with a morphology similar to that described above for *Brachyceratops montanus*. Clearly delineated dorsotemporal channels extend from the dorsotemporal fenestrae into the caudal portion of the sinus. The two channels are separated by a midline projection of the dorsal surface of the parietal. This projection does not overhang the sinus itself, and the parietal is not excavated beneath the channels as seen in the adult condition (e.g., USNM 5420). The right dorsotemporal channel (which is the best preserved) is approximately 7 mm wide and 2 mm in depth. The channels run for around 15 mm before converging in the supracranial sinus. A slight midline ridge, extending for just 1 or 2 mm, marks the caudal end of the sinus. As preserved, the parietal portion of the sinus is 21 mm long along the midline and is 20 mm wide. Bone texture in the floor of the sinus is smooth.

One disarticulated element is identified as the left frontal, based on the pattern of sutures and depressions on one surface of the element that are interpreted as a portion of the supracranial sinuses. Most of the presumed ventral surface of the element is smooth, except for a scarf-joint suture medially on the underside, beneath the presumed sinus. This is probably the suture with the parietal. No definitive interfrontal foramen is apparent, but the relevant region is broken. Furthermore, the medial suture (between the left and right frontals) also is not preserved. A probable portion of the supracranial sinuses, measuring 35 mm long and 11 mm wide (as preserved), occurs on the presumed frontal. The sinus is divided into two portions by a rounded ridge, approximately 11 mm wide, which may represent an incipient transverse buttress. The rostral excavation measures 5 mm below the dorsal surface of the element (and is 14 mm wide as preserved) and the caudal excavation measures 6 mm below the dorsal surface of the

element (and is 11 mm wide as preserved). The edges of the sinus are sharply separated from the bone on the dorsal roof of the skull. The caudal excavation does not undermine the roof of the skull, but the rostral excavation does slightly (creating a small overhang with approximately a millimeter of excavation laterally). The transverse buttress smoothly grades into the rostral and caudal chambers.

Goodwin et al. (2006) identified a structure on the postorbital as the "cornual sinus." This in fact represents the articular surface for the laterosphenoid. Unlike postorbitals from later ontogenetic stages (Farke, 2006), the postorbital in UCMP 15442 does not contribute to the supracranial sinus. The supraoccipital does not display any evidence of pneumatization, but the bone is also broken at its dorsal extent.

RESULTS OF QUANTITATIVE ANALYSIS

Before correction for phylogenetic effects, sinus size was correlated with basal skull length (r=0.849, $P<0.0001$) across Ceratopsia and arguably within Ceratopsoidea (r=0.475, $P=0.054$). Within Ceratopsoidea, sinus size was arguably correlated with relative horn length (r=0.475, $P=0.054$). Phylogenetically independent contrasts of sinus size were not significantly correlated with contrasts of basal skull length (r=0.345, $P=0.091$) across Ceratopsia. Within Ceratopsoidea, sinus size was not significantly correlated with basal skull length (r=0.225, $P=0.403$) or relative horn length (r=0.437, $P=0.090$, respectively). Measurements used in the analysis are given in Table 4-2.

Volumetric estimates for the sinuses of ceratopsids and bovid mammals are presented in Table 4-4. In particular, it is interesting to note that, relative to overall body mass, the supracranial sinuses of ceratopsids are comparatively small when compared to

the frontal sinuses of bovids. Assuming trabecular bone density of 1.4 g/cm^3 (Pressel et al., 2005), the sinuses removed between .4 kg and 6.5 kg of bone from the skull (in *Centrosaurus* and *Triceratops*, respectively).

DISCUSSION

Homologies of the Supracranial Sinuses

Three hypotheses of homology are considered here: 1) homology of the supracranial sinuses across ceratopsids; 2) homology of the frontoparietal depression in *Zuniceratops* and other non-ceratopsids with the supracranial sinuses of ceratopsids; and 3) homology of the transverse buttress in centrosaurines with the transverse buttress in chasmosaurines. These hypotheses are evaluated by considerations of ontogeny, anatomical topology, and mapping characters onto a phylogenetic tree.

Ontogenetic and structural data alike support homology of the sinuses in both clades of ceratopsids. In the smallest known ceratopsid skulls with preservation of the relevant elements, both the frontal and the parietal are involved in the formation of the sinuses (and may even invade the postorbital in specimens of Triceratops; Farke, 2006). Dorsotemporal channels leading from the dorsotemporal fenestrae into a supracranial sinus also occur both in juvenile *Triceratops* as well as "*Brachyceratops*", again suggesting structural homology. Furthermore, the structures are topologically equivalent.

Unfortunately, the disarticulated and incomplete nature of the *Zuniceratops* material, as the lack of informative ontogenetic series for relevant characters, prevents an airtight statement of homology for the sinuses of this taxon with those seen in ceratopsids. However, given the structural similarity (smooth-walled depressions medial

to the body of the horncore on the dorsum of the frontal) of the structure in *Zuniceratops* with that seen in ceratopsids, homology is quite likely.

Numerous authors have posited homology of the frontoparietal depression of non-ceratopsid neoceratopsians (e.g., *Protoceratops*) with the supracranial sinuses of ceratopsids (e.g., Brown and Schlaikjer, 1940; Sampson et al., 1997; Forster, 1996). In mapping characters onto the phylogenetic tree (Fig. 4-2), this certainly appears to be a viable hypotheses—a structural transformation from the frontoparietal depression into the supracranial sinuses. Topologically, homology is also plausible. The structures are both contained within the frontal and parietal bones. Both the depression and the sinuses communicate with the dorsotemporal fenestrae, although this communication generally is much more restricted in ceratopsids (in the form of the dorsotemporal channels). Ontogenetically, the structures also appear similar. Thus, all of the evidence is consistent with homology of the frontoparietal depression and the supracranial sinuses. The differences in size and degree of enclosure may be secondary to a general structural reorganization of the skull in ceratopsids relative to non-ceratopsids (see below).

Homology of the transverse buttress between centrosaurines and chasmosaurines is also probable. *Zuniceratops* also possesses a moderate transverse swelling at a structurally analogous position within its frontoparietal depression, and transverse buttresses are found in nearly all ceratopsids. The sole exception lies with *Chasmosaurus*, a relatively basal chasmosaurine, which lacks a transverse buttress. The most parsimonious scenario suggests origin of the structure prior to the base of Ceratopsidae, with secondary loss in *Chasmosaurus*. Future fossil discoveries may better elucidate the evolution of this feature.

Osteological Boundaries of the Supracranial Sinuses

Despite explicit hypotheses of the bounding bones presented in the literature (Forster, 1996; Gilmore, 1919), the bones actually contributing to the walls of the sinus are obscured by fusion in adults. The ontogenetic and topological information presented here clarifies these relationships.

The frontoparietal depression is exclusively confined to the frontal and parietal in all non-ceratopsoid neoceratopsians. The condition cannot be completely evaluated in *Zuniceratops*, but it seems likely that this is also the case in this taxon.

Juvenile and subadult specimens of ceratopsids from both major clades clearly indicate that the dorsotemporal channels are contained exclusively within the parietal (Fig. 4-10). No evidence suggests that the situation changes in adults. Furthermore, the frontal unambiguously contributes to the supracranial sinus in all taxa, based on ontogenetic series and topographical relationships in adults.

The contribution of the postorbital to the margins of the supracranial sinuses varies ontogenetically and phylogenetically. Based on the position of the postorbital horncore (immediately lateral to the postorbito-frontal suture, based on disarticulated subadult specimens), and the fact that the sinus approaches but never actually invaginates, the base of the horncore, the postorbital does not contribute to the wall of the sinus at any ontogenetic stage in the centrosaurines *Centrosaurus* spp. and *Styracosaurus albertensis*. In *Achelousaurus horneri*, *Albertaceratops nesmoi*, *Einiosaurus procurvicornis*, and *Pachyrhinosaurus* n.sp., the postorbital does not participate in the wall of the sinus in juveniles and some subadults, but it is invaded by the sinus in the adult condition. This contribution is confirmed by the extension of the

sinus under the postorbital boss or horncores in these species (e.g., Sampson, 1995; Sampson et al., 1997). Among chasmosaurines, contribution of the postorbital seems to be ubiquitous for adult specimens (contra Farke, 2006). Note, however, that the condition in *Chasmosaurus* spp. has only been determined for specimens with elongated postorbital horncores; it is possible that the condition is different in those that have more abbreviated horns.

A contribution of the laterosphenoid to the sinus does not appear likely. In specimens of *Centrosaurus* spp. (e.g., TMP 2002.68.12) and *Chasmosaurus* sp. (e.g., TMP 88.36.50), the articular surface for the laterosphenoid cotylus is clearly visible lateral and ventral to the margin of the sinus. Thus, the laterosphenoid does not contribute to the sinus in these taxa. In *Albertaceratops nesmoi* (TMP 2002.69.1), the condition is more ambiguous. The laterosphenoid is just lateral to the transverse buttress, but it cannot be determined if the medial edge of the laterosphenoid contributes to the surface of the sinus at all. In USNM 4286 (*Triceratops* sp.), the laterosphenoids clearly contribute to the lateral wall of the orbit, but sutural contacts indicate beyond a doubt that the laterosphenoids do not border the sinus itself. Instead, they are separated from the sinus by a thin sheet of bone.

Inferred contributions from the supraoccipital and exoccipital (see Fig. 4 in Forster, 1996) are more difficult to evaluate. In juvenile specimens, these bones clearly do not contribute to the walls of the sinus. In adult specimens, however, the structures are completely fused with the surrounding elements, making it impossible to evaluate the relationships. In *Triceratops*, the thinness of the bone separating the sinus and the

occipital plane of the skull is extremely suggestive of the supraoccipital and exoccipital contributing to the sinus for this species.

Contents of the Supracranial Sinuses

The contents of the supracranial sinuses in ceratopsids have been the subject of much speculation. Sampson et al. (1997) listed a whole series of possibilities (such as fat, a venous sinus, muscle, or neural tissue), and Farke (2006) noted the presence of neurovascular impressions within the sinus of some specimens (Fig. 4-8). This effectively excluded hypotheses that the sinuses were occupied by muscle tissue (Sternberg, 1927), but was consistent with the presence of a tight-fitting tissue covering along the walls of the sinus.

Based on examples from extant animals, neurovascular impressions seem to be associated primarily with a tight-fitting membrane (in addition to the periosteum) along the bone (Farke, pers. obs.). A tightly adherent covering is consistent with a pneumatic chamber but is also compatible with several alternative hypotheses. For instance, meninges of the human brain are tightly adherent to the surface of the endocranial cavity and are associated with impressions of the dural sinuses and meningeal arteries. Here, a soft tissue "filling" is clearly associated with the tight tissue covering. Additional, circumstantial, evidence must be used to exclude hypotheses for the contents of the sinus in ceratopsids.

The sheer size of the sinuses in most taxa excludes neural tissue as a viable possibility for the entire contents of the sinuses. The absence of an interfrontal foramen in most specimens precludes the possibility that the sinus held a portion of the brain

itself, and no known ganglia occur in the position (dorsal surface of the head) or with the size seen in ceratopsids.

If the supracranial sinuses hosted only a venous sinus, it would hold a massive amount of blood in the largest ceratopsids (over 4 L; Table 4-4). It is difficult to conceive of a mechanism (in absence of a major muscle) that would keep this quantity of blood circulating adequately within such a large space, to prevent pooling or sepsis. This is particularly highlighted by the relatively small size (or absence) of the neurovascular channels that physically exit the main body of the sinus in most specimens. Complete closure of the interfrontal foramen (as well as its apparent absence in the ontogenetic series) argues against a connection of this putative venous sinus with any of the dural sinuses. The dorsotemporal channels are also not a particularly likely source of major blood flow, as indicated by a complete lack of neurovascular impressions in all specimens that were investigated. Although a venous sinus is conceivable in the frontoparietal depressions of *Protoceratops* and their relatives (C. Holliday, personal com.), it is not a tenable explanation for the supracranial sinus of ceratopsids.

A fatty deposit within the supracranial sinus is possible, but this does not explain the occurrence of the dorsotemporal channels. Fat presumably could be metabolized as necessary through the vasculature feeding the adiopose tissue, without the need for a special set of channels (lacking neurovascular impressions) directed towards the dorsotemporal fenestrae. At least as is typically seen in long bones or the horncores of some antelope (tragelaphines; Farke, personal obs.), the fatty contents of medullary cavities are not associated with large foramina or channels at the ends of bone, nor are they typically lined with completely smooth bone as seen in the ceratopsid sinuses.

Furthermore, there is no known extant analogue for such a mass of fat within the skull itself.

Glandular tissue can also be excluded. Although some birds (e.g., *Diomedea immutabilis*) display a major fossa for a nasal gland within the frontal on the roof of the skull, the fossa communicates with the orbit along a channel that heads rostrally, not caudally towards the dorsotemporal fenestrae, as in the dorsotemporal channels of ceratopsians. No other glands are known to occupy this region of the skull in extant amniotes, so a glandular hypothesis is excluded.

Assuming that the supracranial sinuses of ceratopsids do not represent a hitherto unknown and unique structure, the pneumatic hypothesis (i.e., an air-filled cranial sinus) remains the most viable option. Several aspects of the ceratopsid sinus anatomy are certainly suggestive of a pneumatic origin. The smooth-walled cavity of the sinus, with occasional neurovascular impressions, is consistent with the condition seen in the paranasal sinuses of other animals (Farke, 2006). Similarly, the presence of struts and septae (e.g., the transverse buttress), and accessory cavities, matches the condition seen in pneumatic chambers in other vertebrates. The apparent mode of growth of the sinuses, through invasion of available bone (e.g., up into the horncores) is also consistent with a pneumatic origin (although not exclusive to it). Yet, a major hurdle remains for the pneumatic hypothesis: what is the source of the pneumaticity?

Pneumatic Origin of the Supracranial Sinuses

The floor and walls of the supracranial sinus are remarkable in their consistent lack of potential foramina for a pneumatic diverticulum. No direct communication exists

between the nasal cavity and the supracranial sinuses, as demonstrated by multiple specimens from multiple taxa. Thus, there is no evidence that the supracranial sinuses were paranasal in nature (i.e., pneumatized via an epithelial diverticulum piercing the nasal capsule, as in the antorbital sinus system). Furthermore, no other foramina known in the sinuses indicate direct pneumatization by the tympanic pneumatic system. The interfrontal foramen communicates with the endocranial cavity and is absent in most individuals (as well as in the earliest ontogenetic stage with the region well-preserved, *Brachyceratops montanus*, USNM 7951; Fig. 4-10), so it too must be excluded as a pathway for a pneumatic source.

If the supracranial sinuses were not pneumatized through their walls or floor, a previously-overlooked pathway must be considered: pneumatization from the dorsotemporal fenestrae via the dorsotemporal channels (Fig. 4-1). Although this proposal is somewhat novel, it is the most likely explanation given the data. Furthermore, it explains many puzzling anatomical details of the ceratopsian skull roof.

Under this hypothesis, a pneumatic diverticulum accompanied the adductor musculature up to the margins of the dorsotemporal fenestrae. The diverticulum then proceeded rostrally, within the dorsotemporal channels, to excavate the dorsal roof of the skull and form the supracranial cavities. Thus, the dorsotemporal channels themselves represent a pneumatic pathway. This hypothesis is certainly consistent with the ontogenetic data, in that all of the relevant features are present at the earliest preserved ontogenetic stages. Precedent for pneumatic diverticula sandwiched between muscles is seen in the suborbital diverticulum of the antorbital sinus in birds (Witmer, 1995) and in the cervical region of birds (O'Connor, 2006).

Unfortunately, the association of this hypothetical diverticulum with the muscular tissue means that the pathway to the ultimate air source (paranasal, paratympanic, or pharyngeal) cannot be traced. The gap between the pterygoid, basioccipital, and supraoccipital (c.f., fig. 6 of Forster, 1996) represents one possible route by which the air space of the tympanic cavity or the auditory tube could meet the adductor musculature. A pharyngeal diverticulum could meet the adductor musculature nearer their insertion on the lower jaw. The distance from the nasal cavity probably eliminates a paranasal source.

Several predictions can be made from the hypothesis proposed here. First, additional pneumatic fossae in association with the diverticulum, aside from the supracranial sinuses themselves, are likely. One possible example is seen on the medial surface of the dorsotemporal fenestrae in the *Torosaurus utahensis* type specimen, USNM 15583 (Fig. 4-6; described above). A second prediction is that in specimens in which the dorsotemporal channels are partly or completely obscured by bone (Fig. 4-5), a patent canal should remain to connect the dorsotemporal fenestrae with the supracranial sinuses. Further preparation is needed on the relevant specimens in order to confirm this prediction.

The pneumatic hypothesis, accompanied by the ontogenetic data, also presents an alternative explanation for the formation of the interfrontal foramen. As indicated by USNM 5951 (Fig. 4-10), the interfrontal foramen is absent in at least some juvenile specimens. This suggests, then, that the foramen does not represent the failure of sutures to unite. Instead, the foramen may develop through the active removal of bone on the sinus's side. If the bone became thin enough, a foramen then formed secondarily. The

association of the foramen with the general region of the frontoparietal suture may be coincidental, due to the fact that the brain is closest to the roof of the skull at this point. Regardless, given the comparative rarity of genuine interfrontal foramina (indisputable only in one specimen), the significance of this character is questionable.

Even if the pneumatic hypothesis is ultimately discarded, any alternative hypotheses must explain the consistent connection of the dorsotemporal fenestrae with the supracranial sinuses via the dorsotemporal channels.

Neurovasculature of the Supracranial Sinuses

First, as has been noted both in the above descriptions and previously in the literature (Farke, 2006), numerous blood vessels communicate between the supracranial sinuses and the horncores. No major blood vessels were observed to communicate between the sinuses and the endocranial cavity or the nasal cavity. In all specimens for which the neurovascular paths could be observed, all vessels from the sinus communicate with the dorsal part of the orbit (Fig. 4-8A).

Based on the vascular patterns in extant archosaurs (Sedlmayr, 2002), the arterial supply and venous drainage to and from the horns, sinus, and dorsal orbit probably came from branches of the supraorbital artery, a branch of the profundus artery. In birds, and potentially crocodilians, these vessels contribute to a rete system that probably helps cool the brain or portions of the brain. A rete is certainly possible in ceratopsids, too. Thus, as in goats (Taylor, 1966), the horns of ceratopsids may have had a thermoregulatory function, among other functions. Further work is needed to document and interpret the vascular supply of the skull in ceratopsids.

Sinuses in Bovids and Ceratopsians

The frontal sinuses of bovids are often invoked as analogies for the supracranial sinuses of ceratopsians in both form and function (e.g., Forster, 1996). Beyond the obvious difference that bovid sinuses arise directly from the nasal cavity whereas those of ceratopsids don't, and the similarity that the sinuses in both groups sometimes enter the horncores, might other structural patterns inform our understanding of the sinuses in ceratopsians?

The size of the frontal sinuses in bovids is more closely correlated to the size of the frontal bone itself rather than skull or horn size (although all of these factors were significantly correlated), but the former relationship was greatly reduced (and the others reduced somewhat) when phylogenetic factors were taken into account at a family-wide level (see Dissertation Chapter 3). Within more restricted clades, however, frontal sinus morphology still tracked that of the containing frontal bone. Furthermore, no statistically significant relationship existed between sinus morphology and behaviors such as head butting once phylogeny was considered. These results were interpreted to mean that phylogeny was the most important factor in determining sinus morphology and "opportunistic pneumatization" (sensu Witmer, 1997) was secondary. Thus, frontal sinuses are not particularly adapted for any function in most bovids. Similarly, finite element modeling of a goat head (see Dissertation Chapter 2) found that sinuses offered only modest benefits in shock absorption, but were associated with the removal of "structurally unnecessary" bone. Furthermore, the sinuses in bovids were poorly placed relative to the horns for the purpose of protecting the brain from loads to the horns.

These results, along with anatomical differences outlined below, caution the inference of shock-absorption of the sinuses in ceratopsids from sinuses in bovids.

Unfortunately, sufficient data aren't available to evaluate the relationship between the size of the sinus and the size of the frontal or the rest of the skull roof in ceratopsids, in a manner parallel to the analyses of bovids. Qualitatively, however, it is interesting to note that no ceratopsids secondarily lost their supracranial sinuses, as seen in bovids. Additionally, none of the ceratopsids examined have an especially deep or especially shallow sinuses for their skull size; most of the variation in sinus extent was related to its lateral boundaries.

The statistically significant correlation between sinus size and skull size in ceratopsians was reduced when accounting for phylogeny. This suggests that phylogeny is correlated with sinus size in ceratopsians, as in bovids. Also similar to bovids, the extent of the sinus in ceratopsoids has little relationship to horn length, also suggesting that the sinuses in this clade are not simply pneumatizing available bone (large horns are not necessarily invaded by a large sinus). It is also interesting to note that, relative to body size (used for comparison instead of skull size, due to the drastically different skull proportions between the clades), the sinuses of ceratopsids are much smaller relative to those seen in bovids (Table 4-4).

Function of the Sinuses in Ceratopsids

A phylogenetic test of the functional significance of the supracranial sinuses as a whole is hampered by the fact that the structures only evolved once within Ceratopsia. Additionally, although there are parallels between centrosaurine and chasmosaurine

ceratopsids (e.g., extension of the sinus into the postorbital), these independent origins do not occur enough times for a meaningful statistical analysis. Consequently (and unfortunately), the following discussion must necessarily interpret the functional morphology of the supracranial sinuses in a largely anecdotal manner. Two major evolutionary events are discussed: 1) development and expansion of a frontoparietal depression; and 2) secondary closure of this frontoparietal depression to form a supracranial sinus.

The function of the frontoparietal depression itself is unclear. It occurs in taxa both with and without elongated parietosquamosal frills and first appears in taxa that completely lack postorbital ornamentation. Thus, the function and origin of the frontoparietal depression remains enigmatic. Among known specimens of adult neoceratopsians, the depression reaches its greatest extent in *Zuniceratops*. No adaptive or functional scenario has been presented for the development of this structure (if, indeed, such a function even existed), and it is difficult to reconstruct such a scenario based on current data. Assuming that the frontoparietal depression of *Protoceratops* and others is correctly homologized with the supracranial sinuses of ceratopsids, the ultimate origin of the sinuses was not associated with horn use or shock absorption at all.

Brown and Schlaikjer (1940) suggested that secondary closure of the frontoparietal depression to form the supracranial sinuses resulted from the need to strengthen the skull against forces applied to the horns (assuming the horns were loaded at least occasionally) and in order to better support the frill. Because elongated horns evolved prior to the base of Ceratopsidae and the occurrence of a true sinus, this explanation seems the most plausible. A completely open depression on the skull would

have been a weak point under loading, and the initial secondary roofing, seen in all ceratopsids, would have served to strengthen the skull against such loads (even if the frontal fontanelle remained open). Based on reconstructions, the basal skull length of *Zuniceratops* (which had elongated postorbital horns but only a frontoparietal depression) is estimated at approximately 400 mm, whereas the basal centrosaurine *Albertaceratops* (which had elongated horns and a true sinus) had an estimated basal skull length approaching 1000 mm. It is thus hypothesized that the initial appearance of a supracranial sinus was more influenced by an abrupt increase in maximum skull size at the base of Ceratopsidae (and a presumed increase in loading to the horns), rather than the appearance of postorbital horns (which occurred before the true sinus). Given that the appearance of an enclosed sinus occurred only once in ceratopsids, this hypothesis cannot be tested further with the present data.

In concert with the change in overall skull size, the creation of a sinus from a relatively shallow frontoparietal depression may also be associated with a reorganization of the skull as ceratopsids evolved from a *Protoceratops*-like ancestor. Dodson (1993) noted that the orbits of ceratopsids (as typified by *Centrosaurus*) are placed considerably dorsally on the skull relative to the condition seen in *Protoceratops*, and the quadrates are also reoriented. The endocranial cavity is also relatively lower within the skull in ceratopsids as compared to *Psittacosaurus* and non-ceratopsid neoceratopsians (Fig. 4-1). This suggests, then, that the greatly enlarged sinuses of ceratopsids may have developed alongside this deepening of the skull (although a cause/ effect relationship cannot be determined at present).

In terms of position within the skull, the sinuses of ceratopsians are better placed than those of many bovids to buffer the brain from blows to the head. In ceratopsids, unlike most bovids, the sinuses completely intervened between the brain and the horns (Fig. 4-1). Thus, the sinuses of ceratopsids could protect the brain more adequately. Yet, this comes with a cost – not only were the horns further away from the brain, but they were also farther away from the occipital condyle, the axis of rotation for the skull. Consequently, forces applied to the horns have a greater moment arm about the occipital condyle, compared to a hypothetical condition in which the horns were not atop a thickened skull roof with sinus. This means that greater forces would be necessary to move the horns and also that greater stresses would be incurred within the skull as a whole during horn use due to the horns' greater distance from the occipital condyle. Adaptations against this greater stress could include complete closure of the frontal fontanelle and the obliteration of most cranial sutures. Yet, it is important to note that it is not necessarily the sinuses that offer the advantage, but the separation of the horns from the braincase itself.

The sinuses probably had only a minor role in reducing overall cranial weight, as indicated by estimates of mass reduction of no more than 6.5 kg of bone. This is only a fraction of estimated skull mass in *Triceratops* (220 kg; Farke, 2006).

Bovids as Ceratopsid Analogs

In addition to differences in the placement of the sinuses relative to the horns and braincase between ceratopsians and bovids, two other important structural divergences further limit the use of bovids as functional analogs for ceratopsids (some of which were

summarized by Farke, 2004). First, the brain is much more tightly related to the walls of the endocranial cavity in bovids than presumably was the case in ceratopsians. The surface of the endocranial cavity in ceratopsians largely lacks impressions for most endocranial structures (see fig. 8 in Forster, 1996), unlike the condition seen in mammals and birds. In the latter groups, the brain nearly completely fills the endocranial cavity and many features of the brain are reflected in the overlying bone. The relatively loose fit of the brain within the endocranial cavity for *Triceratops* and relatives may have helped insulate the brain somewhat from any blows or vibrations applied to the skull. Thus, other modes of shock absorption may have been less necessary than for animals with neural tissue more closely related to the surrounding bone.

A second major difference between bovids and ceratopsids concerns the orientation of the horns. In most extant bovids, the horns project caudally from the skull – not rostrally or dorsally as seen in ceratopsids (Farke, 2004). As a consequence, the parasagittal loads (whether dorsoventral or rostrocaudal) commonly experienced in bovids would have been difficult to induce in ceratopsids (whose horn orientation primarily permitted loads in the mediolaterally direction). The horn orientation also would preclude ramming behavior in most ceratopsids (except perhaps for *Pachyrhinosaurus* and other taxa with postorbital bosses). In all, ceratopsid horns probably experienced loads very different from those in bovids.

CONCLUSIONS

Although it cannot be proven incontrovertibly, many of the features of the ceratopsid supracranial sinuses are consistent with a pneumatic origin for these

structures. Any alternative explanations for the contents of the sinuses must account for the intimate linkage between the sinuses and the dorsotemporal channels proceeding from the rostral margins of the dorsotemporal fenestrae. Ontogenetic and phylogenetic data support the homology of the sinuses across ceratopsids and also suggest that the sinuses are homologous with the frontoparietal depression of non-ceratopsid neoceratopsians.

The development of a roofed sinus from the ancestral frontoparietal depression probably was related to the reorganization of the ceratopsian skull roof during the evolution of ceratopsids from their *Protoceratops*-like ancestors, particularly in the elevation of the orbits and the dropping of the braincase relative to the dorsum of the skull. Although shock absorption is not a likely function for the sinuses in many bovids, numerous structural contrasts with ceratopsians prevent direct application of a bovid analogy. New approaches are undoubtedly needed to better understand the overall evolution of the ceratopsid skull.

Figure 4-1. Schematic cross-sections of ceratopsian skulls illustrating the frontoparietal depression or supracranial sinuses (both in black) in relation to the endocranial cavity (light gray) and the rest of the braincase (dark gray). Reconstructions are based on CT scans and examination of original specimens. The orbit is indicated by dotted lines. **A**, *Psittacosaurus* sp.; **B**, *Protoceratops andrewsi*; **C**, "*Brachyceratops montanus*"; **D**, *Centrosaurus apertus*; **E**, *Chasmosaurus belli*; and **F**, *Triceratops horridus*. Scale bars equal 10 cm.

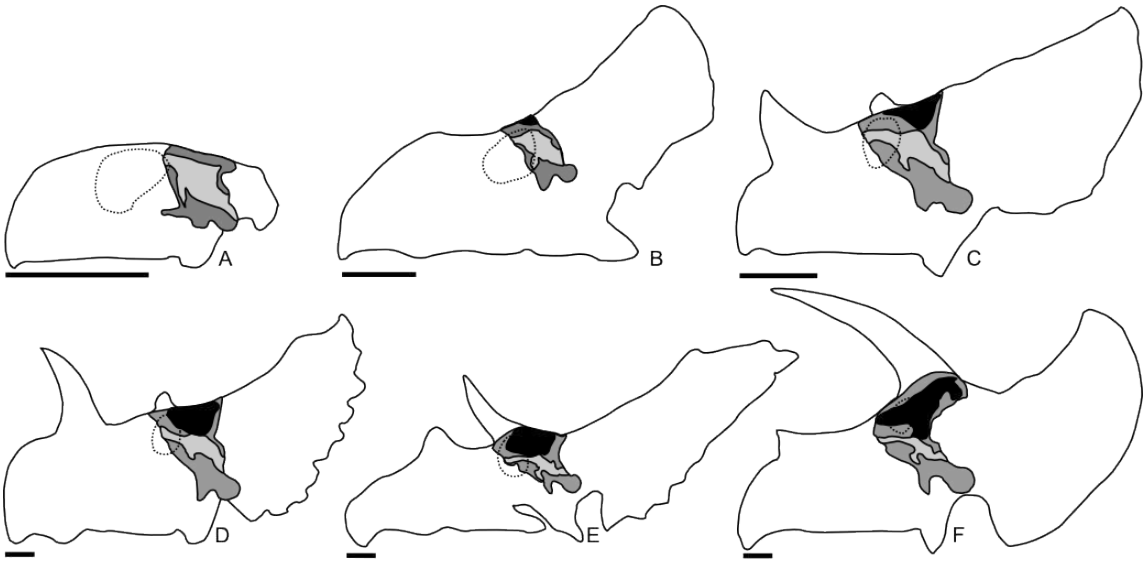
A
B
C
D
E
F

Figure 4-2. Simplified phylogeny of Ceratopsia (after various sources; see text) used for the comparative analyses in this study, also illustrating the distribution of a frontoparietal depression (light gray) and supracranial sinuses (dark gray) within the clade.

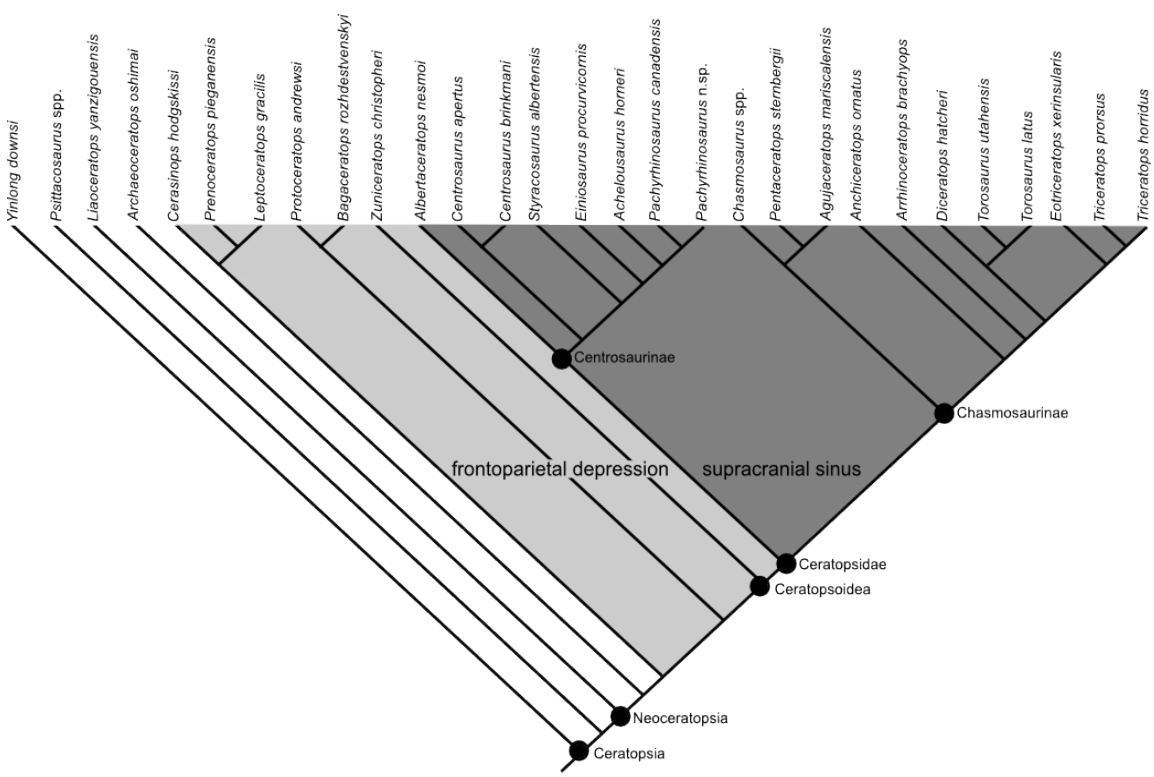
Yinlong downsi
Psittacosaurus spp.
Liaoceratops yanzigouensis
Archaeoceratops oshimai
Cerasinops hodgskissi
Prenoceratops pieganensis
Leptoceratops gracilis
Protoceratops andrewsi
Bagaceratops rozhdestvenskyi
Zuniceratops christopheri
Albertaceratops nesmoi
Centrosaurus apertus
Centrosaurus brinkmani
Styracosaurus albertensis
Einiosaurus procurvicornis
Achelousaurus horneri
Pachyrhinosaurus canadensis
Pachyrhinosaurus n.sp.
Chasmosaurus spp.
Pentaceratops sternbergii
Agujaceratops mariscalensis
Anchiceratops ornatus
Arrhinoceratops brachyops
Diceratops hatcheri
Torosaurus utahensis
Torosaurus latus
Eotriceratops xerinsularis
Triceratops prorsus
Triceratops horridus
Centrosaurinae
Chasmosaurinae
frontoparietal depression
supracranial sinus
Ceratopsidae
Ceratopsoidea
Neoceratopsia
Ceratopsia

Figure 4-3. Skull roof of *Protoceratops andrewsi*, IGM 100-1246, in dorsal view, illustrating the morphology of the frontoparietal depression. Scale bar equals 5 cm. Abbreviations: **dtf**, dorsotemporal fenestra; **f**, frontal; **o**, orbit; **p**, parietal.

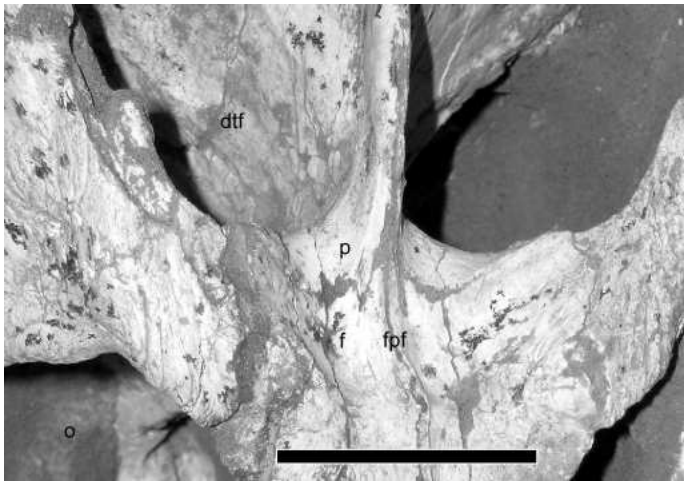
dtf
p
f
fpf
o

Figure 4-4. Right oblique dorsolateral view of caudal skull roof of *Anchiceratops ornatus*, AMNH 5251, showing features related to the dorsotemporal fenestrae, channels, and frontoparietal fontanelle. The scale bar equals 10 cm. Abbreviations: **cc**, confluens of dorsotemporal channels; **dc**, dorsotemporal channel; **dtf**, dorsotemporal fenestra; **fpf**, frontoparietal fontanelle; **ph**, postorbital horncore. Arrows indicate the pneumatic pathway hypothesized in this paper.

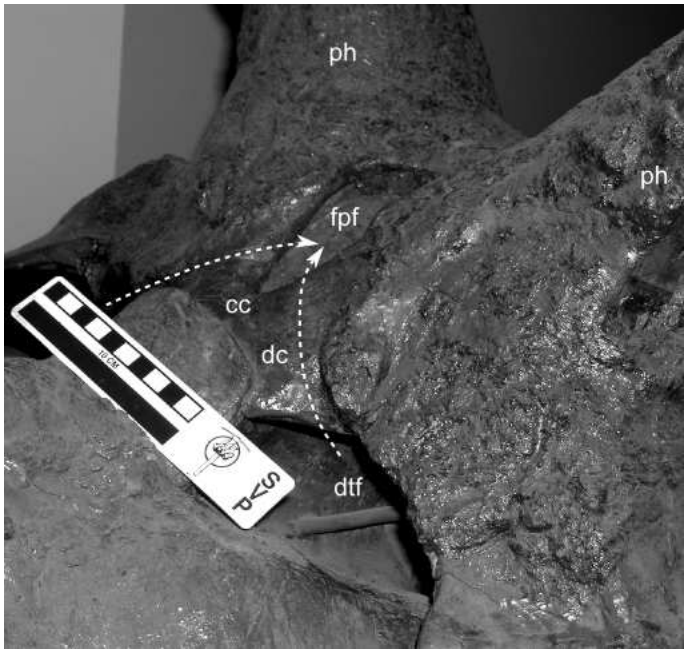
ph
ph
fpf
cc
dc
dtf

Figure 4-5. Dorsal view of caudal skull roofs of **A,** *Diceratops hatcheri*, USNM 2412, and **B***, Triceratops horridus*, USNM 2100, showing features related to the dorsotemporal fenestrae, channels, and frontoparietal fontanelle. In particular, note the apparent separation between the dorsotemporal channels and the dorsotemporal fenestrae in both specimens. The rostral end of the specimens is to the top of the figure. The scale bars equal 10 cm. Abbreviations: **cc**, confluens of dorsotemporal channels; **dc**, dorsotemporal channel; **dtf**, dorsotemporal fenestra; **fpf**, frontoparietal fontanelle; **ph**, postorbital horncore. The boxed area on the inset image shows the approximate location of the photographs.

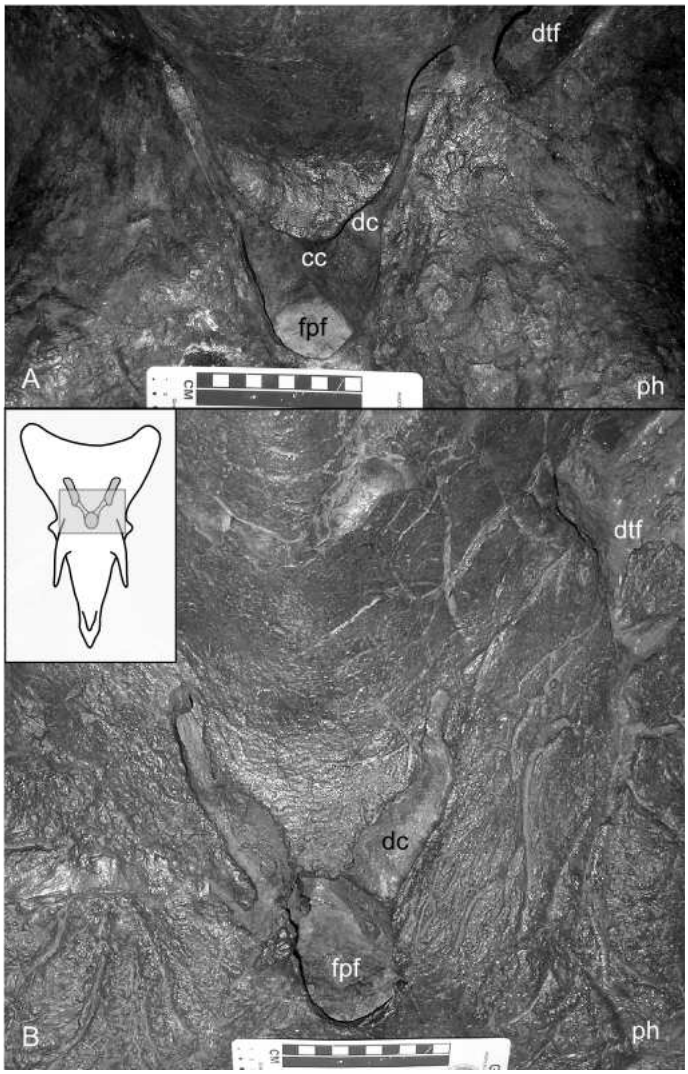
dtf
dc
cc
fpf
A
ph
dtf
dc
fpf
B
ph

Figure 4-6. Rostral parietal of *Torosaurus utahensis*, USNM 15583, in **A**, dorsal, and **B**, lateral views, detailing features related to the dorsotemporal fenestrae and dorsotemporal channels. The rostral end of the specimen is at the left side of the figure. Scale bars equal 10 cm. Abbreviations: **af**, accessory foramen; **d**, diverticulum; **dc**, dorsotemporal channels; **df**, dorsotemporal fenestra. The black area on the inset line drawing approximates the region preserved in the specimen.

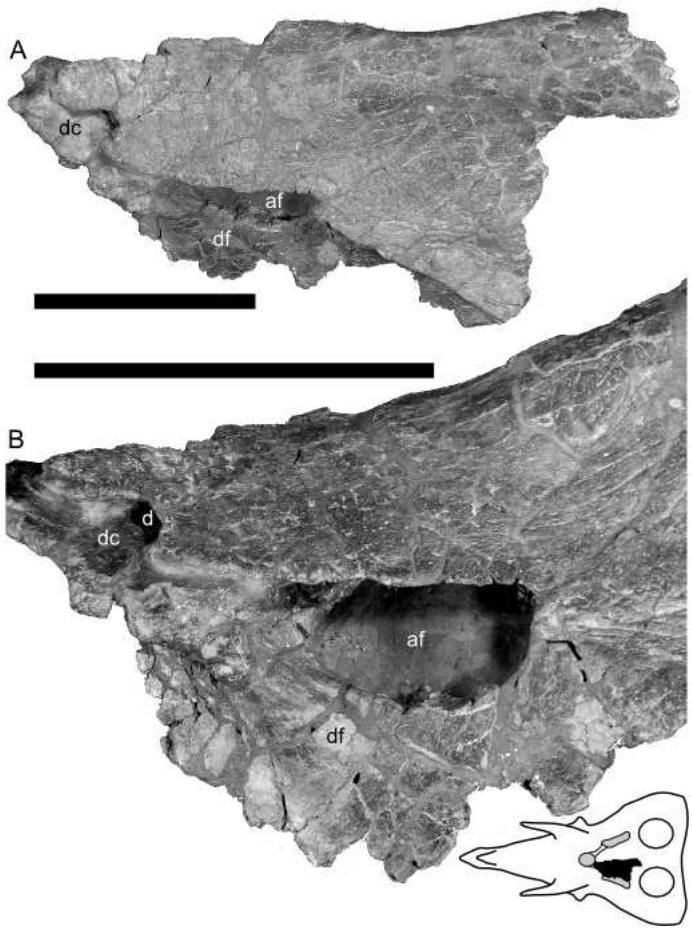
A
dc
af
df
B
d
dc
af
df

Figure 4-7. Postorbitals of *Centrosaurus brinkmani*, illustrating features related to the supracranial sinuses. **A**, TMP 2002.68.18, right postorbital and associated bones in medial view. **B**, TMP 2002.68.32, right postorbital and associated bones in dorsal view, with box indicating area enlarged in C. **C**, TMP 2002.68.32, detail of right frontal in dorsal view, illustrating rostral extension of sinus onto dorsum of skull. The rostral end of the specimens is at the left side of the picture. Abbreviations: **cc**, caudal chamber; **fpf**, frontoparietal fontanelle; **ls**, laterosphenoid articulation; **rc**, rostral chamber; **re**, rostral extension; **tb**, transverse buttress. The top scale bar, for A and B, equals 10 cm. The bottom scale bar, for C, measures 2 cm.

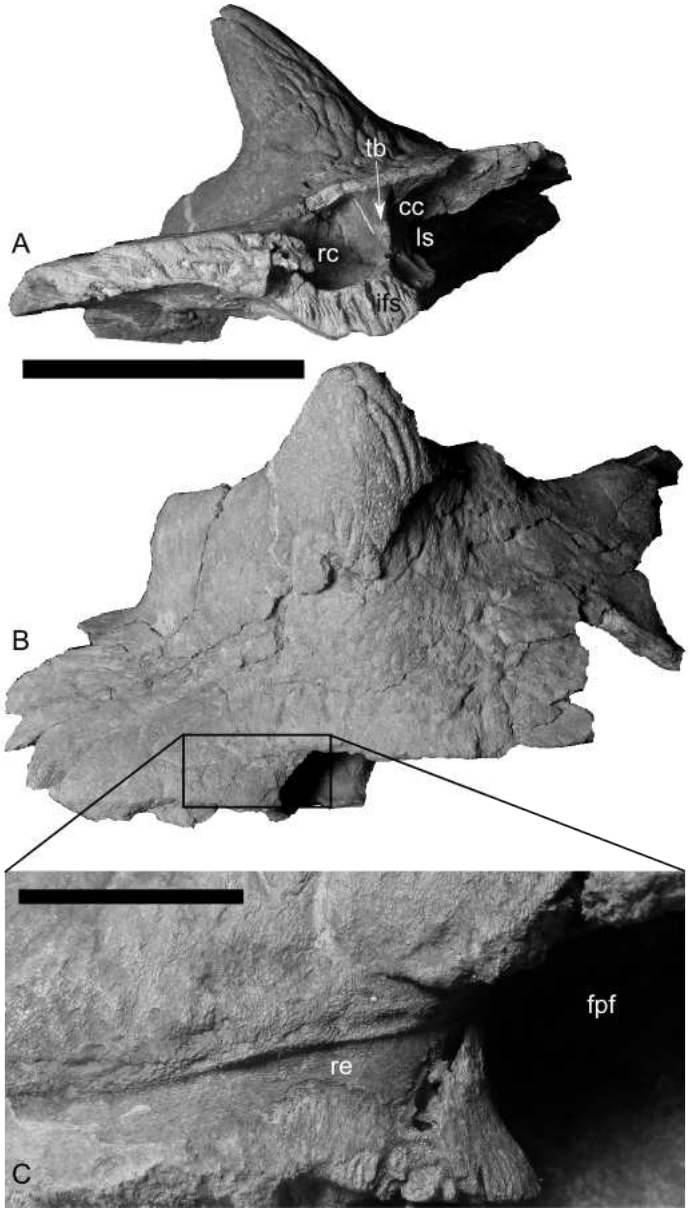
A
tb
cc
ls
rc
ifs
B
C
fpf
re

Figure 4-8. Postorbitals of ceratopsids illustrating neurovascular impressions. **A**, ROM 12789, *Chasmosaurus* sp., ?right postorbital in ventral view; **B**, ROM 12787, Centrosaurinae indet., left postorbital in medial view. The white arrow indicates the presumed origin of the blood vessel within the orbit; the dotted line indicates the path of the vessel within the bone separating the sinus and the orbit; the black line and arrow indicate the path of the vessel within the wall of the sinus and into the body of the postorbital horncore. Scale bars equal 5 cm. Abbreviations: **o**, orbit; **ss**, supracranial sinus.

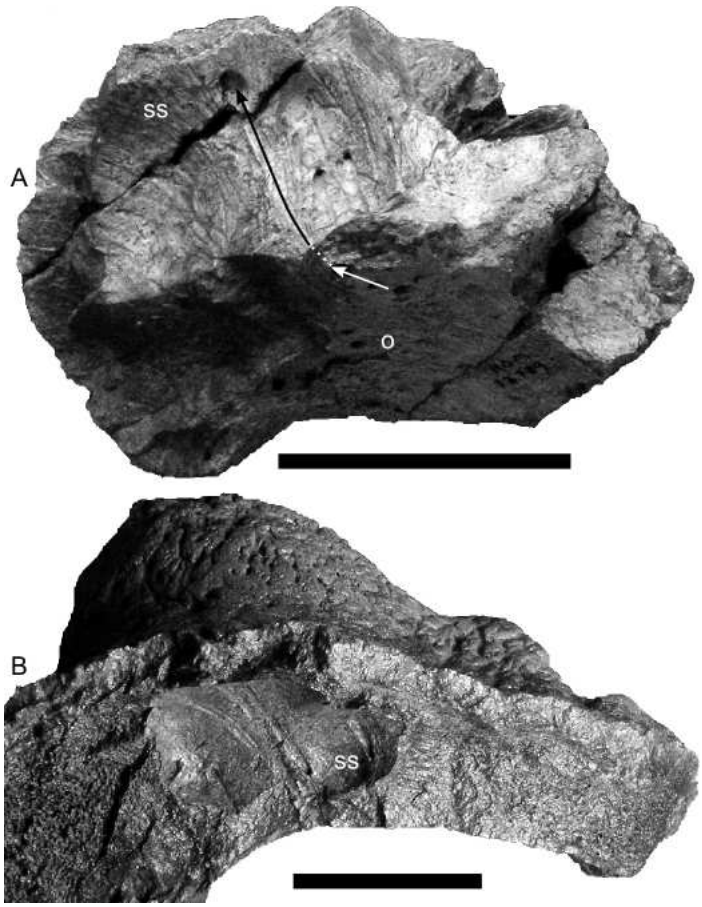
A
SS
O
B
SS

Figure 4-9. Three-dimensional reconstructions from CT scan data for a partial skull of *Chasmosaurus* sp., TMP 79.11.147, illustrating the supracranial sinuses. **A**, skull in dorsal view; **B**, same view with bone rendered transparently; **C**, skull in left lateral view; **D**, endocast of supracranial sinus in ventral view, with rostral end to left of image; **E**, parasagittal section of skull illustrating supracranial sinus; **F**, skull in left lateral view with bone rendered transparently. Abbreviations: **ec**, endocranial cavity; **ss**, supracranial sinus. Scale bar equals 10 cm.

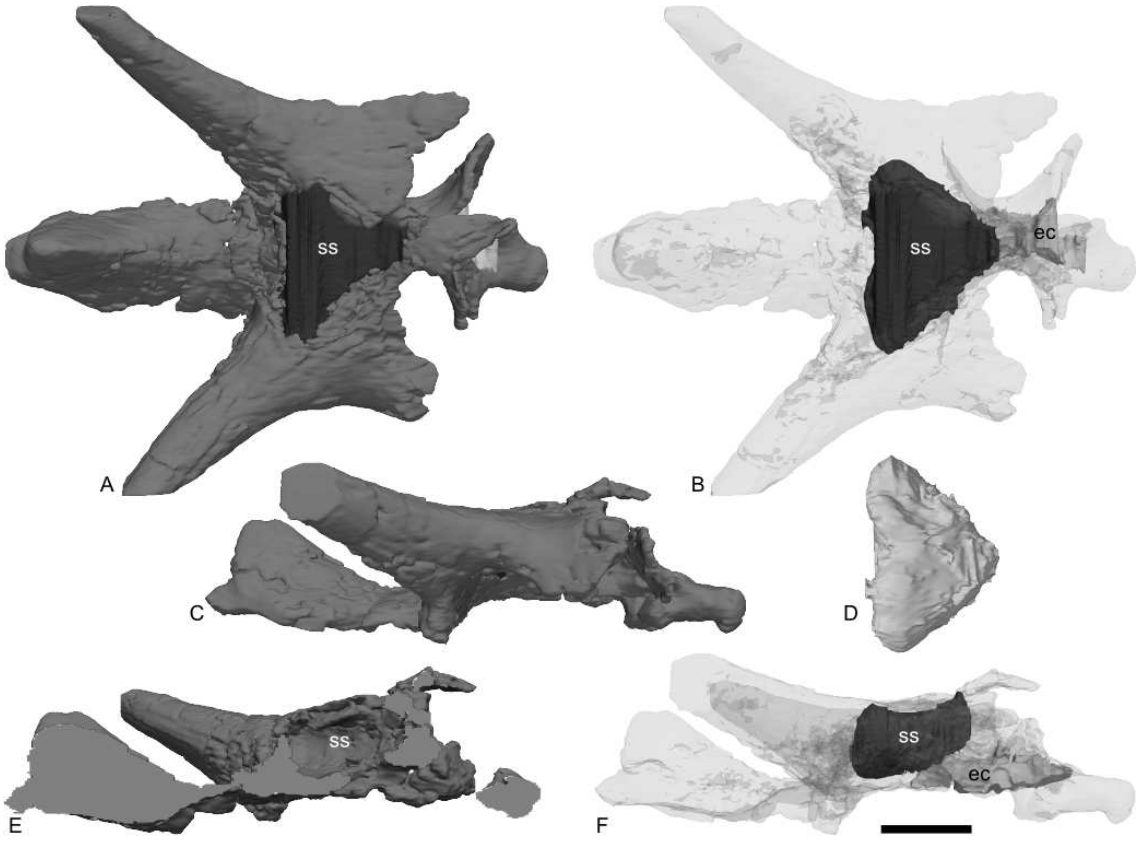
A
ss
B
ss
ec
C
D
E
ss
F
ss
ec

Figure 4-10. Dorsal view of the skull roof of *Brachyceratops montanus*, USNM 7950 and 7951, illustrating features relevant to the supracranial sinuses. The rostral end of the skull is to the bottom of the figure. Sutural boundaries, in transparent white, have been overlain on the original photograph. The area of the supracranial sinus also is indicated by a transparent overlay. Each square on the scale bar equals 1 cm. Abbreviations: **dc**, dorsotemporal channel; **df**, dorsotemporal fenestra; **f**, frontal; **l**, lacrimal; **p**, parietal portion of supracranial sinus; **pb**, parietal bar; **pf**, prefrontal; **po**, postorbital; **scs**, supracranial sinus.

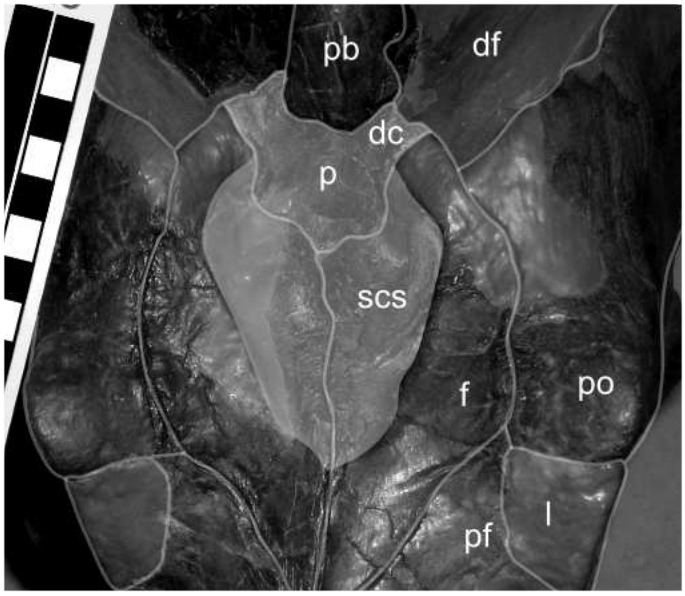
pb
df
dc
p
scs
f
po
l
pf

Table 4-1. Specimens studied first-hand. *indicates specimen that was CT scanned.

Taxon	Specimens
Achelousaurus horneri	MOR 681
Agujaceratops mariscalensis	TMM 43098-1
Albertaceratops nesmoi	TMP 2002.3.35, 2002.69.1*, 2002.69.10
Anchiceratops ornatus	AMNH 5251; CMN 8535; ROM 802; UW 2419
Arrhinoceratops brachyops	ROM 796
Brachyceratops montanus	USNM 7950, 7951, 14765,
Centrosaurinae indet.	AMNH 5342*; CMN 8790; MOR 591; ROM 3521, 12782, 12787; USNM 12745;
Centrosaurus apertus	CMN 8795, 8798; ROM 767, 43214; TMP 79.11.20, 79.11.157, 82.16.11, 82.18.139
Centrosaurus brinkmani	TMP 2002.68.5, 2002.68.10, 2002.68.11, 2002.68.12, 2002.68.13, 2002.68.18, 2002.68.21, 2002.68.30, 2002.68.31, 2002.68.32, 2002.68.127, 2002.68.130, 2002.68.142, 2002.68.129
Cerasinops hodgskissi	MOR 300; USNM 13864
Chasmosaurus belli	ROM 839, 843; YPM 2016
Chasmosaurus irvinensis	CMN 41357
Chasmosaurus russelli	CMN 2280, 8800; TMP 83.25.1
Chasmosaurus sp.	ROM 12789; TMP 67.8.17, 67.17.5, 79.11.147*, 88.36.5
Diceratops hatcheri	USNM 2412
Einiosaurus procurvicornis	MOR 373 (multiple specimens), 456 (multiple specimens)
Eotriceratops xerinsularis	TMP 2002.57.7
Leptoceratops gracilis	CMN 8887, 8889
Pachyrhinosaurus albertensis	CMN 8867, 9485
Pachyrhinosaurus n.sp.	TMP 86.55.249, 87.55.110, 88.55.187, 89.55.21, 89.55.484, 89.55.808, 89.55.1131, 89.55.1243
Pentaceratops sternbergi	USNM 12741, 12743
Prenoceratops pieganensis	MNHCM unnumbered
Protoceratops andrewsi	AMNH 6408, 6414, 6429, 6444, 6637; IGM 100-1246
Psittacosaurus spp.	AMNH 6254, IGM 100-1132
Styracosaurus albertensis	CMN 344
Torosaurus latus	MOR 1122
Torosaurus utahensis	USNM 15583
Triceratops spp.	CMN 8528; UCMP 154452; USNM 2416, 4286, 4842, 5740, 7280, 8027, 8059; YPM 1822
Zuniceratops christopheri	MSM P2101, P2102, P3812

Table 4-2. Measurements used in the statistical analysis. *indicates measurement estimated from figure. Explanations of the sinus character states are given in the text.

Taxon	Skull Length	Source	Sinus	Horn Length	Source
Yinlong downsi	153	Xu et al. 2006*	0	NA	
Psittacosaurus spp.	203	Sereno et al. 2007	0	NA	
Liaoceratops yanzigouensis	111	Xu et al. 2002	0	NA	
Archaeoceratops oshimai	145	You and Dodson 2003	0	NA	
Prenoceratops pieganensis	223	after *Cerasinops*	1	NA	
Cerasinops hodgskissi	223	Chinnery and Horner 2007*	1	NA	
Leptoceratops gracilis	349	CMN 8889	1	NA	
Protoceratops andrewsi	357	Dodson 1976	1	NA	
Bagaceratops rozhdestvenskyi	124	Maryanska and Osmolska 1975	1	NA	
Zuniceratops christopheri	414	Wolfe 2000*	1	200	MSU
Albertaceratops nesmoi	1000	Ryan 2007*	4	415	Ryan 2007
Centrosaurus apertus	835	ROM 767	2	95	ROM 767
Centrosaurus brinkmani	835	after *C. apertus*	2	101	TMP 2002.68.18
Styracosaurus albertensis	851	CMN 344	2	67	CMN 344
Pachyrhinosaurus n.sp.	722	Rothschild and Tanke 1997*	4	113	TMP 89.55.1131
Achelousaurus horneri	875	Sampson 1995	4	100	MOR
Einiosaurus procurvicornis	670	Sampson 1995	4	81	MOR 373-6-24-6-4
Chasmosaurus spp.	978	ROM 843	3	370	AMNH 5401

Table 4-2 (continued).

Taxon	Skull Length	Source	Sinus	Horn Length	Source
Pentaceratops sternbergii	1030	Lehman 1998	4	900	Lehman 1998
Agujaceratops mariscalensis	722	TMM 43098-1	3	430	Forster et al. 1993
Anchiceratops ornatus	800	Sternberg 1929	4	632	ROM 802
Torosaurus latus	1304	Farke 2006	4	853	MOR 981
Torosaurus utahensis	878	Lehman 1996*	4	520	Sullivan et al. 2004
Eotriceratops xerinsularis	1216	photo of TMP 2002.57.7 reconstruction	4	770	TMP 2002.57.7
Triceratops horridus	1180	Forster 1996	4	749	USNM 2100
Triceratops prorsus	1270	Forster 1996	4	750	YPM 1822

Table 4-3

Anatomical terminology applicable to the supracranial sinuses, for this study and others. In order to conserve space, only the first use of a term in the literature is recorded. *indicates new terminology. References include: [1]Sampson, 1995; [2]Forster, 1996; [3]Marsh, 1891; [4]Lambe, 1913; [5]Sternberg, 1927; [6]Gilmore, 1914; [7]Maryanska and Osmólska, 1975; [8]Brown and Schlaikjer, 1940.

This study	*Previous studies*
Supracranial sinuses[1]: Excavation within at least the frontal and parietal bones on the roof of the skull, at least partially enclosed by bone dorsally	Frontal sinus complex[2], supracranial cavities[1]
Cornual diverticulum of supracranial sinus*: Portion of sinus extending into the base of the postorbital horncore	Cornual sinus[2]
Frontoparietal fontanelle*: Fontanelle involving frontal and parietal bones, at dorsum of supracranial sinus	Pineal foramen[3], postfrontal fontanelle[4], frontal fontanelle[5]
Dorsotemporal channels*: Channels of smooth bone leading from the dorsotemporal fenestrae into the supracranial sinus	Parietal sulci[2]
Interfrontal foramen*: A foramen between the supracranial sinus and endocranial cavity	Frontoparietal foramen[1], postfrontal foramen[6]
Frontoparietal depression*: Conjoined depression within the frontal and parietal bones on the roof of the skull, not enclosed by bone dorsally.	Frontal depression[7], parieto-frontal depression[8]

Table 4-4. Estimated sinus volumes and body masses for selected ceratopsids and bovids. Note that sinus volumes in ceratopsids are relatively smaller than in bovids, when compared by body mass. Body masses for ceratopsids are derived from Paul and Christiansen (2000) and those for bovids are derived from Silva and Downing (1995). Part of the sinus for ROM 43214 was broken away, so the volume is estimated based on the reconstructed extent of the sinus.

Taxon	**Specimen**	**Estimated sinus volume**	**Measurement method**	**Maximum body mass**
Anchiceratops ornatus	ROM 802	720 ml	sand	1,180 kg
Centrosaurus apertus	ROM 43214	300 ml	sand	1,460 kg
Chasmosaurus sp.	TMP 79.11.147	932 ml	CT scan	1,520 kg
Triceratops sp.	USNM 5420	4,659 ml	Point digitizer	6,420 kg
Bison bison	YPM 3404	2,886 ml	CT scan	1,000 kg
Ovis canadensis	YPM 1489	1,525 ml	CT scan	156 kg
Syncerus caffer	YPM 16009	4,462 ml	CT scan	664 kg

Summary, significance, and future directions

The primary goal of this dissertation was to use two clades, Bovidae (Mammalia) and Ceratopsidae (Dinosauria), as model groups for investigating the function and evolution of cranial sinuses. Specifically, it was hoped that the behavioral and morphological variation in these groups would permit exploration of functional hypotheses such as shock absorption or opportunistic pneumatization. I particularly wanted to investigate the feasibility of using sinus morphology to infer behavior and function in extinct clades, such as Ceratopsidae. In the end, the research succeeded in many aspects of this, although it also raised many additional questions.

Frontal Sinuses and Head-Butting in Goats: A Finite Element Analysis

The first chapter of the dissertation utilized finite element modeling (FEM) to investigate the function of the frontal sinuses in goats during head-butting behavior. Specifically, I wished to test the hypotheses: 1) that the frontal sinuses function as shock absorbers; and 2) that sinuses form in unloaded regions of the skull (consistent with the hypothesis of opportunistic pneumatization). A series of models representing variable morphology (with and without sinuses) was created and loaded under a variety of conditions. It was found that sinuses did have an effect on shock absorption, but under some loading conditions a model lacking both sinuses and a vaulted frontal performed nearly as well. Based on patterns of principal strains along the surface of the endocranial cavity, sinuses in fact are placed rather poorly to protect the endocranial cavity from most blows to the horns. The sinuses were found to coincide with regions of bone in the frontal under relatively low stress. Thus, the modeling partially supports the hypothesis of sinuses as shock absorbers, but is consistent with the "opportunistic pneumatization"

hypothesis, that sinuses remove bone that is unnecessary for the structural support of the skull.

These results from the FEM are significant as one of the first studies to model the mechanical role of sinuses within the skull. Furthermore, it is the first biomechanical investigation of the shock absorption hypothesis for the frontal sinuses of bovids. Finally, the study also presents some of the first biomechanical evidence consistent with the "opportunistic pneumatization" hypothesis.

Additional lines of inquiry are numerous. For instance, goats represent only one type of sinus morphology and head-butting behavior among bovids. Cape buffalo (*Syncerus caffer*) ram heads at the very base of the horns, which are situated on the forehead. This contrasts with the location of impacts in goats, which are often further out on the horn. Might the sinuses have a more important role as shock absorbers in taxa such as the Cape buffalo? Further modeling is necessary in order to evaluate this hypothesis. The present study also relied on static models, rather than dynamic models. Thus, the impact process was not modeled directly. With the collection of the necessary data on impact accelerations, a dynamic model would undoubtedly more accurately reflect real-world conditions. Finally, it would be very interesting to examine the mechanical behavior of the brain during impact, rather than the indirect proxy of the bone lining the endocranial cavity.

Evolution and Functional Morphology of the Frontal Sinuses in Bovidae (Mammalia: Artiodactyla), and Implications for the Evolution of Cranial Pneumaticity

The second chapter of the dissertation described and quantified the morphology of the frontal sinuses in 62 species of bovids, based primarily upon CT scan data. Here, I tested three specific hypotheses: 1) Enlarged and complex frontal sinuses are associated with head-butting behavior; 2) Frontal sinus size most closely tracks frontal bone size; and 3) Phylogeny is correlated with sinus morphology. Based on comparative statistical analyses accounting for phylogeny, no link was found between head-butting behavior and sinus morphology (largely in agreement with the results of the FEM). Additionally, the results indicated that the volume of the frontal sinus was correlated significantly with the size of the frontal bone, but not with the size of the horns or the skull. This result held in most cases even after accounting for phylogeny, and was interpreted as being consistent with the "opportunistic pneumatization" hypothesis (although not clear proof, given the problems of unraveling correlation and causation between the size of the frontal bone and frontal sinuses).

Significantly, this portion of the dissertation represents the most in-depth analysis of the scaling of a cranial sinus. Previous analyses have examined relationships between sinus size and skull size or snout size, but never specifically examining a sinus's relationship with an individual element. Additionally, the methods used to quantify sinus morphology (based on methods used for analyzing trabecular bone) were novel to this study and show great promise for examining sinus morphology in other taxa. Finally, this is the most comprehensive analysis of sinus morphology within any clade of non-

primate mammals.

Within Bovidae alone, numerous opportunities remain to study the sinuses in more depth. Only adult males were examined here, but the ontogeny of the sinuses remains unknown in most taxa. Furthermore, little is known about the extent of sexual dimorphism in the sinuses of most taxa (beyond some caprine species). An additional question centers on the homology of portions of the frontal sinus in bovids. Do all frontal sinuses in all bovids arise by a similar developmental pattern? Developmental histology studies are needed to answer this question.

Perhaps most interesting is the fact that bovids likely present multiple losses of the frontal sinus, rather than multiple origins. What factors led to the loss of the frontal sinuses in several lineages? In cephalophines (duikers), the nasal cavity is pinched inward by enlarged fossae for the hypertrophied preorbital glands. Did this cause the loss of the frontal sinus? Do issues of cranial packing associated with small skull size result in the loss of frontal sinuses in other bovids? Further comparative work is needed to evaluate these issues.

Evolution, Homology, and Function of the Supracranial Sinuses in Ceratopsian Dinosaurs

The third and final chapter of the dissertation described and interpreted the supracranial sinuses of ceratopsian dinosaurs. Two main questions were addressed: 1) what was the pneumatic origin, if any, for the sinuses; and 2) what was the function of the sinuses?

Supracranial sinuses were found to have originated at the base of the clade

Ceratopsidae, and the structures were probably formed by the enclosure of a frontoparietal depression found in more basal taxa, along with invasion of adjacent elements. It was concluded that the morphology of the sinuses indicates that they are probably pneumatic, but this cannot be demonstrated irrefutably. If the sinuses were pneumatic, the air source would have had to access the roof of the skull via the dorsotemporal fenestrae. The supracranial sinuses simply may have developed as a consequence of a structural reorganization of the skull at the base of Ceratopsidae, although a role in shock absorption still cannot be ruled out.

This study is unique in its depth and breadth. Previous studies of ceratopsids described the sinuses to some degree, but often as isolated structures. Furthermore, the homology and detailed anatomy of several previously puzzling structures (such as the interfrontal foramen and the dorsotemporal channels) was clarified on the basis of the comparative data presented here.

Any future advances in ceratopsids likely will have to await the discovery of additional material. In particular, more detailed ontogenetic series (especially of articulated skulls) would be helpful to fill in several stages in the development of the sinuses. Likewise, the discovery and description of taxa at key points in the evolution of the sinuses are also desirable. A major question that remains is whether or not the sinuses in ceratopsids are truly pneumatic. Without soft tissue, this question may never be answered conclusively.

Perhaps most importantly, numerous structural differences were noted between the frontal sinuses of bovids and the supracranial sinuses of ceratopsids. These differences raise serious questions about analogizing the two groups. In particular, the

sinuses of ceratopsids differed from those of bovids in position relative to the horns (completely beneath them) and endocranial cavity (covering the entire extent). Among other issues, this difference limits the utility of the FE analysis for goats being analogized directly to the function of the sinuses in ceratopsids. Differences in horn orientation and inferred fighting style also caution against a direct ceratopsid/bovid analogy. In the end, alternative lines of evidence (such as paleopathology or histology) may be far more useful than comparative functional analysis when it comes to inferring cranial function in extinct taxa such as *Triceratops*, which differ in so many respects from their modern "analogs."

Tying It All Together

In the end, where does this work leave our understanding of the function of the frontal sinuses in bovids and the supracranial sinuses in ceratopsids? Based on the combined comparative analysis and FEM of bovid skulls, evidence of a shock absorptive function for the frontal sinuses is mixed. The results of the FEM are consistent with the hypothesis that sinuses form in regions of unloaded bone, but the comparative analysis suggests that phylogeny may also be highly correlated with some aspects of sinus morphology and head-butting behavior. The size of the frontal sinus in bovids is much more closely related to the size of the frontal bone than to the size of the skull or horns. Finally, the function of the supracranial sinuses in ceratopsids, if any, remains just as elusive as at the beginning of the project. Structural needs may also play a role in ceratopsid sinus morphology, but still more work is necessary.

Broader Significance

This dissertation represents the most comprehensive and integrative analysis of sinus morphology and evolution offered to date. A philosophical advance is the recognition of two criteria necessary for pneumatization – 1) presence of a pneumatic diverticulum; and 2) presence of bone capable of being pneumatized. Interestingly, many previous studies have mentioned one or the other, but nothing that I have found in the literature that explicitly identified *both* as mutual prerequisites for the development of a sinus. It is hoped that this paradigm will guide future research on sinus morphology.

Additionally, this dissertation lays out a set of guidelines that may be helpful for future studies on sinus anatomy. First, it is necessary to choose the proper scaling variables for quantitative analysis. It should not be expected that a regression of frontal sinus volume on cranial length will give meaningful results, if frontal sinus volume is most strongly correlated with the volume of the frontal bone (as demonstrated here). This has particular implications for previous studies on sinus volume in primates—work identifying an isometric or allometric relationship between skull length and maxillary sinus volume may in fact just be documenting the relationship between the volume of the *maxilla* and the length of the skull. Second, studies of sinus function must be analyzed within a phylogenetic framework. As demonstrated in the chapter on bovid sinus anatomy, consideration of phylogeny made a difference during analysis of behavior and sinus morphology. Third, inferences of function in extinct animals require an in-depth understanding of function in their extant analogs. Here, it was found that the assumption of sinuses as shock absorbers in bovids, which was then extended to ceratopsids, may have been faulty. Indeed, structural differences between the two clades

render any direct functional analogies extremely suspect. Finally, the use of multiple lines of evidence – finite element modeling, quantitative comparative approaches, and examination of fossil taxa – has proven quite informative, and is recommended for any further studies of sinuses.

Future Directions

Although the results presented here are consistent with the idea of sinuses as resulting from the removal of "unnecessary" bone, the results are not conclusive. As shown in the study on bovids, phylogeny may also be correlated with sinus morphology. Developmental studies, in concert with additional modeling in other taxa, are necessary in this regard. In particular, it would be important to see if sinuses have uniform potentials for expansion across all taxa, or if rates of bone remodeling vary between species. Do sinuses produce a truly optimal structure (as often implied), or are they simply "good enough?" Experimental work, perhaps through automated loading of developing skulls in a model organism, might be particularly informative.

The approach used here for bovids certainly could be applied in other clades and on other sinuses. Additional data from non-bovid taxa are needed to verify if the patterns observed here are consistent across vertebrates with sinuses.

Work is also needed to compare the processes of cranial and post-cranial pneumaticity. Are cranial and postcranial pneumaticity linked in any way? Are similar developmental processes at work? Can one be used as a functional analog for the other?

Finally, the issue of the ultimate origin of sinuses needs to be addressed. In the end, bovids present a case study for multiple losses of a sinus – not multiple origins. Is

this perhaps a general pattern across taxa with sinuses? In-depth sampling of other clades is necessary to test this. What selective pressures, if any, coincided with the independent origin of sinuses in archosaurs and synapsids? How have the functional and developmental roles of the sinuses changed through evolution? Here, the fossil record promises to be most informative.

A resolution to the question of "What do sinuses do?" is not likely anytime soon. With new methods and new ways of thinking, however, it may ultimately be answered.

Bibliography

Alvarez, F. 1990. Horns and fighting in male Spanish ibex, *Capra pyrenaica*. Journal of Mammalogy 71:608-616.

Ashman, R. B., J. Y. Rho, and C. H. Turner. 1989. Anatomical variation of orthotropic elastic moduli of the proximal human tibia. Journal of Biomechanics 22:895-900.

Behrents, R. G., D. S. Carlson, and T. Abdelnour. 1978. In vivo analysis of bone strain about the sagittal suture in *Macaca mulatta* during masticatory movements. Journal of Dental Research 57:904-908.

Blaney, S. P. A. 1990. Why paranasal sinuses? Journal of Laryngology and Otology 104:690-693.

Blanton, P. L., and N. L. Biggs. 1968. Eighteen hundred years of controversy: the paranasal sinuses. American Journal of Anatomy 124:135-147.

Bouvier, M., and W. L. Hylander. 1981. Effect of bone strain on cortical bone structure in macaques (*Macaca mulatta*). Journal of Morphology 167:1-12.

Brown, B., and E. M. Schlaikjer. 1940. The structure and relationships of *Protoceratops*. Annals of the New York Academy of Sciences 40:133-266.

Buntjer, J. B., M. Otsen, I. J. Nijman, M. T. R. Kuiper, and J. A. Lenstra. 2002. Phylogeny of bovine species based on AFLP fingerprinting. Heredity 88:46-51.

Caro, T. M., C. M. Graham, C. J. Stoner, and M. M. Flores. 2003. Correlates of horn and antler shape in bovids and cervids. Behavioral Ecology and Sociobiology 55:32-41.

Chinnery, B. 2004. Description of *Prenoceratops pieganensis* gen. et. sp. nov. (Dinosauria: Neoceratopsia) from the Two Medicine Formation of Montana. Journal of Vertebrate Paleontology 24:572-590.

Chinnery, B. J., and J. R. Horner. 2007. A new neoceratopsian dinosaur linking North American and Asian taxa. Journal of Vertebrate Paleontology 27:625-641.

Coleman, M. N. 2008. What does geometric mean, mean geometrically? Assessing the utility of geometric mean and other size variables in studies of skull allometry. American Journal of Physical Anthropology 135:404-415.

Coleman, M. N., and M. W. Colbert. 2007. Technical note: CT thresholding protocols for taking measurements on three-dimensional models. American Journal of Physical Anthropology 133:723-725.

Currey, J. D. 2002. Bones: structure and mechanics. Princeton University Press,

Princeton, NJ, 436 pp.

Dodson, P. 1993. Comparative craniology of the Ceratopsia. American Journal of Science 293A:200-234.

Dodson, P., and P. J. Currie. 1988. The smallest ceratopsid skull--Judith River Formation of Alberta. Canadian Journal of Earth Sciences 25:926-930.

Dumont, E. R., J. Piccirillo, and I. R. Grosse. 2005. Finite-element analysis of biting behavior and bone stress in the facial skeletons of bats. The Anatomical Record Part A 283A:319-330.

Edinger, T. 1950. Frontal sinus evolution (particularly in the Equidae). Bulletin of the Museum of Comparative Zoology at Harvard College 103:411-496.

Estes, R. D. 1991. Behavior Guide to African Mammals. University of California Press, Berkeley, 611 pp.

Farke, A. A. 2004. Horn use in *Triceratops* (Dinosauria: Ceratopsidae): testing behavioral hypotheses using scale models. Palaeontologia Electronica 7:10 pp.

Farke, A. A. 2006. Morphology and ontogeny of the cornual sinuses in chasmosaurine dinosaurs (Ornithischia: Ceratopsidae). Journal of Paleontology 80:780-785.

Farke, A. A. 2007. Morphology, constraints, and scaling of frontal sinuses in the hartebeest, *Alcelaphus buselaphus* (Mammalia: Artiodactlya, Bovidae). Journal of Morphology 268:243-253.

Fernández, M. H., and E. S. Vrba. 2005. A complete estimate of the phylogenetic relationships in Ruminantia: a dated species-level supertree of the extant ruminants. Biological reviews of the Cambridge Philosophical Society 80:269-302.

Forster, C. A. 1990. The cranial morphology and systematics of *Triceratops* with a preliminary analysis of ceratopsian phylogeny. Ph.D. Dissertation. University of Pennsylvania, Department of Geology, 227 pp.

Forster, C. A. 1996. New information on the skull of *Triceratops*. Journal of Vertebrate Paleontology 16:246-258.

Garland, T., P. H. Harvey, and A. R. Ives. 1992. Procedures for the analysis of comparative data using phylogenetically independent contrasts. Systematic Biology 41:18-32.

Gatesy, J., and P. Arctander. 2000. Hidden morphological support for the phylogenetic

placement of *Pseudoryx nghetinhensis* with bovine bovids: a combined analysis of gross anatomical evidence and DNA sequences from five genes. Systematic Biology 49:515-538.

Geist, V. 1966. The evolutionary significance of mountain sheep horns. Evolution 20:558-566.

Gentry, A. W. 1992. The subfamilies and tribes of the family Bovidae. Mammal Review 22:1-32.

Gilmore, C. W. 1914. A new ceratopsian dinosaur from the Upper Cretaceous of Montana, with note on *Hypacrosaurus*. Smithsonian Miscellaneous Collections 63:1-10.

Gilmore, C. W. 1917. *Brachyceratops*, a ceratopsian dinosaur from the Two Medicine Formation of Montana, with notes on associated fossil reptiles. United States Geological Survey Professional Paper 103:1-45.

Gilmore, C. W. 1919. A new restoration of *Triceratops*, with notes on the osteology of the genus. Proceedings of the United States National Museum 55:97-112.

Goodwin, M. B., W. A. Clemens, J. R. Horner, and K. Padian. 2006. The smallest known *Triceratops* skull: new observations on ceratopsid cranial anatomy and ontogeny. Journal of Vertebrate Paleontology 26:103-112.

Hatcher, J. B., O. C. Marsh, and R. S. Lull. 1907. The Ceratopsia. United States Geological Survey Monograph 49:1-300.

Henderson, D. M. 1999. Estimating the masses and centers of mass of extinct animals by 3-D mathermatical slicing. Paleobiology 25:88-106.

Herring, S. W., and S. Teng. 2000. Strain in the braincase and its sutures during function. American Journal of Physical Anthropology 112:575-593.

Hibbeler, R. C. 1997. Mechanics of Materials, Third Edition. Prentice Hall, Upper Saddle River, New Jersey, 855 pp.

Heyne, K., and G. H. Schumacher. 1967. Biometrische Untersuchungen an den Nebenhöhlen der Nase von *Ovis aries*. Anatomischer Anzeiger 120:433-443.

Hildebrand, T., A. Laib, R. Müller, J. Dequeker, and P. Rüegsegger. 1999. Direct three-dimensional morphometric analysis of human cancellous bone: microstructural data from spine, femur, iliac crest, and calcaneus. Journal of Bone and Mineral Research 14:1167-1174.

Hildebrand, T., and P. Rüegsegger. 1997. A new method for the model-independent assessment of thickness in three-dimensional images. Journal of Microscopy 185:67-75.

Hönig, J. F., H. A. Merten, R. Schütte, U. A. Grohmann, and A. Cassisis. 2002. Experimental study of the frontal sinus development on Goettingen miniature pigs. Journal of Craniofacial Surgery 13:418-426.

Hönig, J. F., R. Schütt, and H. A. Merten. 1999. Tierexperimentelle Untersuchungen zur Stirnhöhlenentwicklung nach kraniofazialer Austauschplastik des Os frontale beim Göttinger Miniaturschwein. Mund-, Kiefer- und Gesichtschirurgie 3:325-330.

Jaslow, C. R. 1987. A Functional Analysis of Skull Design in the Caprini. Ph. D. Dissertation. University of Chicago, Department of Anatomy, 144 pp.

Jaslow, C. R. 1990. Mechanical properties of cranial sutures. Journal of Biomechanics 23:313-321.

Jaslow, C. R., and A. A. Biewener. 1995. Strain patterns in the horncores, cranial bones and sutures of goats (*Capra hircus*) during impact loading. Journal of Zoology 235:193-210.

Kingdon, J. 1982a. East African Mammals: An Atlas of Evolution in Africa. Volume III Part D (Bovids). Academic Press, London, 394-746 pp.

Kingdon, J. 1982b. East African Mammals: An Atlas of Evolution in Africa. Volume III Part C (Bovids). Academic Press, London, 393 pp.

Kitchener, A. C. 1985. The effect of behaviour and body weight on the mechanical design of horns. Journal of Zoology 205:191-203.

Kitchener, A. C. 1987. Fracture toughness of horns and a reinterpretation of the horning behaviour of bovids. Journal of Zoology, London 213:621-639.

Kitchener, A. C. 1988. An analysis of fighting of the blackbuck (*Antilope cervicapra*) and the bighorn sheep (*Ovis canadensis*) and the mechanical design of the horns of bovids. Journal of Zoology 214:1-20.

Kitchener, A. C. 1991. The evolution and mechanical design of horns and antlers, pp. 229-253 in J. M. V. Rayner and R. J. Wootton (eds.), Biomechanics in Evolution. Cambridge University Press, Cambridge.

Koppe, T., T. Klauke, S. Lee, and G. Schumacher. 2000. Growth pattern of the maxillary sinus in the miniature pig (*Sus scrofa*). Cells Tissues Organs 167:58-67.

Koppe, T., T. Moormann, C. P. Wallner, and O. Rohrer-Ertl. 2005. Extensive enlargement of the maxillary sinus in *Alouatta caraya* (Mammalia, Primates, Cebidae): an allometric approach to skull pneumatization in Atelinae. Journal of Morphology 263:238-246.

Koppe, T., and H. Nagai. 1997. Growth pattern of the maxillary sinus in the Japanese macaque (*Macaca fuscata*): reflections on the structural role of the paranasal sinuses. Journal of Anatomy 190:533-544.

Koppe, T., and H. Nagai. 1999. Quantitative analysis of the maxillary sinus in catarrhine primates, pp. 121-132 in The Paranasal Sinuses of Higher Primates: Development, Function, and Evolution. Quintessence Publishing, Carol Stream, Illinois.

Koppe, T., T. C. Rae, and D. R. Swindler. 1999. Influence of craniofacial morphology on primate paranasal pneumatization. Annals of Anatomy 181:77-80.

Koppe, T., O. Röhrer-Ertl, S. Breier, and C. Wallner. 2006. Maxillary sinus atelectasis in a wild born gibbon (*Hylobates moloch*). Primates 47:140-144.

Lalueza-Fox, C., J. Castresana, L. Sampietro, T. Marques-Bonet, J. A. Alcover, and J. Bertranpetit. 2005. Molecular dating of caprines using ancient DNA sequences of Myotragus balearicus, an extinct endemic Balearic mammal. BMC Evolutionary Biology 5:70.

Lambe, L. M. 1913. A new genus and species of Ceratopsia from the Belly River Formation of Alberta. The Ottawa Naturalist 27:109-116.

Lehman, T. M. 1990. The ceratopsian subfamily Chasmosaurinae: sexual dimorphism and systematics, pp. 211-229 in K. Carpenter and P. J. Currie (eds.), Dinosaur Systematics: Approaches and Perspectives. Cambridge University Press, Cambridge.

Lehman, T. M. 1996. A horned dinosaur from the El Picacho Formation of West Texas, and review of ceratopsian dinosaurs from the American Southwest. Journal of Paleontology 70:494-508.

Lehman, T. M. 1998. A gigantic skull and skeleton of the horned dinosaur *Pentaceratops sternbergi* from New Mexico. Journal of Paleontology 72:894-906.

Levy, M. L., B. M. Ozgur, C. Berry, H. E. Aryan, and M. L. J. Apuzzo. 2004. Birth and evolution of the football helmet. Neurosurgery 55:656-61; discussion 661-2.

Lieberman, D. E., J. D. Polk, and B. Demes. 2004. Predicting long bone loading from cross-sectional geometry. American Journal of Physical Anthropology

123:156-171.

Lull, R. S. 1903. Skull of *Triceratops serratus*. Bulletin of the American Museum of Natural History 19:685-695.

Lundrigan, B. 1996. Morphology of horns and fighting behavior in the family Bovidae. Journal of Mammalogy 77:462-475.

McDonald, J. N. 1981. North American Bison: Their Classification and Evolution. University of California Press, Berkeley, 316 pp.

McHenry, C. R., P. D. Clausen, W. J. T. Daniel, M. B. Meers, and A. Pendharkar. 2006. Biomechanics of the rostrum in crocodilians: A comparative analysis using finite-element modeling. The Anatomical Record Part A: Discoveries in Molecular, Cellular, and Evolutionary Biology 288A:827-849.

Makovicky, P., and M. A. Norell. 2006. *Yamaceratops dorngobiensis*, a New Primitive Ceratopsian (Dinosauria: Ornithischia) from the Cretaceous of Mongolia. American Museum Novitates 3530:1-42.

Marsh, O. C. 1891. The gigantic Ceratopsidae, or horned dinosaurs, of North America. American Journal of Science 41:167-178.

Maryanska, T., and H. Osmólska. 1975. Protoceratopsidae (Dinosauria) of Asia. Palaeontologia Polonica 33:133-181.

Matthee, C. A., and S. K. Davis. 2001. Molecular insights into the evolution of the family Bovidae: a nuclear DNA perspective. Molecular and Biological Evolution 18:1220-1230.

Metzger, K. A., W. J. T. Daniel, and C. F. Ross. 2005. Comparison of beam theory and finite-element analysis with in vivo bone strain data from the alligator cranium. The Anatomical Record Part A 283A:331-348.

Molnar, R. E. 1977. Analogies in the evolution of combat and display structures in ornithopods and ungulates. Evolutionary Theory 3:165-190.

Moore, W. J. 1981. The Mammalian Skull. Cambridge University Press, Cambridge, 369 pp.

Murray, P. D. F., and J. S. Huxley. 1925. Self-differentiation in the grafted limb-bud of the chick. Journal of Anatomy 59:379-384.

O'Connor, P. M. 2006. Postcranial pneumaticity: An evaluation of soft-tissue influences on the postcranial skeleton and the reconstruction of pulmonary anatomy in

archosaurs. Journal of Morphology 267:1199-1226.

Ostrom, J. H. 1966. Functional morphology and evolution of the ceratopsian dinosaurs. Evolution 20:290-308.

Paul, G. S., and P. Christiansen. 2000. Forelimb posture in neoceratopsian dinosaurs: implications for gait and locomotion. Paleobiology 26:450-465.

Paulli, S. 1900a. Über die Pneumaticität des Schädels bei den Säugerthieren. Eine morphologische Studie. I. Über den Bau des Siebbeins. Über die Morphologie des Siebbeins und die Pneumaticität bei den Monotremen und den Marsupialiern. Gegenbaurs Morphologisches Jahrbuch 28:147-178.

Paulli, S. 1900b. Über die Pneumaticität des Schädels bei den Säugerthieren. Eine morphologische Studie. II. Über die Morphologie des Siebbeins und die der Pneumaticität bei den Ungulaten und Proboscіden. Gegenbaurs Morphologisches Jahrbuch 28:179-251.

Paulli, S. 1900c. Über die Pneumaticität des Schädels bei den Säugerthieren. Eine morphologische Studie. III. Über die Morphologie des Siebbeins und die Pneumaticität bei den Insectivoren, Hyracoideen, Chiropteren, Carnivoren, Pinnipedien, Edentaten, Rodentiern, Prosimiern und Primaten, nebst einer zusammenfassende übersicht über die Morphologie des Siebbeins und die der Pneumaticität des Schädels bei den Säugethieren. Gegenbaurs Morphologisches Jahrbuch 28:483-564.

Pidancier, N., S. Jordan, G. Luikart, and P. Taberlet. 2006. Evolutionary history of the genus *Capra* (Mammalia, Artiodactyla): Discordance between mitochondrial DNA and Y-chromosome phylogenies. Molecular Phylogenetics and Evolution 40:739-749.

Pressel, T., A. Bouguecha, U. Vogt, A. Meyer-Lindenberg, B. Behrens, I. Nolte, et al. 2005. Mechanical properties of femoral trabecular bone in dogs. BioMedical Engineering OnLine 4:17 pp.

Preuschoft, H., H. Witte, and W. Witzel. 2002. Pneumatized spaces, sinuses and spongy bones in the skulls of primates. Anthropologischer Anzeiger 60:67-79.

Purvis, A. 1995. A composite estimate of primate phylogeny. Philosophical Transactions: Biological Sciences 348:405-421.

Radhakrishnan, P., and J. J. Mao. 2004. Nanomechanical properties of facial sutures and sutural mineralization front. Journal of Dental Research 83:470-475.

Rae, T. C. 2008. Paranasal pneumatization in extant and fossil Cercopithecoidea. Journal

of Human Evolution 54:279-286.

Rae, T. C., R. A. Hill, Y. Hamada, and T. Koppe. 2003. Clinal variation of maxillary sinus volume in Japanese macaques (*Macaca fuscata*). American Journal of Primatology 59:153-158.

Rae, T. C., and T. Koppe. 2000. Isometric scaling of maxillary sinus volume in hominoids. Journal of Human Evolution 38:411-423.

Rae, T. C., and T. Koppe. 2003. The term "lateral recess" and craniofacial pneumatization in Old World Monkeys (Mammalia, Primates, Cercopithecoidea). Journal of Morphology 258:193-199.

Rae, T. C., T. Koppe, F. Spoor, B. Benefit, and M. McCrossin. 2002. Ancestral loss of the maxillary sinus in Old World monkeys and independent acquisition in Macaca. American Journal of Physical Anthropology 117:293-296.

Rae, T. C., U. Viðarsdóttir, N. Jeffery, and A. Steegmann. 2006. Developmental response to cold stress in cranial morphology of *Rattus*: implications for the interpretation of climatic adaptation in fossil hominins. Proceedings of the Royal Society B: Biological Sciences 273:2605-2610.

Rayfield, E. J. 2005. Aspects of comparative cranial mechanics in the theropod dinosaurs *Coelophysis*, *Allosaurus* and *Tyrannosaurus*. Zoological Journal of the Linnean Society 144:309-316.

Rayfield, E. J., A. C. Milner, V. B. Xuan, and P. G. Young. 2007. Functional morphology of spinosaur 'crocodile-mimic' dinosaurs. Journal of Vertebrate Paleontology 27:892-901.

Rebholz, W., and E. Harley. 1999. Phylogenetic relationships in the bovid subfamily Antilopinae based on mitochondrial DNA sequences. Molecular Phylogenetics and Evolution 12:87-94.

Rossie, J. B. 2005. Anatomy of the nasal cavity and paranasal sinuses in *Aegyptopithecus* and early Miocene African catarrhines. American Journal of Physical Anthropology 126:250-267.

Rossie, J. B. 2006. Ontogeny and homology of the paranasal sinuses in Platyrrhini (Mammalia: Primates). Journal of Morphology 267:1-40.

Roux, W. 1881. Der züchtende Kampf der Teile, oder die “Teilauslese” im Organismus (Theorie der “funktionellen Anpassung”). Wilhelm Engelmann, Leipzig.

Rubin, J., C. Rubin, and C. R. Jacobs. 2006. Molecular pathways mediating mechanical

signaling in bone. Gene 367:1-16.

Ryan, M. J., R. Holmes, and A. P. Russell. 2007. A revision of the late Campanian centrosaurine ceratopsid genus *Styracosaurus* from the Western Interior of North America. Journal of Vertebrate Paleontology 27:944-962.

Ryan, M. J. 2007. A new basal centrosaurine ceratopsid from the Oldman Formation, Southeastern Alberta. Journal of Paleontology 81:376-396.

Ryan, M. J., and A. P. Russell. 2005. A new centrosaurine ceratopsid from the Oldman Formation of Alberta and its implications for centrosaurine taxonomy and systematics. Canadian Journal of Earth Sciences 42:1369-1387.

Sampson, S. D. 1995. Two new horned dinosaurs from the Upper Cretaceous Two Medicine Formation of Montana; with a phylogenetic analysis of the Centrosaurinae (Ornithischia: Ceratopsidae). Journal of Vertebrate Paleontology 15:743-760.

Sampson, S. D., M. J. Ryan, and D. H. Tanke. 1997. Craniofacial ontogeny in centrosaurine dinosaurs (Ornithischia: Ceratopsidae): taxonomic and behavioral implications. Zoological Journal of the Linnean Society 121:293-337.

Schaffer, W. M. 1968. Intraspecific combat and the evolution of the Caprini. Evolution 22:817-825.

Schaffer, W. M., and C. A. Reed. 1972. The co-evolution of social behavior and cranial morphology in sheep and goats (Bovidae, Caprini). Fieldiana 61:1-88.

Schreiber, A., I. Seibold, G. Notzold, and M. Wink. 1999. Cytochrome b gene haplotypes characterize chromosomal lineages of anoa, the Sulawesi dwarf buffalo. Journal of Heredity 90:165-176.

Sedlmayr, J. C. 2002. Anatomy, evolution, and functional significance of cephalic vasculature in Archosauria. Ph.D. Dissertation. University of Ohio, Biological Sciences, 398 pp.

Seebacher, F. 2001. A new method to calculate allometric length-mass relationships of dinosaurs. Journal of Vertebrate Paleontology 21:51-60.

Shea, B. 1977. Eskimo craniofacial morphology, cold stress and the maxillary sinus. American Journal of Physical Anthropology 47:289-300.

Silva, M., and J. A. Downing. 1995. Handbook of Mammalian Body Masses. CRC Press, Boca Raton, 359 pp.

Smith, T. D., J. B. Rossie, G. M. Cooper, M. P. Mooney, and M. I. Siegel. 2005. Secondary pneumatization of the maxillary sinus in callitrichid primates: insights from immunohistochemistry and bone cell distribution. The Anatomical Record Part A: Discoveries in Molecular, Cellular, and Evolutionary Biology 285A:677-689.

Sternberg, C. M. 1927. Homologies of certain bones of the ceratopsian skull. Transactions of the Royal Society of Canada 21:135-143.

Strait, D. S., Q. Wang, P. C. Dechow, C. F. Ross, B. G. Richmond, M. A. Spencer, et al. 2005. Modeling elastic properties in finite-element analysis: how much precision is needed to produce an accurate model? The Anatomical Record Part A 283A:275-287.

Taylor, C. R. 1966. The vascularity and possible thermoregulatory function of the horns in goats. Physiological Zoology 39:127-139.

Tyson, H. 1977. Functional craniology of the Ceratopsia (Reptilia: Ornithischia) with special reference to Eoceratops. Unpublished M.Sc. thesis. University of Alberta, Department of Zoology, 339 pp.

Van Rietbergen, B., R. Huiskes, F. Eckstein, and P. Ruegsegger. 2003. Trabecular bone tissue strains in the healthy and osteoporotic human femur. Journal of Bone and Mineral Research 18:1781-1788.

van Vuuren, B. J., and T. J. Robinson. 2001. Retrieval of four adaptive lineages in duiker antelope: Evidence from mitochondrial DNA sequences and fluorescence in situ hybridization. Molecular Phylogenetics and Evolution 20:409-425.

Vrba, E. S. 1979. Phylogenetic analysis and classification of fossil and recent Alcelaphini Mammalia: Bovidae. Biological Journal of the Linnean Society 11:207-228.

Vrba, E. S., and G. B. Schaller. 2000. Phylogeny of Bovidae (Mammalia) based on behavior, glands and skull morphology, pp. 203-222 in Antelopes, deer, and relatives: fossil record, behavioral ecology, systematics, and conservation. Yale University Press, New Haven, CT.

Wang, Q., D. S. Strait, and P. C. Dechow. 2006. A comparison of cortical elastic properties in the craniofacial skeletons of three primate species and its relevance to the study of human evolution. Journal of Human Evolution 51:375-382.

Weidenreich, F. 1924. Über die pneumatischen Nebenräume des Kopfes. Ein Beitrag zur Kenntnis des Bauprinzips der Knochen, des Schädels und des Körpers. Zeitschrift für Anatomie und Entwicklungsgeschichte 72:55-93.

Weidenreich, F. 1941. The brain and its role in the phylogenetic transformation of the human skull. Transactions of the American Philosophical Society 31:320-442.

Willows-Munro, S., T. J. Robinson, and C. A. Matthee. 2005. Utility of nuclear DNA intron markers at lower taxonomic levels: Phylogenetic resolution among nine *Tragelaphus* spp. Molecular Phylogenetics and Evolution 35:624-636.

Witmer, L. M. 1995. Homology of facial structures in extant archosaurs (birds and crocodilians), with special reference to paranasal pneumaticity and nasal conchae. Journal of Morphology 225:269-327.

Witmer, L. M. 1997. The evolution of the antorbital cavity of archosaurs: a study in soft-tissue reconstruction in the fossil record with an analysis of the function of pneumaticity. Society of Vertebrate Paleontology Memoir 3:1-73.

Wolfe, D. G. 2000. New information on the skull of *Zuniceratops christopheri*, a neoceratopsian dinosaur from the Cretaceous Moreno Hill Formation, New Mexico. Bulletin of the New Mexico Museum of Natural History and Science 17:93-94.

Wu, X., D. B. Brinkman, D. A. Eberth, and D. R. Braman. 2007. A new ceratopsid dinosaur (Ornithischia) from the uppermost Horseshoe Canyon Formation (upper Maastrichtian), Alberta, Canada. Canadian Journal of Earth Sciences 44:1243-1265.

Xu, X., C. A. Forster, J. M. Clark, and J. Mo. 2006. A basal ceratopsian with transitional features from the Late Jurassic of northwestern China. Proceedings of the Royal Society B: Biological Sciences 273:2135-2140.

Zuckerkandl, E. 1887. Das Periphere Geruchsorgan der Säugethiere. Verlag von Ferdinand Enke, Stuttgart, 116 pp.